Optical Studies of Capped Quantum Dots

Optical Studies of Capped Quantum Dots

Optische Studies van Oppervlakte Gemodificeerde Quantum Dots

(met een samenvatting in het Nederlands)

PROEFSCHRIFT

TER VERKRIJGING VAN DE GRAAD VAN DOCTOR AAN DE UNIVERSITEIT UTRECHT OP GEZAG VAN DE RECTOR MAGNIFICUS, PROF. DR. W. H. GISPEN, INGEVOLGE HET BESLUIT VAN HET COLLEGE VOOR PROMOTIES IN HET OPENBAAR TE VERDEDIGEN OP MAANDAG 7 FEBRUARI 2005 DES MIDDAGS TE 14:30 UUR

DOOR

SANDER FREDERIK WUISTER

GEBOREN OP 3 JULI 1976 TE LEIDSCHENDAM

Promotor: Prof. Dr. A. Meijerink
Co-promotor: Dr. C. de Mello Donegá

Faculteit Scheikunde
Universiteit Utrecht

CIP-GEGEVENS KONINKLIJKE BIBLIOTHEEK, DEN HAAG
Wuister, Sander Frederik
Optical studies of capped quantum dots
Sander Frederik Wuister. - Utrecht: Universiteit Utrecht,
Faculteit Scheikunde, Debye Instituut.
Proefschrift Universiteit Utrecht. Met samenvatting in het Nederlands.
ISBN 90-393-3951-1

Contents

Chapter 1.

Introduction

Abstract

This chapter gives an introduction into the unique properties of semiconductor quantum dots (QDs). First the history of the synthesis of luminescent QDs and the discovery of quantum size effects is reviewed. The sections that follow explain the size dependent optical properties of QDs, the important role of capping molecules in the synthesis of luminescent QDs and basic theory involved in explaining energy transfer processes. Finally a summary of this thesis given.

1.1 History

Before one can study the size dependent properties of semiconductor nanocrystals (NCs) or quantum dots (QDs) there is need for a controlled synthesis of these nanocrystals. The synthesis of nanocrystals is not trivial and it is for this reason that in the field of QD research there is fruitful interaction between chemists and physicists. Already in the middle ages semiconductor nanocrystals were present in colored glass panes and in the 1920's the size dependent properties of ZnS nanocrystals were reported. It took however until 1982 for the field of semiconductor nanocrystals to emerge as a rapidly expanding new area of research. In this year the groups of Henglein, Brus and Gratzel [1-3] reported on the synthesis of colloidal solutions CdS nanoparticles to study photochemical and catalytic processes as a possible alternative for TiO_2 nanocrystals. Soon it was observed by both Brus (for CdS) and Ekimov (for CuCl) that optical properties of these semiconductor nanocrystals were size dependent and the term quantum size effects was introduced [4,5]. With the increased control over the size and size dispersion Brus was able to show that the absorption spectrum of small colloidal CdS crystallites shifts to the red as the particles were growing. This shift is related to confinement of the conduction band electron and/or the valence band hole and will be discussed in more detail in the next section.

The first colloidal solutions of QDs were prepared by the reaction of Cd^{2+} (from a dissolved Cd salt) and S^{2-} (from H_2S) in the presence of a polymer or SiO_2 nanoparticles. Later inverse micelles [6], yielding QDs that were soluble in non-aqueous solvents, and also thiols [7] were used to gain better control over size of the CdS nanocrystals. In the initial experiments the focus was on controlling the particle size and the luminescence quantum efficiency (QE) of the QDs was low, typically less than 1%. The first paper reporting highly luminescent QDs appeared in 1987 [8] where Hengleins group showed that the luminescence QE of CdS nanocrystals increased from less than 1% to over 50% by growing a $Cd(OH)_2$ shell over the CdS core. This marks the beginning of the research on highly luminescent QDs.

It took about 5 years after the first papers on quantum size effects in CdS before the first report on colloidal CdSe nanocrystals appeared [9] and, again some 5 years later, the next element in group VI of the periodic table (Te) was used in combination with Cd to study quantum size effects in CdTe semiconductor nanocrystals [10]. No data on CdPo have so far been reported… A major breakthrough in the synthesis of colloidal semiconductor QDs was reported in 1993 by Murray, Norris and Bawendi [11]. Inspired by the work of Steigerwald [12] a synthesis method was developed with $Cd(Me)_2$ and elemental Se as precursors in a matrix of the coordinating ligands tri-octylphosphine (TOP) and tri-octylphosphineoxide (TOPO). The precursors were injected in the hot

TOP/TOPO matrix (around 300 °C) resulting in a rapid nucleation of CdSe crystallites in a supersaturated solution. Controlled growth at a somewhat lower temperature resulted very monodisperse CdSe QDs with a luminescence QE above 10%. This paper initiated a burst of activity in the field of chemically prepared colloidal QDs which is for example illustrated by the fact that the Murray paper has been cited over 1300 times. Further improvement of the QE and stability of the CdSe QDs was achieved by overcoating of the CdSe QDs with a ZnS shell [13,14]. Interestingly, a similar observation was already made by Brus in 1982 who observed an increase in luminescence intensity of CdS QDs upon growing a ZnS layer over the QDs [2]. The high temperature QD synthesis was further developed by introducing different coordinating ligands, for example primary amines, and resulted in the synthesis of highly luminescent CdS [15], CdSe [16,17] and CdTe [18,19] QDs with or without a passivating shell of a wider bandgap II-VI semiconductor. Various groups have systematically investigated the influence of synthesis conditions (precursor ratio, growth temperature and time, solvent composition) on the particle size, size distribution and luminescence efficiency [20-22]. This has resulted in synthesis methods that monodisperse QDs that have luminescence quantum efficiencies above 50%. In spite of all this research the success of the QD synthesis still depends strongly on the skills and experience of the individual chemist involved in the synthesis.

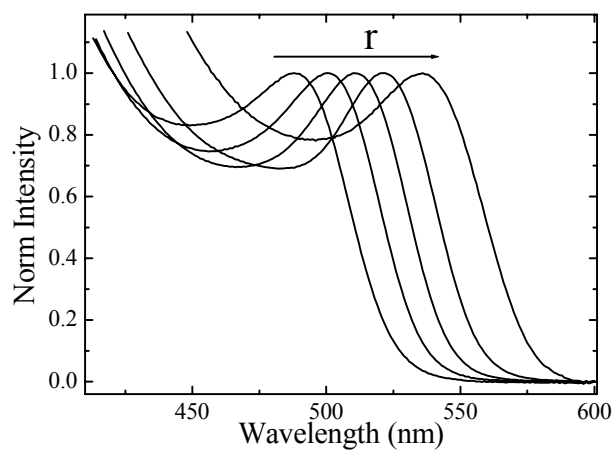

Figure 1.1 Normalized absorption spectra of TOP/DDA capped CdTe QDs of different sizes dispersed in toluene. The size (r) increases (from left to right) as the particles are growing.

1.2 Quantum size effects

The observation by Brus that the absorption edge shifts to longer wavelengths as the CdS nanocrystals grow is a generally observed effect for nanometer sized semiconductor particles. In Figure 1.1 the effect is illustrated for CdTe QDs. Absorption spectra are shown for CdTe nanocrystals with sizes between 2 nm and 3 nm. As the particle size increases from 2 nm to 3 nm the absorption edge shifts from 520 nm to 640 nm. Related to this shift, the color of the QD solution changes from yellow to red. The shift of the absorption edge as a function of particle size is due to quantum size effects. In the bulk semiconductor the Bohr radius of the free exciton is determined by the spatial extension of the wavefunctions of the conduction band electron and valence band hole. Typically, the Bohr radius is several nm in II-VI semiconductors (e.g. 3 nm for CdS, 5 nm for CdSe and 7 nm for CdTe). As the particle size becomes of the order of the exciton Bohr radius or smaller, these wavefunctions are confined by the edges of the nanocrystals and the kinetic energy of the charge carriers (electron and/or hole) increases. This causes the observed shift of the absorption edge to higher energies as the particle size decreases. The first model describing the relation between the bandgap energy and particle size was based on a 'particle in a box' model and results in the following equation [23]:

$$E = E_g + \frac{\hbar^2 \pi^2}{2R^2}\left[\frac{1}{m_e} + \frac{1}{m_h}\right] - \frac{1.8e^2}{4\pi\varepsilon_\infty \varepsilon_0 R} + smaller\,terms \qquad (1.1)$$

In this equation E_g is the bandgap energy of the bulk semiconductor, the second term describes the increase in energy due to confinement effects (proportional to R^2) while the third term describes the decrease in energy due to Coulomb attraction between electron and hole (proportional to $1/R$). This equation gives a good fit of the experimentally observed relation between E and R for the weak confinement regime but cannot explain the observations in the strong confinement regime where the effective mass approximation with infinite barriers breaks down. More recent work, for example by Zunger, has shown that for a correct description of the size dependence of the optical bandgap, also polarization effects have to be taken into account [24]:

$$E = E_g + \frac{\hbar^2 \pi^2}{2R^2}\left[\frac{1}{m_e} + \frac{1}{m_h}\right] + (E_e^{pol} + E_h^{pol} - J_{e,h}) \qquad (1.2)$$

In this equation E_e^{pol} and E_h^{pol} are the self-polarization of the electron and hole, respectively. The Coulomb interaction term is represented by $J_{e,h}$. These

polarization terms depend on the dielectric constants of both the quantum dot and the medium surrounding the quantum dot. In most cases the polarization terms and the Coulomb terms are opposite in sign and almost cancel each other. As a result, the size dependence of the optical bandgap is mainly determined by the bandgap of the bulk semiconductor and the confinement effects.
In addition to a change in the absorption energy, the reduction in size gives rise to the appearance of discrete energy levels at the band edges. For a bulk semiconductor the density of states is low at the band edge. The density of states in the quasi-continuum of energy levels increases rapidly above the conduction band edge and below the valence band edge (see Figure 1.2, left hand side) resulting in a sharp absorption edge and a structureless strong absorption continuum for a bulk semiconductor. For semiconductor quantum dots the situation is different. Due to the limited number of atoms in the QD (typically 100-10 000) discrete atomic like energy levels appear at the edges of the bands (see Figure 1.2, right hand side). This quantum size effect is reflected in the absorption spectra by the appearance of discrete absorption bands [25]. In Figure 1.1 a local maximum is observed corresponding to the lowest energy transition. At higher energies more structure can be observed due to transitions to higher discrete energy levels. For smaller particles the structure becomes more pronounced as the separation between the levels increases. The width of the absorption bands is for a large extent determined by the particle size distribution. A large size distribution results in broader bands due to a distribution in absorption energies for different sizes QDs within the ensemble.

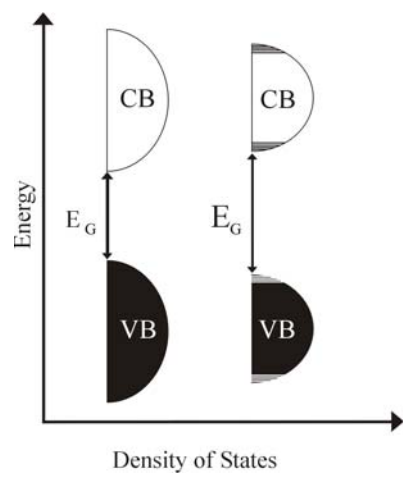

Figure 1.2 Schematic representation of the band structure of a bulk semiconductor (left) and of a semiconductor nanocrystal in the quantum size regime (right).

1.3 Capping molecules

In section 1.1 the key role of capping molecules in the synthesis of highly luminescent QDs was mentioned. In this section the role of the capping molecules is considered in more detail. Capping molecules play a role in three important aspects of QD synthesis:

(1) Control the growth of QDs
(2) Prevent aggregation of QDs (by steric hindrance or charge)
(3) Passivate dangling bonds at the QD surface

(1) Capping molecules have a chemical group with an affinity for either cation (e.g. TOPO, thiols and amines coordinate with Cd^{2+}) or the anion (e.g. TOP, capable of forming a TOP-Se complex). Under the growth conditions of the semiconductor nanocrystals the complexing properties of the coordinating molecules play an important role. The nanocrystal grows within a shell of capping molecules. The final particle size is determined by the growth kinetics. If bonding with the surface atoms of the QD is too weak there will be uncontrolled growth of the semiconductor beyond the quantum size regime. If the bonding is too strong the particle growth is inhibited. To obtain QDs of the desired nm size the growth conditions have to chosen such that the binding of the capping molecules is neither too strong nor too weak. The growth rate, and thus the particle size, is determined by the nature and concentration of the capping molecules, the growth temperature and precursor concentrations.
(2) Semiconductor QDs are not a thermodynamically stable phase. There will be a thermodynamically driven tendency for aggregation of QDs. Capping molecules play a key role in preventing aggregation. In apolar solvents the QDs are sterically stabilized by the long apolar alkyl chains of the capping molecules. In polar solvents the stabilization can also occur via (positive or negative) charges on the capping molecules.
(3) Since QDs are extremely small crystallites, the surface to volume ratio is large. At the crystal surface the periodicity of the crystal breaks down which may result in states within the bandgap (i.e. a state between the bottom of the conduction band and the top of the valence band). These surface states act as recombination centers for the excitons by first trapping one of the charge carriers followed by radiative or non-recombination with the other charge carrier. In the case of radiative recombination an emission band is observed on the long wavelength side of the excitonic emission band. This emission is referred to as defect emission or trap emission. Due to the large lattice relaxation involved in the trapping and recombination process, often the presence of surface states leads to non-radiative recombination. The non-

radiative losses lower the luminescence quantum efficiency and are undesirable in applications which rely on efficiently luminescing QDs. In Figure 1.3 the different recombination processes for an exciton are depicted schematically. Capping molecules are capable of passivating surface states. Perfectly capped QDs can have a very high luminescence QE with values close unity.

A different approach to reduce non-radiative losses at the surface is to grow a shell of higher bandgap material around the semiconductor core. The higher bandgap material confines the charge carriers, resulting in quantum size effects in the semiconductor core, and prevents the formation of surface states. These so-called core-shell QDs can have high quantum efficiencies and a higher stability against (photo-)oxidation. In Figure 1.4 emission spectra are shown for CdS QDs in water. The growth of a $Cd(OH)_2$ shell around the QDs results in a strong increase of the luminescence QE [8]. More recent examples of core-shell QDs are CdSe(ZnS) [13,14], CdSe(CdS) [26] and CdSe(ZnSe) [17]. The wider bandgap shell is capable of preventing non-radiative losses at surface states. For the growth and stability of the colloidal solutions of QDs capping molecules are still required and cap the surface of the shell.

1.4 Energy transfer

The optical properties of individual QDs are determined by the quantum size effects and the presence of (surface) defect states. As discussed in the previous

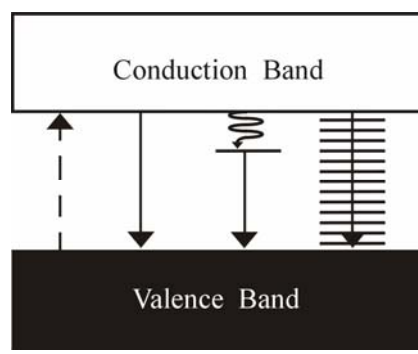

Figure 1.3 Schematic representation of different relaxation pathways of the exciton. From left to right excitation, radiative exciton recombination, defect related emission and non-radiative relaxation are depicted.

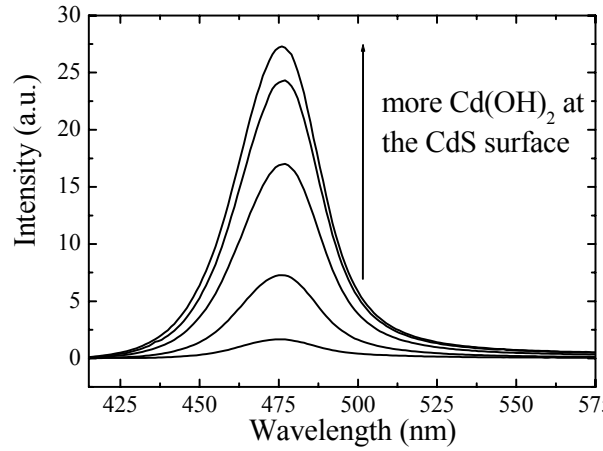

Figure 1.4 Emission spectra of colloidal CdS QDs in water capped with $Cd(OH)_2$. The concentration of QDs is the same for all samples, only the amount of $Cd(OH)_2$ at the CdS surface increases. The CdS QDs are stabilized by a polyphosphate polymer.

section, high quality QDs can have an efficient excitonic emission at a wavelength corresponding to the bandgap energy. If the distance between QDs is large, the luminescence properties of the (ensemble of) individual QDs is observed. However, when the distance between QDs becomes smaller energy transfer can occur. Energy transfer between different QDs or between QDs and other luminophores (e.g. dye molecules) is important in various applications [27,28]. For example, when QDs are used as luminescent labels in biological systems, energy transfer from a QD attached to one biomolecule (e.g. a protein) to a dye molecule attached to another biomolecule is observed when the biomolecules bind. In the bound state energy transfer from the QD (the donor) to the dye molecule (the acceptor) can occur because of the close proximity and the luminescence probes the binding of biomolecules. In another application energy transfer from smaller (wider bandgap) QDs to larger (smaller bandgap QDs) is proposed in carefully engineered structures of smaller and larger QDs to achieve a directional flow of the excitation energy [29]. Possible applications are in QD lasers or light emitting diodes [28,30].
Energy transfer processes involving QDs are assumed to involve dipole-dipole interaction. For energy transfer through dipole-dipole interaction the transfer rate can be calculated using equation derived by Forster [31]:

$$\Gamma_{ET} = \frac{2\pi}{\hbar}\frac{\mu_D^2\mu_A^2\kappa^2}{r^6 n^4}\Theta \qquad (1.3)$$

where μ_D and μ_A are donor and acceptor electric dipole moments, κ is an orientation factor (κ^2 is $^2/_3$ for randomly oriented dipoles), Θ is the spectral overlap integral, n is the refractive index and r is the distance between the two dipoles. The dipole strength of a luminescing entity can directly be derived from its radiative decay rate. For QDs this dipole moment is large at room temperature in view of the nanosecond decay time. The overlap integral (Θ) is determined by the overlap between the emission of the donor and the absorption of the acceptor (the resonance condition). The energy transfer rate is strongly dependent on the distance and decreases with the sixth power of the distance between the donor and acceptor. The Forster equation for energy transfer has been derived assuming interacting point dipoles, i.e. the distance between the dipoles is much larger than the spatial extension of the oscillating dipoles. This approximation may not be valid for energy transfer processes involving QDs with large delocalized excitons.

1.5 Summary of the thesis

This thesis, containing 9 chapters, can be divided in four sections. The first part (chapters 2, 3 and 4) focuses on the synthesis of CdTe QDs and the capping exchange by thiols. In chapter 2 the synthesis conditions for the synthesis of CdTe QDs in TOP and dodecylamine (DDA) are explored by varying the reaction temperature and the synthesis duration. CdTe QDs with sizes between 2.4 nm and 2.9 nm were obtained. The QE gradually increases during the synthesis to 45% for the best samples. A luminescence decay time of 10 ns (1/e value) was obtained for these samples. The formation of two sizes of CdTe clusters from Cd and Te precursors was observed. A stepwise growth is observed from the smaller to the larger cluster size.

The TOP/DDA capped CdTe QDs are transferred into water by the use of capping exchange with amino-ethanethiol•HCl or mercaptopropionic acid (chapter 3). This results in an increase of the photoluminescence QE (up to values of 60%), a decrease of the defect related emission and a monoexponential exciton lifetime of ~ 20 ns. The synthesis of highly luminescent QDs with monoexponential radiative luminescence decay is an important condition for the research described in other chapters of this thesis.

Chapter 4 describes the capping exchange with different types of thiols for TOP/DDA capped CdTe QDs. After capping exchange the QDs can be suspended in water, ethanol or organic media, depending on the type of thiol used for capping exchange. A monoexponential decay with a decay time of ~20 ns and a high QE are obtained for four different thiols. Capping exchange using the same thiols for TOP/TOPO/HDA capped CdSe QDs results in a quenching of the exciton luminescence. The striking difference between these two II-VI

semiconductor QDs is explained by the difference in the energy of the valence band top. Hole trapping by the thiol molecule at the QD surface is possible for CdSe but not for CdTe and explains the luminescence quenching in thiol-capped CdSe QDs. If the redox potential of a thiol is very high (like for 4-mercaptophenol), quenching of the luminescence is also observed for CdTe QDs.
Many theoretical models have been developed for the dependence of the radiative decay time on the solvent refractive index. The experimental work to verify the proposed models is limited and restricted to Eu^{3+}. In chapter 5 (second part) experimental work on the influence of local field effects on the spontaneous emission rate is presented with CdTe and CdSe QDs as probe. The radiative decay time of QDs with a monoexponential exciton decay is measured in solvents with a refractive index ranging from 1.37 to 1.50. The observed dependence of the radiative decay rate on the refractive index n, is weaker than predicted by two well-known models. A good agreement is found with a recently proposed fully microscopic model for local field enhancement of the spontaneous emission rate.
The third part (chapters 6 and 7) presents the remarkable phenomenon "luminescence temperature antiquenching" observed for two different model systems. Chapter 6 describes the surprising recovery of the luminescence intensity of alkylamine capped CdSe QDs dispersed in toluene. This increase in intensity is accompanied by an increase of the luminescence life time and occurs as a sharp transition around 250K (within 15K). The transition temperature systematically increases by increasing the length of the alkylamine capping molecules. This indicates that a phase transition in the capping layer is involved and directly affects reconstruction of the CdSe surface. Surface reconstruction is required to remove surface (quenching) states.
For water-soluble amino-ethanethiol capped CdTe QDs (chapter 7) a pronounced luminescence temperature antiquenching is observed: the excitonic emission of efficient luminescing CdTe QDs is almost completely quenched when cooled to 230 K and fully recoveres at 270 K. Here, a phase transition in the solvent (from liquid to solid) is held responsible for the luminescence antiquenching. The transition temperature decreases as an increasing concentration of a freezing point depressing agent (methanol) is present. Strain is induced to the capping molecules as the water solidifies to ice. For short (C_2) capping molecules the strain is propagated to the QD surface atoms, affecting the surface reconstruction. For longer (C_{11}) capping molecules the strain is dissipated in these flexible molecules and no luminescence temperature antiquenching is observed.
The last part of the this thesis (chapter 8 and 9) concerns energy transfer in two nanocrystalline systems. Chapter 8 discusses energy transfer between QDs in a QD solid. Efficient energy transfer is observed from smaller QDs to larger QDs. The energy transfer rate is proportional to the dipole strength of the exciton emission, which is a strong function of temperature. Also energy transfer in two

heteronuclear QD solids (consisting of green emitting and orange emitting QDs) is studied. Efficient energy transfer is observed from green emitting to orange emitting QDs. Changing the concentration of orange emitting QDs results in different kinetics of the energy transfer.
In Chapter 9 energy transfer involving a different type of nanocrystals is reported. Nanocrystals of $Y_3Al_5O_{12}$ (YAG) doped with Ce^{3+} are insulator nanocrystals in which quantum size effects do not play a role. However, YAG:Ce nanocrystals have a photostability that exceeds that of QDs and make these nanocrystals interesting as luminescent labels requiring a high photostability. The last chapter discusses energy transfer between nanocrystalline YAG:Ce and Tetramethyl rhodamine isothiocyanate (TRITC), a functionalized dye. Efficient energy transfer is observed from the Ce^{3+} ions to the TRITC molecules upon photoexcitation of the NC YAG:Ce – TRITC conjugates.

References

[1] A. Henglein, *J. Phys. Chem.* **1982**, 86, 2291
[2] R. Rossetti, L.E. Brus, *J. Phys. Chem.* **1982**, 86, 4470
[3] D. Duonghong, J. Ramsden, M. Grätzel, *J Am. Chem. Soc.* **1982**, 104, 2977
[4] R. Rossetti, J.L. Ellison, J.M. Gibson, L.E. Brus, *J. Chem. Phys.* **1984**, 80, 4464
[5] A.I. Ekimov, A. A. Onushchenko, *Fizika i Tekhnika Poluprovodnikov* **1982**, 16, 1215
[6] Y. M. Tricot, J. H. Fendler, *J. Phys. Chem.* **1986**, 90, 3369
[7] Y. Nosaka, K. Yamaguchi, H. Miyama, H. Hayashi, *Chem. Lett.* **1988**, 4, 605
[8] L. Spanhel, M. Haase, H. Weller, A. Henglein *J. Am. Chem. Soc.* **1987**, 109, 5649
[9] N. M. Dimitrijevic, P.V. Kamat, *J. Phys. Chem.* **1987**, 91, 2096
[10] T. Rajh, O. I. Micic, A. J. Nozik, *J. Phys. Chem.* **1993**, 97, 11999
[11] C.B. Murray, D.B. Norris and M.G. Bawendi, *J. Am. Chem. Soc.* **1993**, 115, 8706
[12] S. M. Stuczynski, J.G. Brennan, M. L. Steigerwald, *Inorg. Chem.* **1989**, 28, 4431
[13] M. A. Hines, P. Guyot-Sionnest, *J. Phys. Chem.* **1996**, 100, 468-471
[14] B. O. Dabbousi, J. Rodriguez-Viejo, F. V. Mikulec, et *al. J. Phys. Chem. B* **1997**, 101, 9463
[15] W. W. Yu, X. Peng, *Angew. Chem. Int. Ed* **2002**, 41, 23681
[16] D.V. Talapin, A. L. Rogach, A. Kornowski, M. Haase, H. Weller, *Nano Lett.* **2001**, 1, 207
[17] P. Reiss, J. Bleuse, A. Pron, *Nano Lett.* **2002**, 2, 781
[18] D.V. Talapin, S. Haubold, A. L. Rogach, A. Kornowski, M. Haase and H. Weller, *J. Phys. Chem. B* **2001**, 105, 2260
[19] S. F. Wuister, A.F. van Driel, A. Meijerink, *Phys. Chem. Chem. Phys.* **2003**, 5, 1253
[20] L. Qu, X. Peng, *J. Am. Chem. Soc.* **2002**, 124, 2049
[21] D. V. Talapin, A. L. Rogach, E. V. Shevchenko, A. Kornowski, M. Haase, H. Weller, *J. Am. Chem. Soc.* **2002**, 124, 5782
[22] C. de Mello Donegá, S. G. Hickey, S. F. Wuister, D. Vanmaekelbergh, A. Meijerink, *J. Phys. Chem. B* **2003**, 107, 489
[23] L. E. Brus, *J. Chem. Phys.* **1984**, 80, 4403
[24] A. Francescetti, A. Williamson, A. Zunger, *J. Phys. Chem. B* **2000**, 104, 3398
[25] A. P. Alivisatos, *J. Phys. Chem. B* **1996**, 100, 13226
[26] X. Peng, M.C. Schlamp, A. V. Kadavanich, A. P. Alivisatos, *J. Am. Chem. Soc.* **1997**, 119, 7019

[27] M. Bruchez Jr., M. Moronne, P. Gin, S.A. Weiss, A.P. Alivisatos, *Science* **1998**, 281, 2013
[28] S. Coe, W. -K. Woo, M.G. Bawendi, V. Bulovic, *Nature* **2002**, 420*,* 800
[29] S.A. Crooker, J.A. Hollingsworth, S. Tretiak, V.I. Klimov *Phys. Rev. Lett.* **2002**, 89, 186802-1
[30] V. I. Klimov, A. A. Mikhailovsky, S. Xu, A. Malko, J.A. Hollingsworth, C. A. Leatherdale, H. Eisler, M. G. Bawendi, *Science* **2000**, 290*,* 314
[31] T. Förster, *Naturwissenschaften*, **1946**, 33, 166

Chapter 2.

Luminescence and growth of CdTe quantum dots and clusters

Abstract

Highly luminescent CdTe quantum dots (QDs) were synthesized in a mixture of TOP and DDA. The growth of the particles in the reaction mixture was followed in time for three different temperatures. The reaction temperature determined the final diameter of the QDs (2.4 nm at 145ºC, 2.7 nm at 165ºC and 2.9 nm at 180ºC). For all three temperatures a fast initial growth is observed in the first 30 minutes and is followed by a slower growth to the final particle size. The small particles that are initially formed show a defect related emission. After several minutes an excitonic emission is observed. The quantum efficiency gradually increases from 10% to 45% for the best samples (after four hours). A good correlation between quantum efficiency and luminescence lifetime is observed. A luminescence lifetime of approximately 10 ns is found for the exciton emission in the CdTe particles with the highest quantum efficiency. The formation of small CdTe clusters of discrete sizes from Cd and Te precursors is observed in the reaction mixture at room temperature. The stability of the CdTe clusters depends on the reaction conditions and a stepwise growth from a smaller to a larger cluster size is observed.

2.1 Introduction

In the last two decades the interest in semiconductor quantum dots (QDs) has increased rapidly [1]. The physical and chemical properties of semiconductor QDs differ from bulk semiconductors. Due to quantum size effects the band gap energy can be tuned and the formation of atomic like levels occurs at the edges of the band gap [2]. Since most II-VI semiconductors have a direct band gap, the II-VI QDs form a new and promising class of luminescent materials that may find extensive application as luminescent labels in biological systems [3,4].

The development of the TOP/TOPO (tri-octylphosphine/tri-octylphosphineoxide) synthesis, a high temperature organic synthesis with organo-metallic precursors, marks an important step forward in making efficiently luminescing QDs [5]. Via this synthesis method monodisperse QDs of CdS, CdSe and CdTe showing excitonic emission can be obtained. Since the initial publication on making high quality CdSe quantum dots via the TOP/TOPO method, a variety of similar synthesis routes for efficiently luminescing II-VI QDs has been published, including methods based on different coordination molecules (e.g. HDA (hexadecylamine) instead of TOPO) [6, 7] and methods to cap the QDs with a thin layer of a wider bandgap material [8,9].

The preparation of high quality CdTe QDs is more complicated than for CdS and CdSe because Te is very sensitive to oxygen [10]. Recently a room temperature synthesis for CdTe has been reported using aqueous solutions and thiol capping molecules [11]. Stable, thiol capped particles with quantum yields up to 18% were obtained [12]. More recently Talapin et al. published an article where CdTe was formed from $Cd(Me)_2$ and Te in a TOP/DDA (dodecylamine) mixture, leading to QDs with a quantum efficiencies up to 65% [13]. To obtain a better understanding of the influence of the reaction conditions on the growth and luminescence of CdTe QDs, this chapter follows the growth of CdTe QDs for a TOP/DDA synthesis in time for different reaction temperatures by recording absorption and emission spectra and by measuring both the quantum efficiencies and luminescence life times for samples taken at various time intervals during the growth. In addition the initial formation of CdTe clusters of discrete sizes and the discontinuous growth of these clusters is reported.

2.2 Experimental

Synthesis

For the synthesis of CdTe a method similar to the one described by Talapin et al. [13] was used. In general the reaction times and temperatures are lower the in Ref [13]. In a three necked flask 10 g of dry DDA and 7 mL of TOP were heated to 50^{o}C. To this solution 0.22 gr (1.54 mmol) $Cd(Me)_2$ in 7 mL of TOP and 0.16 gr (1.25 mmol) Te powder were added. A Cd/Te ratio of about 1.25 was used in all the synthesis performed unless a different ratio is indicated. The reaction mixture

was heated to 145ºC, 165ºC and 180ºC. To follow the particle growth in time for these temperatures, samples of about 0.5 mL were taken at regular time intervals during the growth of the quantum dots and stored in 3 mL toluene. Excess of Cd and Te was not removed during storage. The point where the reaction mixture turned from grey to green during heating (which was at about 135ºC) was set as t = 0 min. This was the point where the tellurium starts to dissolve and the TOP-Te complex was formed [13].

Apparatus

Emission spectra were recorded on a SPEX Fluorolog spectrofluorometer, equipped with two monochromators (double-grating, 0.22 m, SPEX 1680, model F2002) and a 450 W Xenon lamp as the excitation source. Absorption spectra were measured using a Perkin-Elmer Lambda 16 UV/vis spectrometer. Luminescence lifetime measurements were performed with a Pico Quant picosecond laser (λ_{ex} = 406 nm, 2.5 MHz) and monochromator (1350 lines mm^{-1} grating, blazed at 500 nm) in combination with a fast Hamamatsu photo-multiplier tube (H5738P-01) for light detection. Luminescence decay curves were obtained by pulse height analysis using a Time Harp 100 computer card. Quantum efficiencies were measured against commercial Rhodamine B with a known quantum efficiency of 90%. A correction for reabsorption was done by dividing the emission spectrum by the (for the path length corrected) transmission spectrum.

2.3 Results and discussion

2.3.1 Temperature dependence of particle growth

Figure 2.1a shows the absorption spectra (normalized to the first absorption maximum) of samples of CdTe QDs taken at different time intervals for a reaction temperature of 165°C. At the times indicated a sample was taken from the top of hot reaction mixture and diluted into 3 mL of toluene. Figure 2.1b shows the emission spectra of these CdTe samples. The QDs have an excitonic emission with a full width at half maximum (FWHM) of approximately 35 nm (1200 cm^{-1}), indicating that relatively monodisperse particles are obtained.

Hardly any defect related emission is seen in the emission spectra of fresh samples. Samples stored in toluene show some defect related emission after a few days. Both the absorption and emission spectra show a red shift with reaction time which results from the growth of the QDs. From position of the first maximum in the absorption spectra the average particle size could be determined by using the relationship between the maximum of the first absorption peak and the particle size [11]. A sharp increase in particle size is noted within the first 30 minutes. The particle size increases only slightly at longer timescales and finally reaches a constant value. (See also Figure 2.3b.)

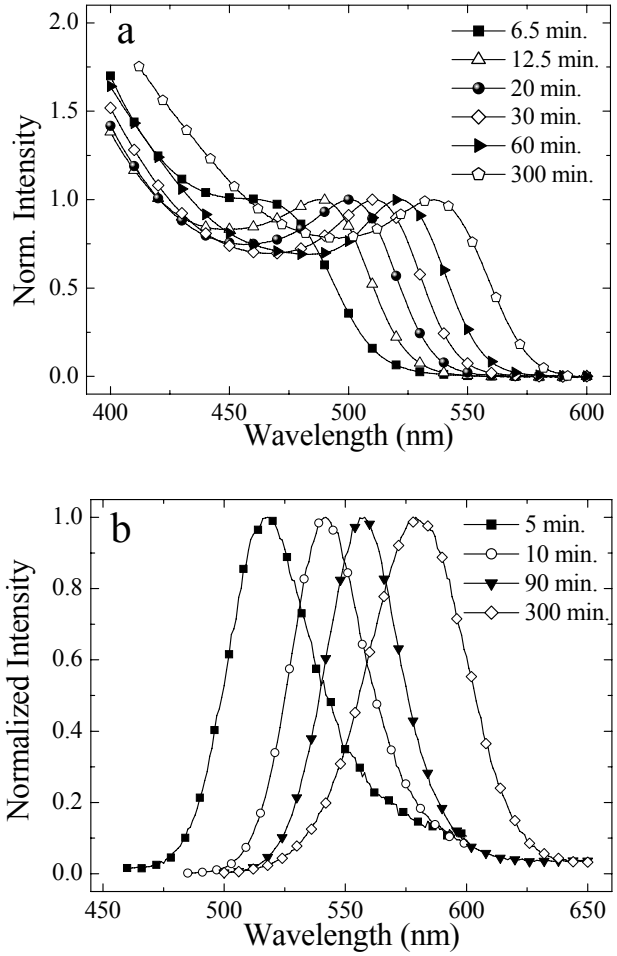

Figure 2.1 (a) Absorption spectra (normalized to the first absorption maximum), (b) emission spectra (normalized to the emission maximum, λ_{ex} = 400 nm of CdTe QDs (diluted in toluene) taken for a synthesis at 165^{o}C at different time intervals (indicated in the figure).

These are samples from a synthesis at the same temperature as in figure 2.1 but taken on a shorter timescale. In addition to emission from the CdTe QDs a peak is observed at 454 nm. This peak can be ascribed to Raman scattering. It is shifted by ~ 3000 cm^{-1} from the excitation wavelength due to excitation of C-H vibrations. The weak Raman peak is always present, but can only be observed in the (scaled) emission spectra of weakly luminescent samples. The initially formed particles show a broad band emission around 600 nm with a low quantum efficiency (< 1%).

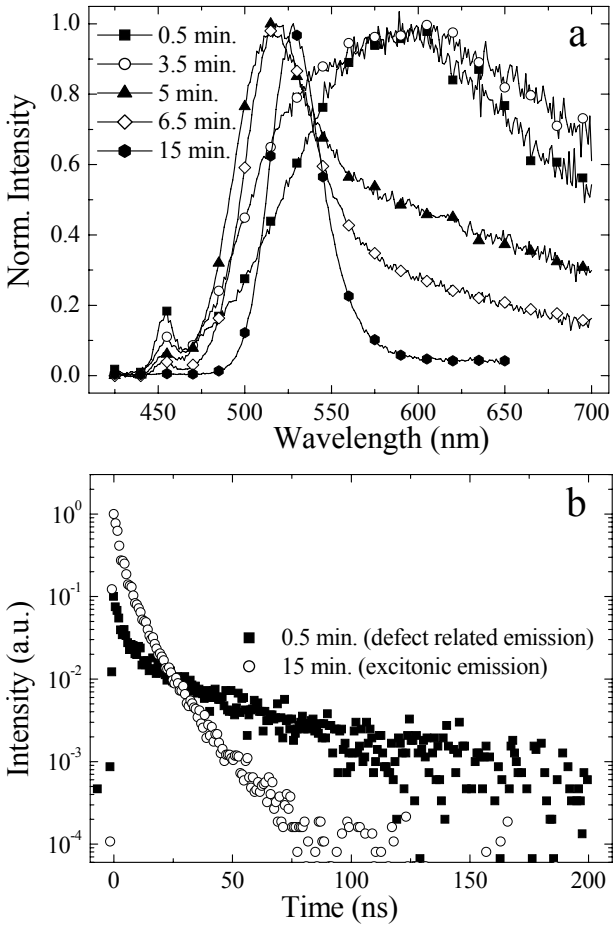

Figure 2.2 (a) Emission spectra (normalized to the emission maximum, λ_{ex} = 400 nm) of CdTe QDs taken for a synthesis at 165°C and diluted in toluene at short time intervals (indicated in the figure). (b) Luminescence decay curves of the CdTe emission (λ_{em} = 600 nm, T=300 K) for a sample after 0.5 minutes and of the CdTe emission (λ_{em} = 525 nm, T= 300 K) for a sample taken after 300 minutes (λ_{ex} = 406 nm).

The luminescence decay curve (see figure 2.2b) is non-exponential, showing a fast initial decay followed by a long-lived tail with $\tau_{1/e}$ (the time at which the intensity has decreased to 1/e of the initial value) of about 200 ns. The relatively long life time and the low efficiency are characteristic of a defect-related emission. Trapping of one of the charge carriers is followed by radiative or non-radiative recombination at the trapping site. Defect related emission is often observed in II-VI QDs [14].

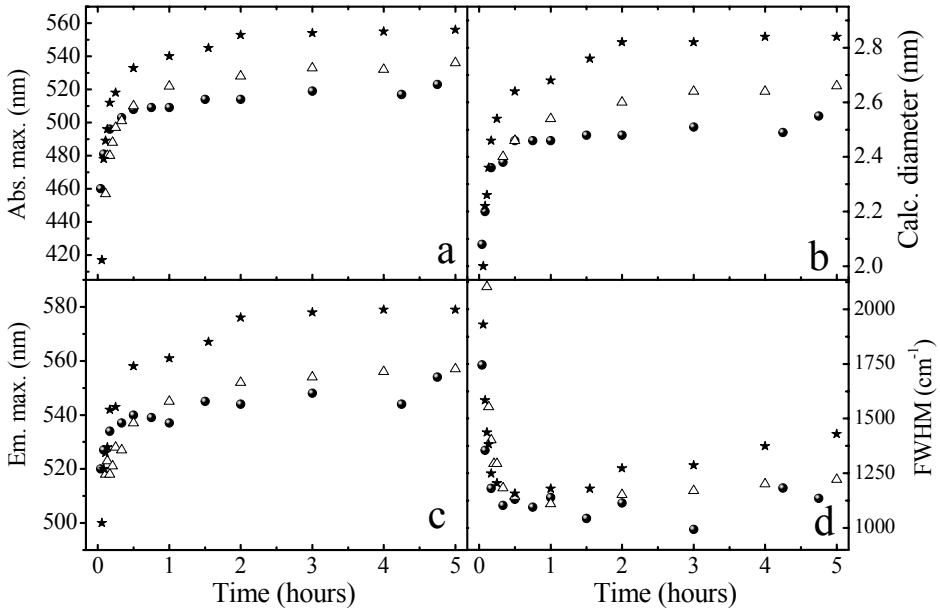

Figure 2.3 (a) Absorption maximum, (b) calculated diameter, (c) emission maximum (λ_{ex} = 400 nm) and (d) FWHM of the CdTe emission peak as function of time for the synthesis of CdTe in TOP/DDA at three different reaction temperatures: 145^{o}C (●), 165^{o}C (△) and 180^{o}C (★)) and recorded room temperature.

For efficiently luminescing QDs this type of emission is undesired. Annealing of defects improved crystallinity and capping of surface sites leads to the disappearance of defect related emission and the appearance of (efficient) excitonic emission.

For the present synthesis conditions and temperature (165ºC), the excitonic emission is clearly observed after 5 minutes. The defect related emission continues to decrease until after about 15 minutes the excitonic emission dominates with a quantum efficiency of about 20% and a short, nearly mono-exponential life time ($\tau_{1/e}$ < 10 ns, see figure 2.2b) typical of excitonic emission. The results presented in figure 2.2 indicate that initially small particles are formed with a relative high concentration of defects. As the particles grow, the surface passivation by DDA and TOP improves and crystals defects are annealed. After 15 minutes mainly excitonic emission is observed but the increase of the quantum efficiency continues for several hours (see below) showing that the annealing of defects and/or capping of the quenching sites at the surface of the quantum dots continues for this period of time.

To study the influence of the reaction temperature on the final particle size also a synthesis at a higher temperature (180ºC) and at a lower temperature (145ºC) was done. Figure 2.3a shows the absorption spectra of the samples in toluene taken from the solution at various times for all three temperatures (T = 145ºC, T =165ºC and T =180ºC). The maximum of the first absorption peak shifts strongly in the first 30 minutes for all three syntheses. After 30 minutes a smaller change is observed, reflecting a slower growth towards a nearly constant particle size. At the lowest reaction temperature (145ºC) a constant value for the first absorption maximum (a constant particle size) is reached sooner than for higher temperatures. Figure 2.3b shows the average particle size with reaction time (determined from the relationship between the maximum of the first absorption peak and the particle size [11]). The final size of the CdTe QDs is determined by the reaction temperature. At higher temperatures larger particles are obtained. This result is comparable to what Cumberland et al [15] recently observed for CdSe QDs formed from clusters. The formation of larger particles at higher growth temperatures can be explained by taking into account the kinetics of the particle formation. Nanocrystalline semiconductor particles grow inside a shell of coordinating ligand molecules. If the binding of the capping molecules is too strong, particle growth is prevented by a strongly bound shell of ligands. On the other hand, weakly coordinating ligands will result in fast growth, resulting in large particles. It is well known that the choice of ligands is crucial for the formation of nm-sized semiconductor crystals. The particles can grow when a ligand molecule detaches and the exposed surface site reacts with a Cd or Te precursor in the solution. The temperature will influence the rate at which the ligands attach and detach from the surface. A higher rate of attaching and detaching at higher temperatures will result in a faster growth rate and thus larger particle sizes. In addition, dissolution of smaller particles may increase with temperature which results in a faster Ostwald ripening and growth to larger particle sizes. By controlling the temperature and the reaction time a good control over the CdTe particle size is obtained for particles between 2 and 3 nm. Figure 2.3c shows the development of the wavelength for the maximum of the excitonic emission peak with time. As expected the position of the maximum of the emission spectra follows the trend of the position of the absorption maximum with time.

In figure 2.3d the FWHM of the emission peak is plotted as function of reaction time for syntheses at 145ºC, 165ºC and 180ºC. The relative large values for the FWHM in the initial stage of the reaction are due to the fact that the emission is partly caused by a broad defect related emission. Within 30 minutes the nature of the peak has changed to exciton emission and a minimum in the FWHM in reached. During further growth the FWHM increases indicating that the size distribution of the QDs increases. An increase in the size distribution has been observed for CdSe and explained in terms of Ostwald ripening after long reaction times [16].

2.3.2 Quantum efficiency and luminescence lifetime

One of the important properties of luminescent quantum dots is the quantum efficiency. For applications and fundamental studies, a high quantum efficiency is usually beneficial. To study how the quantum efficiency develops during the synthesis described in this paper, the quantum efficiency was measured for samples taken from the reaction mixture at 165ºC at regular time intervals. The results are shown in figure 2.4a. During the first two hours the quantum efficiency gradually increases until it levels of around 40%. The gradual increase of the quantum efficiency reflects the improved capping by DDA and TOP and the annealing of defects as discussed above. Since luminescence quenching (non-radiative decay) leads to a shortening of the luminescence lifetime, a correlation between lifetime and quantum efficiency can be expected. In figure 2.4b the luminescence decay curves for the excitonic emission are plotted for different samples taken after

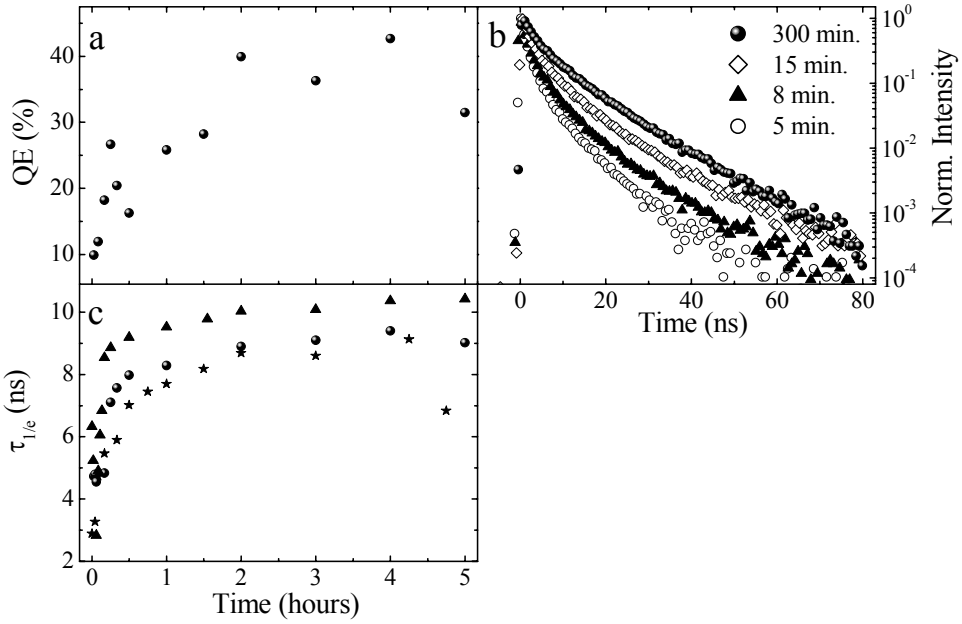

Figure 2.4 (a) Quantum efficiency (measured against commercial Rhodamine B, λ_{ex} = 400 nm) as a function of reaction time for a CdTe synthesis at 165°C. (b) Luminescence decay curves (λ_{ex} = 406 nm) measured for the emission maximum for CdTe samples taken after 5, 8, 15, and 300 minutes from reaction mixture for a synthesis at 165ºC. (c) Luminescence lifetime (λ_{ex} = 406 nm) measured for the emission maximum as function of reaction time for three different temperatures: 145°C (●), 165°C (△) and 180°C (★).

different reaction times at 165ºC. All decay curves show a clear deviation from a single-exponential decay. The faster initial decay reflects the emission from QDs with a faster non-radiative decay rate. A distribution in decay times is expected as the different QDs will have different types and numbers of quenching centers, resulting in a spread of luminescence lifetimes for different quantum dots. Rather than fitting the decay curves to a multi-exponential or other complex equation, an estimate for the average lifetime was obtained from the time in which the emission intensity drops to 1/e of the initial value, $\tau_{1/e}$. An increase of the luminescence decay time with reaction time is observed and can be explained by an increase of the quantum yield as discussed above. The correlation between quantum efficiency and luminescence lifetime is good. Therefore measuring the luminescence lifetime, (an easy experiment) is a fast method to analyze the quantum yield. Still one should be careful since in some situations the quantum yield may be low (due to a large fraction of quenched dots) while a relatively long luminescence lifetime is measured for a small fraction of bright dots with a long-lived excitonic emission [17].
Figure 2.4c shows the luminescence lifetime as a function of reaction time for all samples at 145ºC, 165ºC and 180ºC. For all temperatures a strong increase of the luminescence lifetime is observed in the first minutes of the reaction, indicating an increase in quantum yield. At higher reaction temperatures a faster increase of the luminescence lifetime is observed. This can be explained by faster annealing of defects and a faster surface reorganization at higher temperatures. Since the annealing of defects and surface reorganization involves an activation energy, a faster increase in the quantum yield is expected at higher temperatures.

2.3.3 CdTe clusters

To investigate the stability of CdTe QDs at room temperature, the optical properties of samples from the solution in toluene stored in (not air tight) closed vials under ambient conditions were followed in time. In figure 2.5 absorption spectra are shown for the CdTe synthesis at 145ºC for samples taken after 5 and 20 min. reaction time. In figure 2.5a the absorption spectra have been measured directly after taking the sample. In figure 2.5b the absorption spectra measured after two weeks are shown. Two interesting differences are observed. Firstly, a blue shift in the absorption onset is noted, indicating that the particles decreased in size. This may be due to photo-oxidation of the quantum dots as CdTe is very sensitive to oxygen. Photo-oxidation of semiconductor QDs is a well investigated process for CdS [18,19] and has also been observed for CdSe [20]. As oxidation occurs, the surface layer of the QD lattice is oxidized resulting in a smaller semiconductor particle size and thus in a blue shift of the absorption spectrum.

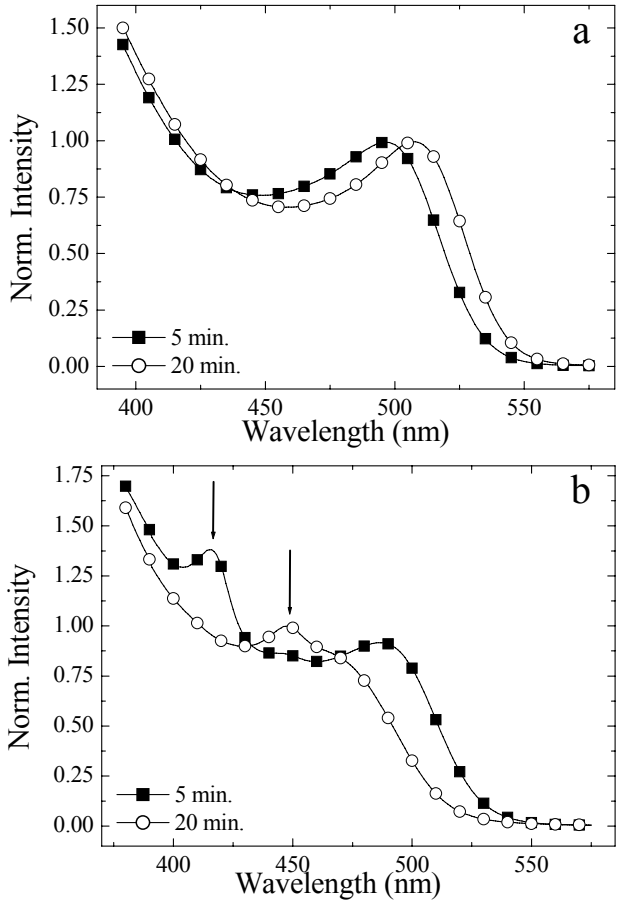

Figure 2.5 (a) Absorption spectra (normalized to the first absorption maximum) of CdTe samples taken after 5 and 20 minutes from the reaction mixture (at 145°C), measured directly after sample extraction and (b) measured 2 weeks later.

The second interesting difference between figure 2.5a and 2.5b is the appearance of two small peaks: one around 450 nm and one around 420 nm. The formation of sharp absorption peaks at similar energies is also observed for aged samples taken after short reaction times for syntheses at 165ºC and 180ºC. Figure 2.6 shows the absorption spectra of CdTe samples from the synthesis at 165ºC (after 1.5 and 2.5 minutes) and at 180ºC (after 1.5 and 3.5 minutes) after one week of aging. The sharp peaks in the absorption spectra seem to be at discrete energies. A peak around 420 nm and one around 450 nm can be clearly distinguished in figure 2.6. It is known that in the small size regime clusters of certain sizes are favored [21, 22].

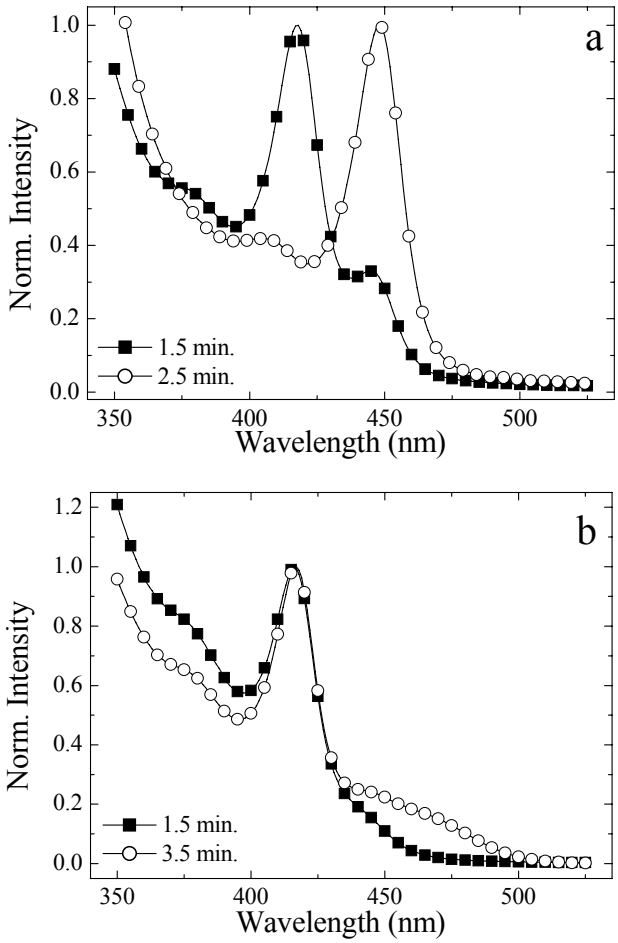

Figure 2.6 Absorption spectra (normalized to the first absorption maximum) of CdTe samples after one week of aging (a) taken after 1.5 and 2.5 minutes from the reaction mixture at 165 ^{o}C and (b) after 1.5 and 3.5 minutes from the reaction mixture at 180^{o}C.

These have been reported for CdS [21] and CdSe [23, 24] and CdTe [11]. Certain sizes can be obtained as these are the thermodynamically stable configurations of the semiconductor in the ultra small size regime. Therefore one could indeed expect very distinct absorption peaks at discrete energies. The shape of the absorption spectra resembles the spectra of clusters b reported by Rogach *et al.* [11], however the absorption peaks are not as sharp as reported here. A possible explanation for the formation of small and stable clusters during aging of the

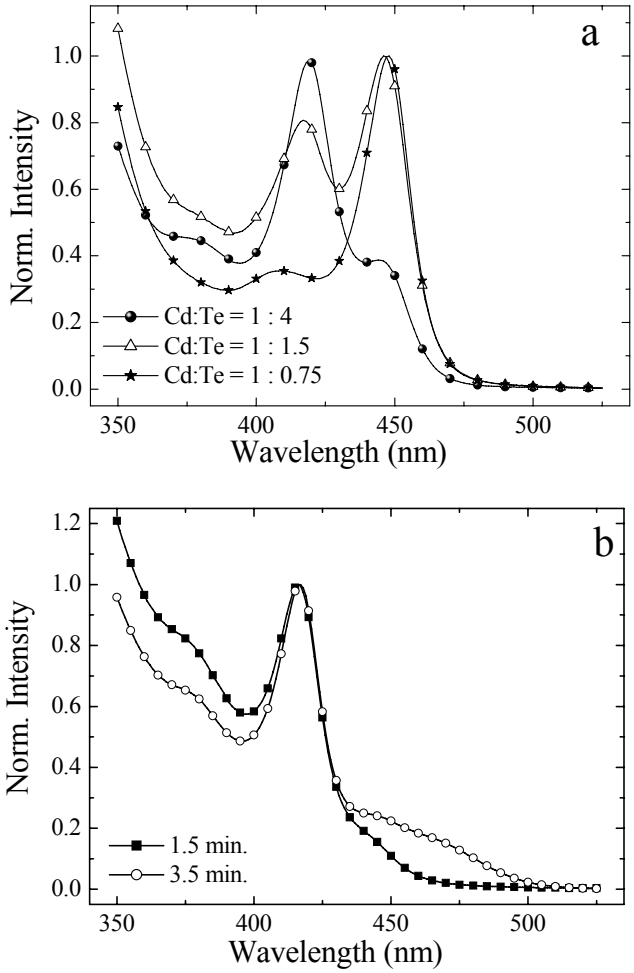

Figure 2.7 (a) Absorption spectra (normalized to the first absorption maximum) of CdTe samples prepared in DDA at 40 °C for Cd:Te ratios of 1:4 (●), 1:1.5 (△) and 1:0.75 (★). (b) Absorption spectra of CdTe samples prepared for a Cd:Te ratio of 1:4 at 40 °C (●) and at 117 °C (△).

samples is that unreacted precursors slowly form small CdTe clusters at room temperature. As the reaction of CdTe QDs is not completed after 20 minutes of reaction time the precursors are expected to be present in the crude reaction mixture. To test this hypothesis, $Cd(Me)_2$ in TOP was added to a mixture of TOP-Te complex (made by dissolving Te overnight in TOP at 180ºC) with DDA that was kept at 40ºC (just above the melting point of DDA). A sample from this

mixture was dissolved into toluene. Figure 2.7a shows the absorption spectra of the mixture in toluene for different Cd:Te ratios. If a large excess of Te (Cd:Te=1:4) is used, a peak at ~ 420 nm is seen. Upon increasing the ratio between Cd and Te to excess Cd, larger clusters (absorption ~ 450 nm) are formed. The positions of these absorption peaks agree very well with the peaks observed in figures 2.6a and b. The sensitivity of the size of the clusters to temperature is illustrated in figure 2.7b. At 40ºC mainly small clusters giving an absorption peak at 420 nm are observed for a Cd:Te ratio of 1:4. Heating the mixture just above 100ºC results in an almost complete transformation into slightly larger clusters absorbing around 450 nm. For clusters this stepwise growth from one thermodynamically stable size to another is expected.

2.4 Conclusions

Insight in the growth and formation of highly luminescent CdTe quantum dots via a TOP/DDA synthesis is obtained by following luminescence from QDs taken at different time intervals for syntheses at different temperatures. For samples taken from the reaction mixture in the first minutes mainly defect related emission is observed. Due to a better surface passivation and defect annealing the excitonic emission rises after about 5 minutes of reaction time until highly luminescent quantum dots with quantum efficiencies up to 45% are obtained after several hours. Particle growth is fast in the first 30 minutes. The final size of the particles is reached after three hours and is determined by the reaction temperature. The particles growth and increase in luminescence quantum efficiency are faster for higher reaction temperatures. A good correlation between the luminescence lifetime of the excitonic emission and the quantum efficiency is observed. Evidence is presented for the formation of thermodynamically stable small clusters from the reaction of precursors at low temperatures (close to room temperature). A stepwise growth from a smaller to a larger stable cluster size is observed.

References

[1] A. P. Alivisatos, *J. Phys. Chem.* **1996**, 100, 13226
[2] L. E. Brus, *J. Chem. Phys.* **1986**, 90, 2555
[3] M. Bruchez, Jr., M. Moronne, P. Gin, S. Weiss, A. P. Alivisatos, *Science* **1998**, 281, 2013
[4] W. C. W. Chan, S. Nie, *Science* **1998**, 281, 2016
[5] C. B. Murray, D. B. Norris, M. G. Bawendi, *J. Am. Chem. Soc.* **1993**, 115, 8706
[6] M. A. Hines, P. Guyot-Sionnest, *J. Phys. Chem. B* **1998**, 102, 3655
[7] D. V. Talapin, A. L. Rogach, A. Kornowski, M. Haase, H. Weller, *Nano Lett.* **2001**, 1, 207
[8] M. A. Hines, P. Guyot-Sionnest, *J. Phys. Chem.* **1996**, 100, 468
[9] B. O. Dabbousi, J. Rodriguez-Viejo, F. V. Mikulec, J. R. Heine, H. Mattoussi, R. Ober, K. F. Jensen, M. G. Bawendi, *J. Phys. Chem. B* **1997**, 101, 9463
[10] M. L. Steigerwald, L. E. Brus, *Annu. Rev. Mater. Sci.* **1989**, 19, 471
[11] A. L. Rogach, L. Katsikas, A. Kornowski, D. Su, A. Eychmüller, H. Weller, *Ber. Bunsen-Ges. Phys. Chem.* **1997**, 101, 1668
[12] A. L. Rogach, *Mater. Sci. Eng. B* **2000**, 69–70, 435
[13] D. V. Talapin, S. Haubold, A. L. Rogach, A. Kornowski, M. Haase, H. Weller, *J. Phys. Chem. B* **2001**, 105, 2260
[14] A. Hässelbarth, A. Eychmüller, H. Weller, *Chem. Phys. Lett.* **1993**, 203, 271
[15] S. L. Cumberland, K. M. Hanif, A. Javier, G. A. Khitrov, G. F. Strouse, S. M. Woessner, C. S. Yun, *Chem. Mater.* **2002**, 14, 1576
[16] X. Peng, J. Wickham, A. P. Alivisatos, *J. Am. Chem. Soc.* **1998**, 120, 5343
[17] Y. Ebenstein, T. Mokari, U. Banin *Appl. Phys. Lett.* **2002**, 80, 4033
[18] A. Henglein, A. Fojtik, H. Weller *Ber. Bunsenges. Phys. Chem.* **1987**, 91, 441
[19] A. van Dijken, D. Vanmaekelbergh, A. Meijerink, *Chem. Phys. Lett.* **1997**, 269, 494
[20] W. G. J. H. M. van Sark, P. L. T. M. Frederix, D. J. Van den Heuvel, H. C. Gerritsen, A. A. Bol J. N. J. van Lingen, C. de Donega, A. Meijerink, *J. Phys. Chem. B* **2001**, 105, 8281
[21] N. Herron, J. C. Calabrese, W. E. Farneth, Y. Wang, *Science* **1993**, 259, 1426
[22] A. P. Alivisatos, *Science* **1996**, 271, 933
[23] V. N. Soloviev, A. Eichhöfer, D. Fenske, U. Banin, *J. Am. Chem. Soc.* **2000**, 122, 2673
[24] V. N. Soloviev, A. Eichhöfer, D. Fenske, U. Banin, *J. Am. Chem. Soc.* **2001**, 123, 2354

Chapter 3.

Highly luminescent water-soluble CdTe quantum dots

Abstract

Colloidal CdTe quantum dots prepared in TOP/DDA (tri-octylphosphine/ dodecylamine) are transferred into water by the use of amino-ethanethiol•HCl (AET) or mercaptopropionic acid (MPA). This results in an increase in the photoluminescence quantum efficiency and a longer exciton lifetime. For the first time, water-soluble semiconductor nanocrystals presenting simultaneously high band-edge photoluminescence quantum efficiencies (as high as 60% at room temperature), monoexponential exciton decays and no observable defect-related emission are obtained.

3.1 Introduction

The research on semiconductor nanocrystals (NCs), also known as quantum dots (QDs), has increased rapidly in the last few decades [1]. The size dependence of their electronic and optical properties is one of the unique features of semiconductor NCs [2], turning them into promising materials for a number of optical applications [3,4]. In particular, semiconductor QDs are very attractive as biological labels [5,6], because of their small size, emission tunability, superior photo-stability and longer photoluminescence (PL) decay times in comparison with dyes [5,6]. One of the major challenges is to obtain water-soluble QDs with a high PL quantum efficiency (QE). Three different approaches have been used to obtain water-soluble semiconductor QDs: ligand-exchange [7-11], encapsulation into a water-soluble shell (e.g. silica [12] or phospholipids [13]) and arrested precipitation in water [14-17]. The ligand exchange method has been applied to highly luminescent (QE≥50%) CdSe(ZnS) [6,11,12], CdSe(CdS) [5] or CdTe [10] QDs prepared in hot coordinating solvents, yielding water-soluble NCs with a lower QE (~10-30% [5,10,11]). In the case of CdSe QDs the emission has been observed to be completely quenched after transfer into water, if no shell of a wider band gap material is used [10]. The encapsulation of the QDs into a water-soluble shell typically yields PL QEs of 20-30% [12,13]. Both of the above-mentioned methods for transferring QDs into water involve several steps and thus have the additional disadvantage of being rather complicated and time consuming. Arrested precipitation in water in the presence of stabilizers (e.g. thiols) is a faster and simpler method to synthesize water-soluble QDs and has been applied to several semiconductors potentially relevant to biolabelling (e.g. CdS, CdSe, CdTe [14-18]). For CdS [14,15] and CdSe [16] this yielded NCs with defect-related emission and a low QE. For CdTe QDs [17,18] both excitonic and defect-related emission bands were observed, and, although samples with no observable trap luminescence were also obtained [17], the typical PL QEs were only 3%-10% [17]. After post-preparative treatment QEs up to ~ 40% were obtained [17]. A strategy to prepare highly efficient (QE >50%) water-soluble QDs is thus still lacking.

In this chapter a novel method is reported that yields highly luminescent water-soluble CdTe QDs, either with a positive or negative surface charge, with no observable defect emission and monoexponential exciton decay.

3.2 Experimental

Synthesis of TOP/DDA capped CdTe QDs

First, highly luminescent CdTe QDs (QE up to 45%) were synthesized in a mixture of TOP/DDA (trioctylphosphine/dodecylamine) by a modified version of the method reported by Talapin *et al.* [19,20]. A mixture of DDA (10 g) and TOP (7 mL) was heated to 50ºC. 0.22 g of $Cd(Me)_2$ in 7 mL TOP and 0.16 g of Te powder (grain size <250 μm) were added to the mixture and the temperature was gradually

raised to either 145ºC, 165ºC or 180ºC, and then kept constant for a few hours, yielding green, yellow or orange emitting NCs with QEs of up to 45% at room temperature. The CdTe QDs thus prepared were then transferred into water by exchanging the TOP/DDA molecules for amino-ethanethiol•HCl (AET) or mercaptopropionic acid (MPA), as described below.

Synthesis of water-soluble CdTe QDs

To prepare CdTe NCs with a positively charged capping, 100 µl of the crude solution of CdTe QDs (with a QE of 48%) in the TOP/DDA coordinating mixture were dissolved in 5 mL chloroform. Subsequently a 0.5 M methanolic solution of AET was added until the particles flocculated. Directly after the flocculation, 5 mL ultra pure water (16 MΩ.cm) was added to the suspension, resulting in a two-phase system (water above chloroform). Upon shaking the NCs were transferred into the water phase.

To prepare negatively charged MPA capped water-soluble CdTe NCs a similar procedure was used, but adding a 0.05 M methanolic solution of MPA-KOH (with 20 mol% excess of KOH) instead of an AET solution. The KOH solution was added to the MPA solution in order to deprotonate the carboxylic groups of MPA. A different batch of TOP/DDA capped CdTe NCs, with a lower QE (9%), was used in order to see the effect of QE improvement by the thiol capping for particles with a lower efficiency. The preparation of TOP/DDA capped CdTe NCs and their subsequent transfer into water were performed under argon or nitrogen. No post-preparative steps were required to clean up the CdTe QDs solution, since TOP and DDA stay in the chloroform phase rather than in the water phase.

Apparatus

Emission spectra were measured at room temperature using a SPEX Fluorolog spectrofluorometer, equipped with two monochromators (double-grating, 0.22 m, SPEX 1680, model F2002) and a 450 W Xenon lamp as the excitation source. A Princeton Instruments liquid nitrogen cooled CCD camera was used to detect the luminescence spectra. Absorption spectra were recorded on a Perkin-Elmer Lambda 16 UV/vis spectrometer. Luminescence lifetime measurements were performed with a Pico Quant picosecond laser (λ_{ex} = 406 nm, 2.5 MHz repetition rate) and monochromator (0.1 m focal length, 1350 lines mm^{-1} grating, blazed at 500 nm) in combination with a fast Hamamatsu photomultiplier tube (H5738P-01) for light detection. Luminescence decay curves were obtained by pulse height analysis using a Time Harp 100 computer card. Quantum efficiencies of the samples were determined using commercial laser dyes as standards (Rhodamine B and Coumarine 153, QE= 90%), as described in detail elsewhere [21].

3.3 Results and discussion

Figure 3.1a shows the emission spectra of a sample of TOP/DDA capped CdTe NCs in chloroform (□, optically clear solution), after addition of 140 µl of a 0.5M methanolic solution of AET (▲, turbid suspension), and after transfer to water (●, optically clear solution). The AET capped CdTe QDs in water are charge-stabilized by a positive surface charge, since the dissociated AET molecules have a NH_3^+ group. Figure 3.2a shows the emission spectra of TOP/DDA capped CdTe NCs in chloroform (□, optically clear solution) and after transfer into water (●, optically clear solution) by ligand-exchange with MPA (negatively charged NCs).

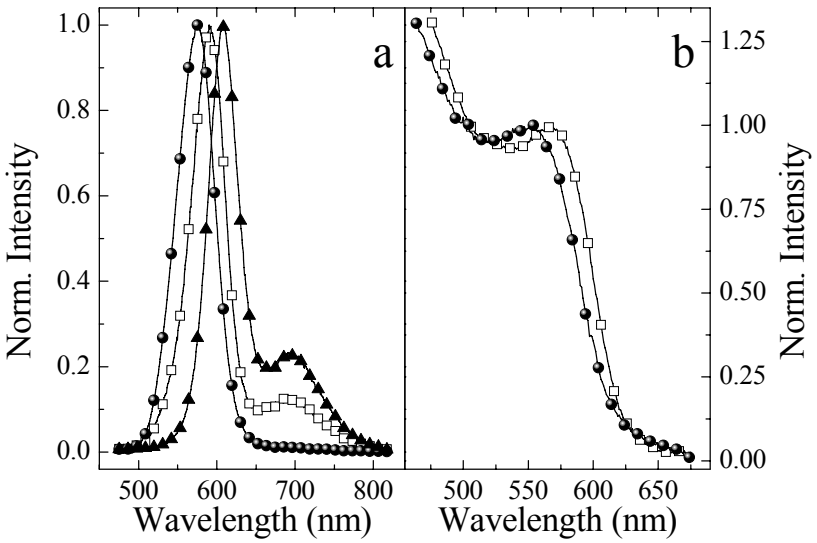

Figure 3.1 a) Emission spectra (λ_{ex}=450 nm) and b) absorption spectra of TOP/DDA capped CdTe NCs in chloroform (□), after addition of 140 µl of 0.5 M AET in methanol (▲) and after transfer into water (●).

The absence of light scattering (optically clear solution) after transfer into water indicates that the clusters of QDs, which were causing the turbidity, fully redisperse in water as individual QDs. The low PL intensity of the flocculated MPA capped CdTe QDs in chloroform prevented the measurement of emission spectra (figure 3.2) or luminescence decay curves (figure 3.5, see below) for this sample.

The CdTe QDs in chloroform present two emission peaks. The narrower peak at higher energy is ascribed to the exciton radiative recombination (band-edge PL) and the broader peak at lower energy is attributed to radiative recombination at defects (trap emission). The relative intensity of the trap emission increases as

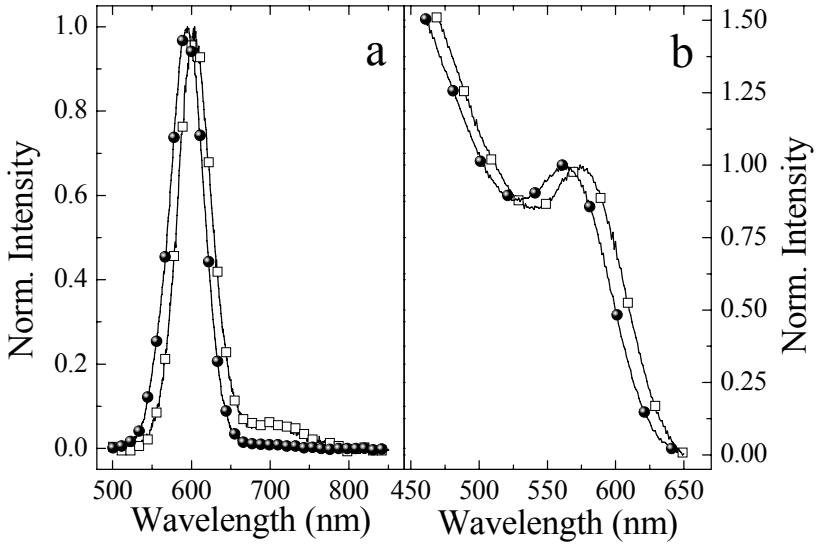

Figure 3.2 a) Emission spectra (λ_{ex}=490 nm) and b) absorption spectra of TOP/DDA capped CdTe NCs in chloroform (□) and after transfer into water with the use of MPA (●).

AET is added to the CdTe QDs in chloroform (figure 3.1a). Moreover, a red shift (61 meV) in the band-edge PL is also observed. The changes observed after the addition of AET can be ascribed to clustering of the QDs due to the modification of the surfactant shell. Since the Cd-thiol bond is much stronger than the Cd-amine bond, AET will replace the TOP/DDA capping molecules of the CdTe QD as soon as it is added. DDA stabilizes the CdTe NCs sterically, while AET capped dots are surface-charged and therefore charge-stabilized in polar media. Since chloroform is not sufficiently polar, the AET capped CdTe QDs will tend to aggregate in chloroform. It must be emphasized that aggregation takes place only when AET or MPA is used. The addition of the same amount of pure methanol does not induce any observable flocculation of the colloidal suspension of DDA-TOP capped CdTe QDs in chloroform.

It has been shown that energy transfer can occur between semiconductor QDs [22,23]. Smaller dots in the excited state can transfer their excitation energy to nearby larger dots in the ground state. The efficiency of this process is strongly dependent on the donor-acceptor distance. In view of the fact that the transitions involved have an electric dipole character, energy transfer via dipole-dipole interaction and a R^{-6} distance dependence is expected [24]. Upon aggregation the average inter-QD distance becomes much shorter. Consequently efficient energy transfer from the smaller NCs (higher energy emission) to the larger NCs in the

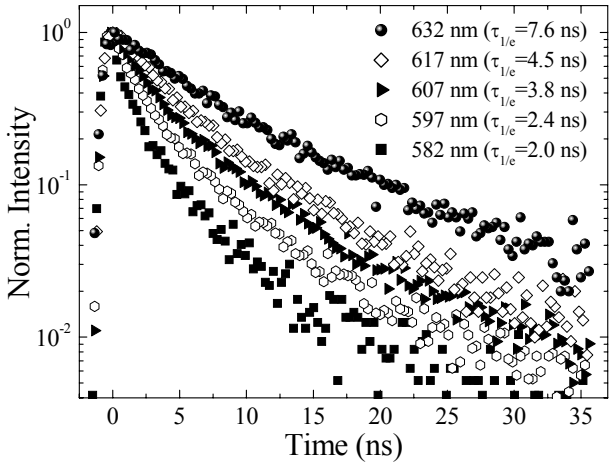

Figure 3.3 Normalized luminescence decay curves taken at different emission wavelengths for TOP/DDA capped CdTe NCs in chloroform, flocculated after addition of 130 µl 0.5 M AET in methanol (λ_{ex}=406 nm). $\tau_{1/e}$ is the time at which the PL intensity has decreased to 1/e of its initial value.

ensemble (lower energy emission) can take place. This explains the red shift observed in the emission spectrum of the CdTe dots after the flocculation induced by the addition of AET.

The increase of the relative intensity of the trap emission in the spectra of the CdTe QDs after the addition of AET can also be explained by the aggregation of the NCs and the accompanying increase of the inter-QD energy transfer rates. Trapping of the exciton at a defect leads to localization of at least one of the charge carriers and to energy relaxation and therefore prevents the QD from transferring its excitation energy to a neighboring QD, since the resonance condition is no longer fulfilled. Therefore, when a smaller QD with exciton emission transfers its excitation energy to a larger QD with a defect-related emission, further energy transfer will be hindered, resulting in a relative increase of the defect related emission accompanied by a decrease in the quantum efficiency.

The energy transfer from the smaller to the larger QDs is also reflected in the lifetimes of the exciton emission. Figure 3.3 shows the luminescence decay curves of a sample of flocculated CdTe NCs in chloroform (with 130 µl AET solution in methanol added) as a function of the emission wavelength (λ_{max}= 607 nm). The time at which the PL intensity has decreased to 1/e of its initial value ($\tau_{1/e}$), is used as a parameter to compare the lifetimes. The lifetime becomes shorter and the exciton decay more nonexponential upon shifting the detection to higher energies

(smaller dots). The shortening of the lifetime for smaller dots is expected because an extra path for depopulating the excited state is created. Since energy transfer happens at a different (faster) rate than the decay of the exciton and a distribution of inter-QD distances is present, a multiexponential decay is expected. By shifting the detection to the lower energy side of the emission peak the PL decay of the larger QDs in the ensemble is probed and the contribution of the energy transfer rates are reduced. This results in both a longer lifetime and a less nonexponential decay for the exciton luminescence.
Upon transferring the CdTe NCs into water using either AET (Figure 3.1a) or MPA (Figure 3.2a) the trap emission is no longer observable indicating that surface defects, rather than lattice defects, must be responsible for trapping the exciton. Furthermore, upon transfer to water a blue shift (of about 120 meV) of the exciton emission is observed with respect to the dots in chloroform. A comparable shift is also observed in the absorption spectra (Fig 3.1b and Figure 3.2b). Talapin *et al.* have also reported a blue shift in the absorption and luminescence spectra when allylamine was added to TOPO capped CdSe NCs [8]. Surface molecule exchange for TOP/DDA capped CdTe QDs with hexanethiol in chloroform (not shown) results in a comparable blue shift in the emission and absorption spectra. This fact indicates that neither the change in solvent nor the charge of the surface molecules can be responsible for the blue shift. Also photo-oxidation, which can result in a blue shift of the exciton emission of the CdTe nanocrystals due to the decrease of the particle size, is not expected since both preparation and surface

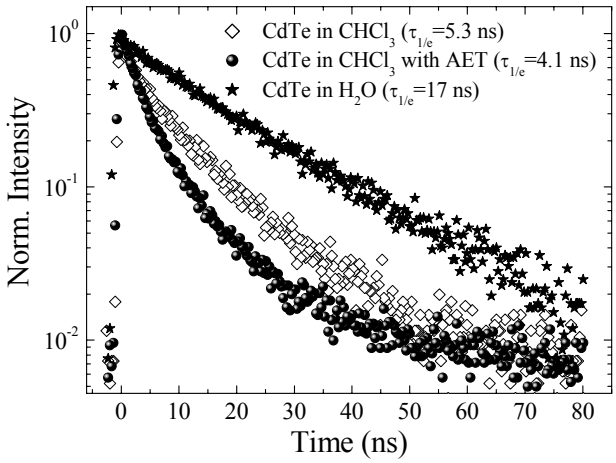

Figure 3.4. Normalized luminescence decay curves (λ_{ex}=406 nm, measured at the maximum of the exciton emission peak) of TOP/DDA capped CdTe QDs in chloroform (●), after addition of 140 µl 0.5 M AET in methanol (◇) and after transfer into water (★).

exchange were performed under inert atmosphere. A possible explanation may be that the stronger bond between the thiol and the Cd atoms at the CdTe NC surface, as compared to the amine-Cd bond, induces a redistribution of electronic density and an increase in confinement energy. Further research is required to clarify the origin of the blue shift.

Figure 3.4 shows the decay curves of the exciton emission of TOP/DDA capped CdTe QDs in chloroform (before and after AET addition) and of the AET-capped CdTe QDs in water. Figure 3.5 shows the decay curves of the exciton emission for TOP/DDA capped CdTe QDs in chloroform and for MPA-capped CdTe QDs in water. After the AET addition the lifetime decreases and becomes dependent on the emission wavelength, as discussed above. In contrast, transfer into water results in a longer lifetime and a monoexponential exciton decay accompanied by an increase in the PL quantum efficiencies, for both AET and MPA capped CdTe NCs. This implies that inter-QD energy transfer is no longer efficient, confirming that the CdTe QDs are fully dispersed in water as individual nanocrystals rather than clusters. Furthermore, the results show that the contribution of nonradiative processes to the exciton decay is significantly reduced after transfer to water. This indicates that the concentration of surface defects is reduced and/or that the exciton trapping at surface defects is less efficient as a consequence of the new capping layer. The AET and MPA capped CdTe particles are stable in water under nitrogen for months, without any indication of aggregation or photodegradation. However, the samples can photodegrade within a day in air.

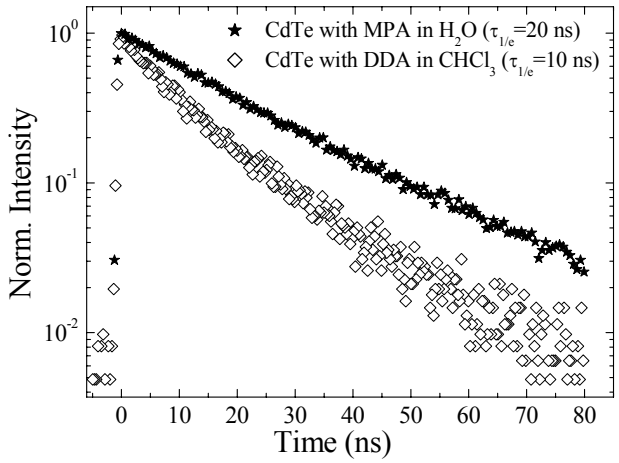

Figure 3.5. Luminescence decay curves (λ_{ex}=406 nm, measured at the maximum of the exciton emission peak) of TOP/DDA capped CdTe NCs in chloroform (◇) and after transfer into water with the use of MPA (★).

The exciton decay behavior observed in the present work for CdTe NCs differs markedly from the results reported by Kapitonov *et al.* [25] for 1-thiolglycerol capped CdTe nanoparticles. The exciton decay curves of the TOP/DDA capped CdTe NCs observed in the present work are slightly nonexponential while Kapitonov *et al.* [25] reported a strongly nonexponential decay, that was analyzed assuming an extremely broad distribution in lifetimes. The difference in the decay kinetics can be explained by the fact that the PL QE of the 1-thiolglycerol capped CdTe nanoparticles investigated by Kapitonov *et al.* is much lower (~3%) [25] than that of the TOP/DDA capped CdTe QDs prepared in this work (up to 45%). The contribution of the non-radiative decay is thus larger for the CdTe QDs capped with 1-thiolglycerol than for those capped with TOP/DDA.

The PL QE increases from 48% for the TOP/DDA capped CdTe NCs in chloroform to 59% for the AET capped nanoparticles in water. The PL QE of the MPA capped nanoparticles increased from 9% to 22%. The relative increase of the PL QE for TOP/DDA capped CdTe samples with a low initial QE is larger than for samples with a high initial QE. The efficiency of the water-soluble QDs is dependent on the quality and PL QE of the original TOP/DDA-capped CdTe QDs, but an increase in QE upon transfer to water is observed for both AET and MPA capped NCs. The increase in PL QE is consistent with the increase of the exciton lifetime discussed above. The fact that even samples with a PL QE of 22% present a monoexponential exciton decay suggests that the emitting NCs in the ensemble have a very high QE. Since the total QE is only 22%, the rest of the ensemble must consist of weakly luminescent (‘dark’) NCs. This is consistent with the observations reported by Ebenstein *et al.* [26] from the investigation of CdSe(ZnS) NCs with an ensemble QE of 48% by correlated atomic force and fluorescence microscopy. The results revealed that the ensembles consisted of highly luminescent (QE close to 100%) and “dark” CdSe(ZnS) QDs.

Talapin *et al.* [10] recently reported the transfer of TOP/DDA capped CdTe NCs into water by using *N*,*N*-dimethyl-2-mercaptoethylammonium chloride. In contrast to the results reported here, the PL QE was observed to decrease from 30-65% to 13-18% after transfer into water [10]. Their method differs from ours in two key aspects. First, we used an aminothiol with a primary amine instead of a tertiary amine. This might affect both the ligand exchange efficiency and the packing density at the NC surface. Second, in the present method the TOP/DDA capped CdTe NCs were not directly transferred into water but were first flocculated with an aminothiol in the absence of water. The aggregated nanoparticles were subsequently transferred to water with the aminothiol ligands already attached to the CdTe NCs surface, thus strongly reducing the interaction between the water molecules and the CdTe surface. The NC surface might be particularly vulnerable during the ligand exchange itself, since some of the coordinating surface sites might be temporarily accessible to water molecules competing with the new ligand. This might, together with a lower crystallinity [17], be the reason for the low initial

QE for CdTe nanocrystals prepared directly in water by arrested precipitation, since in this case a strong competition between the thiol and the water molecules for the CdTe surface sites can be expected. The method reported here is also very attractive for its simplicity compared to other methods for producing water-soluble semiconductor QDs [12,13,27,28]. It also yields water-soluble NCs with photophysical properties superior to those presented by NCs prepared directly in water via arrested precipitation [17,18] (*viz*. a higher QE associated with a monoexponential exciton decay and no defect-related luminescence). QDs with a monoexponential decay offer advantages in studies of QDs in photonic crystals and in energy transfer processes in biological systems where QDs can act as donors. If energy transfer takes place, the decay time of the coupled donor decreases and can be used to accurately determine the energy transfer rate between the QD and an acceptor (*viz.* another QD or dye).

3.4 Conclusions

The capping of TOP/DDA capped CdTe QDs is exchanged by AET and MPA yielding positively and negatively charged QDs respectively that are soluble in water. These water-soluble CdTe QDs show excitonic emission with a monoexponential exciton decay ($\tau_{1/e}$~ 20 ns), a high PL QE (up to 60%).

References

[1] A. P. Alivisatos, *J. Phys. Chem.* **1996**, 100, 13226
[2] L. E. Brus, *J. Chem. Phys.* **1986**, 90, 2555
[3] V. L. Colvin, M. C. Schlamp, A. P. Alivisatos, *Nature* **1994**, 370, 354
[4] V. I. Klimov, A. A. Mikhailovsky, S. Xu, A. Malko, J.A. Hollingsworth, C. A. Leatherdale, H. J. Eisler, M. G. Bawendi, *Science* **2000**, 290, 314
[5] M. Bruchez Jr., M. Moronne, P. Gin, S.A. Weiss, A.P. Alivisatos, *Science* **1998**, 281, 2013
[6] W. C. W. Chan, S. Nie, *Science* **1998**, 281, 2016
[7] C. B. Murray, D. B. Norris, M. G. Bawendi, *J. Am. Chem. Soc.* **1993**, 115, 8706
[8] D. V. Talapin, A. L. Rogach, A. Kornowski, M. Haase, H. Weller, *Nano Lett.* **2001**, 1, 207
[9] L. Qu, Z.A. Peng, X. Peng, *Nano Lett.* **2001**, 1, 333
[10] D.V. Talapin, A.L. Rogach, I. Mekis, S. Haubold, A. Kornowski, M. Haase, H. Weller, *Coll. Surf. A* **2002**, 202, 145
[11] H. Mattoussi, J.M. Mauro, E.R. Goldman, G.P. Anderson, V.C. Sundar, F.V. Mikulec, M.G. Bawendi, *J. Am. Chem. Soc.* **2000**, 122, 12142
[12] D. Gerion, F. Pinaud, S.C. Williams, W.J. Parak, D. Zanchet, S. Weiss, A.P. Alivisatos,. *J. Phys. Chem. B* **2001,** 105, 8861
[13] B. Dubertret, P. Skourides, D.J. Norris, V. Noireaux, A.H. Brivanlou, A. Libchaber, *Science* **2002**, 298, 1759
[14] I. Sondi, O. Siiman, S. Koester, E. Matijevic, *Langmuir* **2000**, 16, 3107
[15] J.O. Winter, T.Y. Liu, B.A. Korgel, C.E. Schmidt, *Adv. Mater.* **2001**, 13, 1673
[16] A.L. Rogach, A. Kornowski, M. Gao, A. Eychmueller, H. Weller, *J Phys. Chem. B* **1999**, 103, 3065
[17] N. Gaponik, D.V. Talapin, A.L. Rogach, K. Hoppe, E.V. Shevchenko, A. Kornowski, A. Eychmueller, H. Weller, *J Phys. Chem. B* **2002**, 106, 7177
[18] S. Wang, N. Mamedova, N.A. Kotov, W. Chen, J. Studer, *Nano Lett.* **2002**, 2, 817
[19] D.V. Talapin, S. Haubold, A.L. Rogach, A. Kornowski, M. Haase H. Weller, *J. Phys. Chem. B* **2001**, 105, 2260
[20] S.F. Wuister, A.F. van Driel A. Meijerink, *Phys. Chem. Chem. Phys.* **2003,** 5, 1253
[21] C. de Mello Donega, S. G. Hickey, S. F. Wuister, D. Vanmaekelbergh, A. Meijerink, *J. Phys. Chem. B* **2003**, 107, 489
[22] C.R. Kagan, C.B. Murray, M. Nirmal, M.G. Bawendi, *Phys. Rev. Lett.* **1996**, 76, 1517
[23] S.A. Crooker, J.A. Hollingsworth, S. Tretiak, V.I. Klimov, *Phys. Rev. Lett.* **2002**, 89, 186802/1

[24] B. Henderson, G.F. Imbusch, *Optical Spectroscopy of Inorganic Solids*, Clarendon Press: Oxford, **1989**, 448
[25] A.M. Kapitonov, A.P. Stupak, S.V. Gaponenko, E.P. Petrov, A.L. Rogach, A. Eychmuëller, *J. Phys. Chem. B* **1999**, 103*,* 10109
[26] Y. Ebenstein, T. Mokari, U. Banin *Appl. Phys. Lett.* **2002**, 80, 4033
[27] A. Schroedter, H. Weller, R. Eritja, W.E. Fordand, J.M Wessels, *Nano Lett* **2002,** 2, 1363
[28] S. Pathak, S.K. Choi, N. Arnheim, M.E. Thompson, *J. Am. Chem. Soc.* **2001,** 123, 4103

Chapter 4.
Influence of thiol capping on the exciton luminescence and decay kinetics of CdTe and CdSe quantum dots

Abstract

Highly luminescent CdSe and CdTe quantum dots (QDs) are prepared in a hot solvent of capping molecules (TOP/TOPO/HDA for CdSe and TOP/DDA for CdTe). The influence of exchange of the capping molecules with different types of thiols (amino ethanethiol, (3-mercaptopropyl) trimethoxysilane, hexanethiol, 2-propenethiol and 4-mercaptophenol) is investigated for both CdSe and CdTe QDs. A remarkable difference is observed: capping exchange with thiol molecules results in an increased luminescence efficiency for CdTe QDs but induces quenching of the excitonic emission of CdSe QDs. The striking difference between the two types of II-VI QDs is explained by the difference in the energy of the to of the valence band. The lower energetic position of the valence band for CdSe results in hole trapping of the photogenerated hole on the thiol molecule thus quenching the luminescence. For CdTe the valence band is situated at higher energies with respect to the redox level of most thiols thus inhibiting hole trapping and maintaining a high luminescence efficiency.

4.1 Introduction

Nanocrystalline semiconductors have attracted great interest over the past decades because their optical and electrical properties are remarkably different from bulk semiconductors [1,2]. Good control over the particle size, together with a high quantum efficiency (QE) can be obtained by several high temperature syntheses in coordinating solvents [3-5]. A high QE, especially in the visible, is crucial for the application of quantum dots (QDs) in biological labels, quantum dot lasers and LEDs [6-9].

Thiols form an important class of capping molecules and thiols with a polar headgroup are used to synthesize water-soluble QDs that can serve as biological labels [10,11]. In the case of CdSe QDs however, the QE strongly decreases after capping exchange with thiols like (3-mercaptopropyl)trimethoxysilane (MPS) [6] and *N*,*N*-dimethyl-2-mercaptoethylammonium chloride [12]. In contrast, we have recently prepared water-soluble, thiol capped CdTe QDs with a high efficiency (up to 60%) and a monoexponential decay [13], demonstrating that the capping exchange with thiols has a beneficial effect on the quantum efficiency (QE) for CdTe QDs. Highly efficient thiol capped CdTe QDs have also been reported by Weller and coworkers [14, 15] in striking contrast with the weakly luminescent thiol capped CdSe QDs reported by the same group [16]. It is the purpose of this chapter to understand the difference between the luminescence behavior of these two related semiconductors upon binding to thiols. Both types of QDs were prepared via well known high temperature synthesis methods. The capping molecules of tri-octylphosphine (TOP) and dodecylamine (DDA) capped CdTe and TOP / tri-octylphosphineoxide (TOPO) / hexadecylamine (HDA) capped CdSe QDs were exchanged with thiols containing different functional groups (both polar and apolar). After capping exchange the CdTe QDs show a strong excitonic emission with a monoexponential decay and a higher QE. However, the same thiols that resulted in an increase of the luminescence lifetime and QE for CdTe QDs induce quenching of the luminescence of CdSe QDs. This remarkable difference between CdSe and CdTe is explained by the difference in the position of the valence band relative to the redox level of the thiol capping molecule.

4.2 Experimental

The syntheses of CdTe and CdSe QDs are performed under a dry argon atmosphere. Capping exchange is performed in a glovebox under nitrogen. All samples are stored in vials under inert atmosphere for luminescence and luminescence life time measurements.

Synthesis of CdTe quantum dots

Highly luminescent CdTe QDs were synthesized in a mixture of TOP/DDA (tri-octylphosphine/dodecylamine) following the method reported by Wuister *et al.* [17,18]. DDA was purified and degassed by heating at 100ºC under vacuum for several hours. In a three necked flask 10 g of dry DDA and 7 mL of TOP were heated to 50ºC. To this solution 0.22 g (1.54 mmol) of $Cd(Me)_2$ in 7 mL of TOP and 0.16 g (1.25 mmol) of Te powder (grain size <250 μm) were added. The reaction mixture was heated to 185ºC for two hours, yielding orange emitting QDs with a QE of 15% at room temperature. The final product (CdTe QDs in TOP/DDA) is a liquid at room temperature.

Synthesis of CdSe quantum dots

Highly luminescent CdSe QDs were prepared by the method reported by de Mello Donegá *et al.* [5]. A total of 20 g of TOPO, 10 g of HDA, and 2 mL of anhydrous triethylorthoformate are transferred into a 250 mL three-necked, round-bottom flask and heated slowly to 330 °C. At this point, the heating mantle was removed and the temperature is allowed to fall. A solution of 10 mL TOP containing 0.79 g Se (as TOP-Se complex) and 0.28 g $Cd(Me)_2$ is quickly injected into the mixture when the temperature reaches 300 °C. After the injection, the temperature was allowed to fall further to 170 °C. The reaction mixture was then stabilized at the desired growth temperature (185°C) for 2 hours yielding orange emitting QDs with a QE of 55% at room temperature.

Capping exchange with thiols can be used to make QDs with surface functionalities that make them soluble in a wide variety of solvents (polar and apolar) and can give the QDs a positive or negative surface charge. The high affinity of the thiol group for the Cd surface atoms with respect to the amines drives the exchange of the amine (HDA or DDA) by the thiol. In the present experiments five different thiols are used with different functional groups: amino ethanethiol, (3-mercaptopropyl)trimethoxysilane, hexanethiol, 2-propenethiol and 4-mercaptophenol.

Capping exchange of CdTe and CdSe QDs with amino-ethanethiol

Either 100 μl of the final product of CdTe QDs in the TOP/DDA coordinating mixture or 0.2 g CdSe in the TOP/TOPO/HDA matrix was dispersed in 5 mL chloroform. Subsequently 100 μl of a 0.5 M methanolic solution of amino-ethanethiol•HCl (AET) was added under nitrogen atmosphere until the particles flocculate. After the flocculation, ultra pure water (16 MΩ.cm) was added to the suspension, resulting in a two-phase system. Upon shaking the QDs were transferred into the water phase, as positively charged particles [13].

Capping exchange of CdTe QDs with (3-mercaptopropyl)trimethoxysilane
For the preparation of CdTe QDs that are soluble into ethanol 20 µl of (3-mercaptopropyl) trimethoxysilane (MPS) was added to 100 µl of the final product of CdTe QDs. After one hour the particles were diluted with 10 mL absolute ethanol and 100 µl NH_3 (aqueous solution, 29%) was added to hydrolyze the methoxy groups of the MPS. The optically clear solution was left overnight under stirring to complete the hydrolyzation of the MPS.

Capping exchange of CdTe QDs with hexanethiol

Hydrophobic thiol capped CdTe QDs were prepared by addition of 50 µl hexanethiol to 100 µl of the crude solution of CdTe QDs in the TOP/DDA coordinating mixture. After one day the particles were soluble in various organic solvents. For the studies reported here, chloroform (5 mL) was used as solvent.

Capping exchange of CdTe and CdSe QDs with allylmercaptan

QDs capped with an alkenylthiol were prepared by addition of 50 µl allylmercaptan (AM, 2-propenethiol) to either 100 µl of the final product of CdTe QDs in the TOP/DDA coordinating mixture or 0.2 g CdSe in the TOP/TOPO/HDA matrix. After one day 5 mL of chloroform was added.

Capping exchange of CdTe and CdSe QDs with 4-mercaptophenol

QDs capped with 4-mercaptophenol were prepared by addition of 20 µg 4-mercaptophenol to either 100 µl of the final product of CdTe QDs in the TOP/DDA coordinating mixture in chloroform or 0.2 g CdSe in the TOP/TOPO/HDA matrix in chloroform.

Apparatus

Emission spectra, recorded with a 0.25 m Acton Research monochromator fitted with a Princeton Instruments liquid nitrogen cooled CCD camera, and luminescence decay curves were measured simultaneously using a Pico Quant laser (λ_{ex} = 406 nm, 2.5 MHz repetition rate, 55 ps pulse width) as excitation source. For luminescence lifetime measurements a monochromator (1350 lines mm^{-1} grating, blazed at 500 nm) in combination with a fast Hamamatsu photomultiplier tube (H5738P-01) was used for light detection. The luminescence decay curves were obtained by time correlated single photon counting (TCSPC) via time-to-amplitude conversion (TAC) with a Time Harp 100 computer card. The ratio of stop to start pulses was kept low (below 0.05) to assure good statistics. All luminescence decay curves were measured at the maximum of the emission peak. The QE of the samples were determined using a SPEX Fluorolog spectrofluorometer, equipped with two monochromators (double-grating, 0.22 m, SPEX 1680, model F2002) and a 450 W Xenon lamp as the excitation source with

commercial laser dyes as standards (Rhodamine B and Coumarine 153, QE= 90%), as described in detail elsewhere [5].

4.3 Results and discussion

4.3.1 Capping exchange with thiols of TOP/DDA capped CdTe quantum dots

CdTe QDs can be grown in a mixture of TOP and DDA, where TOP coordinates to Te and DDA to Cd. Via this method CdTe QDs can be prepared at high temperatures (typically 150-200ºC) yielding QDs with high crystallinity. The size of the particles is determined by the reaction temperature and time. Quantum efficiencies up to 65% have been obtained [17]. Figure 4.1a shows the absorption and emission spectra of CdTe QDs prepared in a mixture of TOP and DDA at a growth temperature of 185ºC. From the position of the first maximum in the absorption spectrum (555 nm) the particle size is estimated to be 3 nm. The emission spectrum shows two bands. The intense band around 590 nm is ascribed to the exciton emission of CdTe QDs. The width of the exciton peak is 50 nm (1450 cm^{-1}) corresponding to a polydispersity of about 15%. The broad band around 675 nm is ascribed to a defect related emission [18]. The decay curve of the exciton emission is depicted in Figure 4.1b. The decay curve is not single exponential. The faster initial decay reflects the emission from QDs with a higher non-radiative decay rate. A distribution in decay times is expected due to a variation in the non-radiative decay rates for different QDs due to a variation in type and number of the quenching centers. This results in a spread of

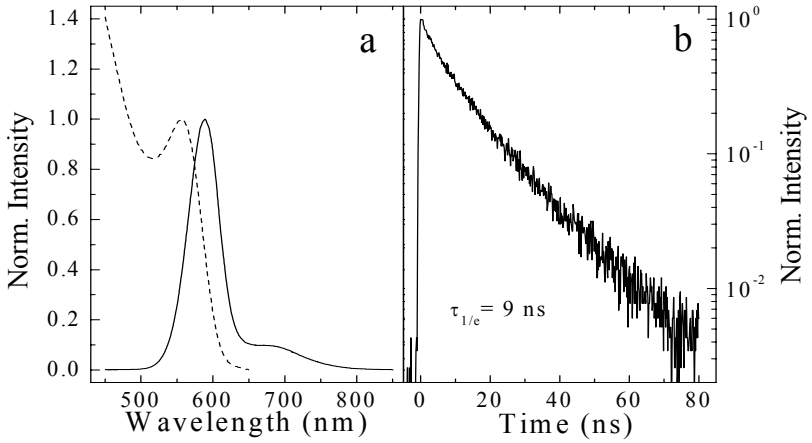

Figure 4.1 (a) Normalized absorption and emission spectra (λ_{ex}= 400 nm) and (b) normalized luminescence decay curves of TOP/DDA capped CdTe QDs.

luminescence lifetimes for different quantum dots. The $\tau_{1/e}$ value (the time at which the intensity has decreased to 1/e of the initial value) is an estimate for the average decay time. For TOP/DDA capped CdTe QDs (with a QE of 15%) the decay time is determined to be about 9 ns, which is comparable to the decay times reported in ref. 15 for CdTe QDs. The features of the TOP/DDA capped CdTe particles as described here (both excitonic and defect related emission and a nonexponential exciton luminescence decay) are characteristic for the TOP/DDA capped CdTe QDs that were used for the surface modification with thiols as will be discussed below.

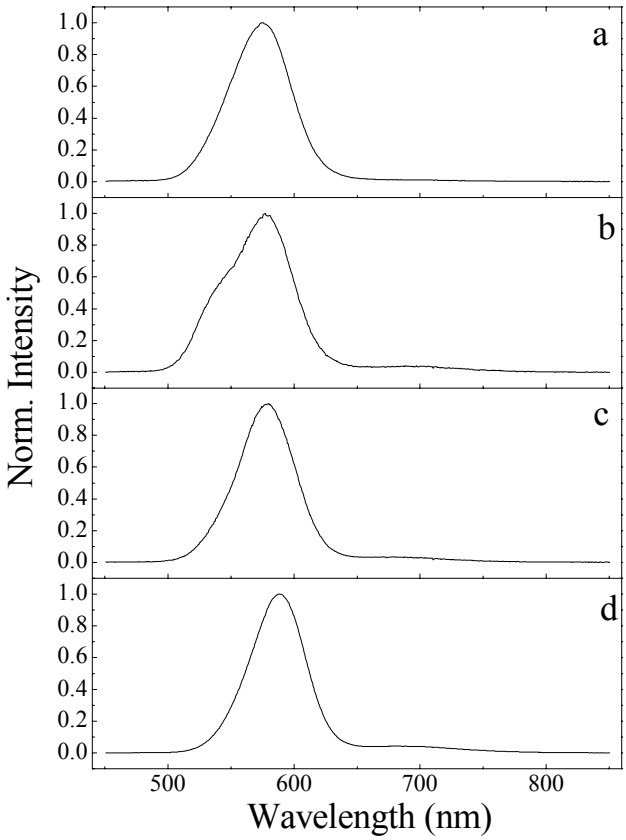

Figure 4.2 Normalized emission spectra (λ_{ex}= 400 nm) for (a) AET (in water), (b) MPS (in ethanol), (c) AM (in chloroform) and (d) HT (in chloroform) capped CdTe QDs.

CdTe QDs grow slowly due to the slow dissolution of Te (as TOP-Te) in the TOP/DDA mixture, thus yielding CdTe with a very high crystallinity [17]. This is one of the factors contributing to the high QE. DDA capping molecules (bound to the Cd sites of the CdTe QD) are not very strongly bound capping molecules compared to for instance thiols [13]. Therefore exchange of the DDA surface molecules for thiols takes place rapidly. This is reflected in the fast precipitation of the QDs after AET addition and the immediate increase in the luminescence intensity and the luminescence decay time upon hexanethiol addition (see below). This makes CdTe QDs, prepared in TOP/DDA, well suited for surface molecule exchange experiments. Four different types of thiols have been used for capping exchange to make the CdTe QDs water-soluble (Amino-ethanethiol•HCl, AET), soluble in ethanol ((3-mercaptopropyl)trimethoxysilane, MPS) and soluble in organic media by capping with saturated (Hexanethiol, HT) and unsaturated (2-propenethiol or allylmercaptan, AM) alkanethiols.

Figure 4.2 shows the emission spectra of CdTe QDs capped with AET (a), MPS (b), AM (c) and HT (d). In all four spectra an intense emission band around 590 nm is observed that is ascribed to the exciton emission. The exciton peak of the MPS capped CdTe QDs has a shoulder at higher energy. The origin of this shoulder is not clear. In some of the spectra (b-d) a defect related emission (around 680 nm) is still observed although the intensity has decreased in comparison to the intensity prior to capping exchange with thiols. This defect related emission originates from surface defects since recapping with AET removes this type emission almost completely [13]. This defect related emission is also observed in efficient samples since the QDs are not all chemically identical. The contribution of the defect related emission to the luminescence signal has reduced from 15% to at most 6% (determined by integrating the peak intensities). The QE increases after capping exchange with thiols and varies between 20 to 40%.

Figure 4.3 shows the luminescence decay curves of CdTe QDs capped with AET (a), MPS (b), AM (c) and HT (d) measured at the maximum of the exciton peak. All luminescence decay curves show a monoexponential behaviour. A monoexponential decay implies that the radiative process is dominant for all *luminescing* QDs. The QE of the luminescing QDs must therefore be close to unity. Since the QE of the ensemble is only 20-40%, about 60-80% of the dots are assumed to be ‘dark’ or weakly luminescent [13, 19, 20]. For AET-, MPS- and HT-capped CdTe QDs the decay time was determined to be 19 ns and for AM capped CdTe QDs a slightly shorter decay time was observed (17 ns). The lifetime is almost independent of the solvent and the functional group of the thiol and is close to the radiative lifetime of CdTe QDs [21]. Clearly, capping exchange with thiol molecules results in a reduced non-radiative decay as is evidenced by the increase of the luminescence QE accompanied by a single exponential decay

of the emission. The higher luminescence efficiency is ascribed to a better surface passivation by the thiol capping molecules. For CdTe QDs with an optimized QE after synthesis in TOP/DDA, capping exchange with AET has been shown to yield water-soluble QDs with a QE as high as 60% [13] which is in agreement with the presently observed beneficial effect of capping exchange with a variety of thiol molecules.

4.3.2 Capping exchange with thiols of TOPO/HDA capped CdSe quantum dots

Monodisperse CdSe QDs with high QE (up to 85%) can be prepared in a mixture of TOP/TOPO-HDA [5]. This yields QDs with an excitonic emission band that can be tuned from green to red, depending on the growth temperature and

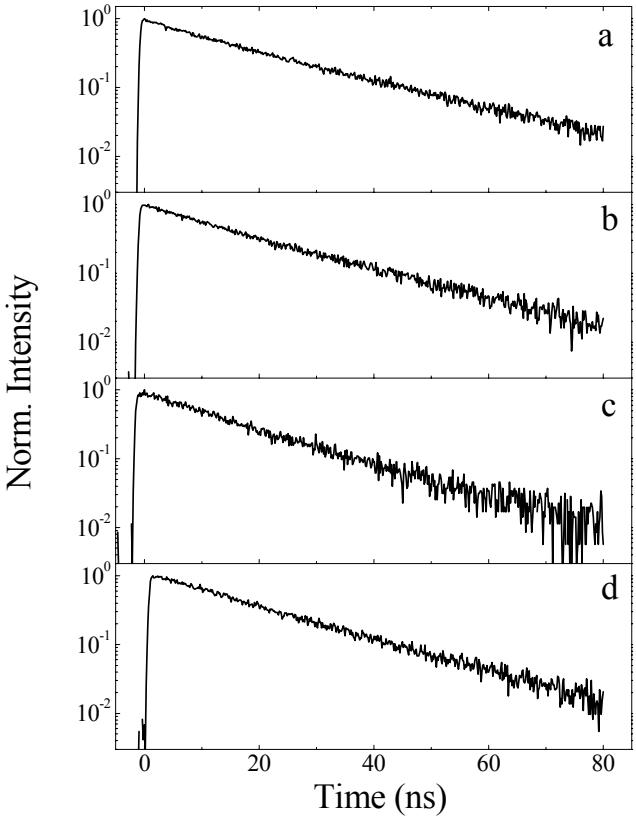

Figure 4.3 Normalized luminescence decay curves (λ_{ex}= 406 nm) of the excitonic emission for (a) AET (in water), (b) MPS (in ethanol), (c) AM (in chloroform) and (d) HT (in chloroform) capped CdTe QDs.

time. Here, CdSe QDs are grown at 185ºC for 2 hours giving orange emitting QDs with a QE of 55%. Figure 4.4a shows the emission spectrum of CdSe QDs (about 3.4 nm in size). The intense peak around 590 nm is assigned to the exciton emission. Due to effective capping of the surface by TOP, TOPO and HDA, no defect related emission is observed. The luminescence decay curve is depicted in Figure 4.4d. A monoexponential decay curve with a $\tau_{1/e}$ value of 28 ns is observed. The value of 28 ns for the luminescence decay time is consistent with the findings of de Mello Donegá *et al*. [5] for a sample with an *ensemble* QE of 85%, indicating that the emission of the CdSe QDs is dominated by radiative recombination.

For capping exchange two different thiols were used: AET and AM. Thiols are capable of partially replacing TOPO at the QD surface [22], while the amine (HDA) can be replaced efficiently by the thiol. AET capped particles were suspended in water and AM capped particles in chloroform. In Figure 4.4 the emission spectra (b, c) and luminescence decay curves (e, f) are depicted for the CdSe QDs after capping exchange with AET and AM. The introduction of thiols to the CdSe surface has a strong effect on the luminescence QE, which drops from

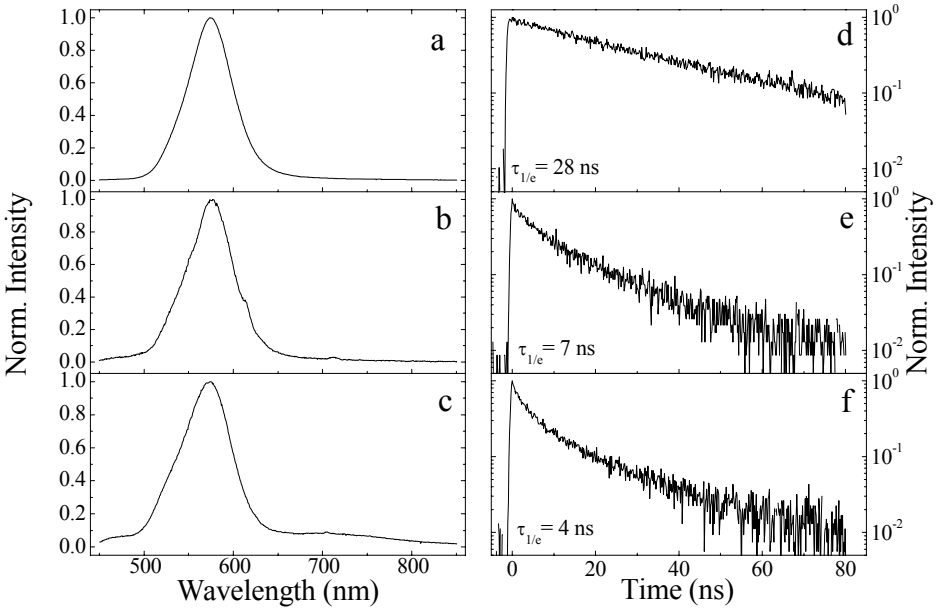

Figure 4.4 Normalized emission spectra (left side, λ_{ex}= 400 nm) and normalized luminescence decay curves (right side, λ_{ex}= 406 nm) of the exciton emission of CdSe QDs capped with TOP/TOPO-HDA in chloroform (a, d), AM in chloroform (b, e) and AET in water (c, f).

55% to a few percent. Still, a weak excitonic emission is observed for the thiol capped samples and in the case of AET capped CdSe QDs in water also a defect related emission is observed around 700 nm. The luminescence decay curves (measured at the maximum of the exciton emission) of the two thiol capped samples show a fast and strongly nonexponential decay. The decay time ($\tau_{1/e}$ value) of the AM capped CdSe QDs in chloroform is 7 ns and of AET capped CdSe QDs in water 4 ns. The fast initial decrease in the luminescence intensity also shows that fast non-radiative decay processes are induced by the thiol capping molecules.

4.3.3 Hole trapping on thiols in CdSe and CdTe quantum dots

Capping exchange with thiols affects the luminescence properties of CdSe QDs in a remarkably different way to that observed for CdTe QDs. Thiols that yield a high QE and a monoexponential decay for CdTe QDs, are observed to almost completely quench the luminescence of CdSe (see above and also [12-16]). This difference is particularly remarkable considering that the two II-VI semiconductors are chemically similar and have comparable band gap energies. An explanation for the strong difference between thiol capped CdSe and CdTe QDs can be found in the energetic position of the top of the valence band. Figure 4.5 depicts the absolute band edge positions of bulk CdSe and CdTe in aqueous solution at pH 1 [23].

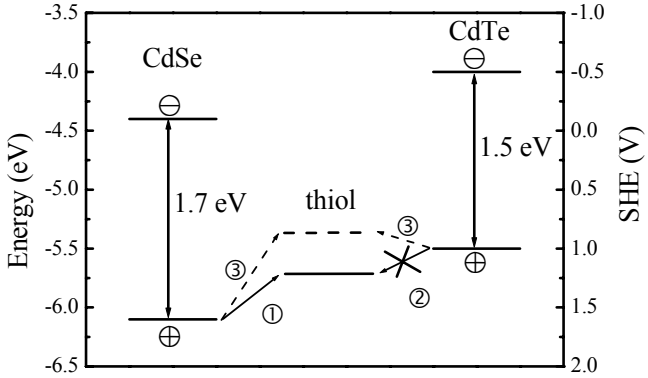

Figure 4.5 Positions of bulk CdSe and bulk CdTe band edges shown both on a vacuum scale and with respect to a standard hydrogen electrode reference. The standard potential expected for a thiol that does not quench the CdTe exciton luminescence is given by a solid line between CdSe and CdTe. Hole trapping can occur from CdSe (process ①) but not from CdTe (process ②). The dashed line indicates the assumed position for the standard potential of a thiol that quenches the luminescence of both CdSe and CdTe (process ③).

Hole trapping from the semiconductor nanocrystal on a thiol is energetically favorable only if the thiol redox energy level is situated at higher energies than the top of the valence band. CdSe (and also CdS) can very efficiently convert thiols into disulfides via a photocatalytic reaction [24]. The first step in this process involves trapping of a photogenerated hole on a thiol molecule that is strongly adsorbed at the CdSe surface. Hole trapping on a thiol molecule results in the creation of a thyil radical and two thyil radicals can be converted into a disulfide. This process is very efficient and observed not only for CdS and CdSe electrodes [24] but also for CdS and CdSe QDs [25, 26]. Hole trapping is inhibited by an energy barrier when the top of the semiconductor valence band is above the thiol redox energy level.

The energy difference between the tops of the valence bands of bulk CdSe and CdTe is more than 0.5 eV. If the redox energy level of a thiol is situated above the top of the valence band of CdSe but below the top of the valence band of CdTe an interesting situation arises (Figure 4.5). Hole trapping is energetically favorable for thiols attached to CdSe (process ①) but not for CdTe (process ②). For radiative recombination both the hole and the electron are needed. If the hole is trapped on a thiol molecule, radiative recombination of the exciton is not possible, resulting in a strongly reduced QE. If the thiol redox energy level is situated between the valence band top of bulk CdSe and CdTe, its different influence on CdSe and CdTe QDs can be explained, since this situation would induce quenching of the luminescence for CdSe QDs while increasing the QE for CdTe QDs through a better surface passivation. The observation of a weak excitonic emission for CdSe QDs capped with AET and AM is explained by a competition between hole trapping and radiative recombination. The rate of radiative exciton recombination is constant while the hole trapping rate depends on the redox energy level of the thiol and therefore on the nature of the thiol. If the redox energy level of the thiol is higher in energy, the trapping will be energetically more favorable. This will increase the trapping rate and therefore decrease the quantum efficiency of the CdSe QDs. The strong initial decrease in intensity that is observed in the luminescence decay curves of the AET and AM capped CdSe QDs also illustrates that hole trapping is a fast process compared to radiative recombination.

For the CdTe QDs capped with e.g. AET or AM the exciton emission is dominated by the radiative process and is characterized by a monoexponential luminescence decay curve with a relatively long decay time ($\tau_{1/e} \sim 19$ ns). This indicates that the hole trapping rate is low. Hole trapping is negligible if the redox energy level of the thiol is situated below the top of the valence band of CdTe (process ② in Figure 4.5). The difference in energy between the top of the valence band of the two semiconductors can thus explain the large difference between the luminescence behavior of thiol capped CdSe and CdTe QDs.

An interesting question arises if it is generally true that thiol capped CdTe QDs show a high QE and a monoexponential luminescence decay, i.e. if hole trapping from the CdTe valence band to a thiol is always inhibited. The thiol 4-mercaptophenol is known to very efficiently quench the luminescence of CdS [27]. Applying this thiol to CdSe QDs resulted in complete quenching of the luminescence (not shown). This indicates that the trapping rate of the photogenerated hole is high when 4-mercaptophenol is attached to the surface of a CdSe QD. Contrary to what would be expected based on the discussion above, capping of CdTe QDs with 4-mercaptophenol decreases the luminescence intensity and leads to a strongly non-exponential luminescence decay (Figure 4.6). In contrast to the behavior observed for other thiols, the luminescence decay curve of 4-mercaptophenol capped CdTe QDs is dominated by fast non-radiative processes reflected in the fast initial intensity decrease and the low QE. This observation shows that hole trapping on the 4-mercaptophenol molecules can be efficient for both CdSe and CdTe QDs (Figure 4.5, process ③) implying that the redox energy level of this thiol lies at higher energies than the top of the valence band for both CdSe and CdTe QDs. A reason for the higher redox energy level of 4-mercaptophenol compared to the other thiols investigated here may be the stabilization of the hole by the phenyl group of the 4-mercaptophenol molecule. This example clearly shows that the redox energy level of the type of thiol used determines the exciton decay kinetics in CdSe and CdTe QDs.

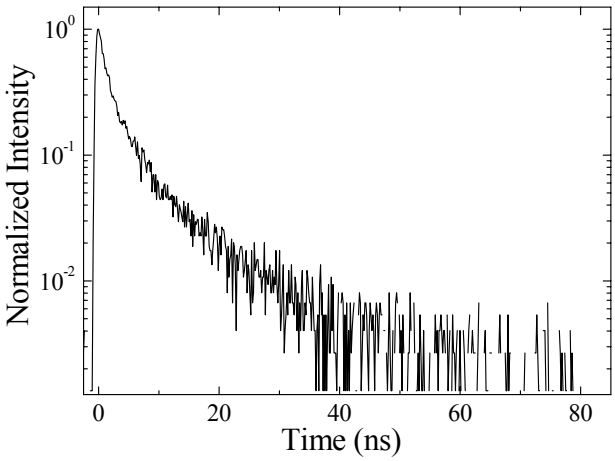

Figure 4.6 Luminescence decay curves (λ_{ex}= 406 nm) of the exciton emission of 4-mercaptophenol capped CdTe QDs.

4.4 Conclusions

The capping of highly efficient TOP/DDA capped CdTe QDs and TOP-TOPO/HDA capped CdSe QDs has been exchanged with thiols containing different functional groups. For CdTe QDs capping exchange with amino ethanethiol (AET), (3-mercaptopropyl)trimethoxysilane (MPS), hexanethiol (HT) and allylmercaptan (AM) yields QDs with higher QEs and a monoexponential decay for the exciton emission. For CdSe QDs capping exchange with AET and AM results in a strong decrease in QE and a faster and nonexponential luminescence decay. The quenching of the exciton emission of CdSe QDs is explained by trapping of the photogenerated hole on the thiol capping molecules. The remarkable difference between thiol capped CdTe and CdSe QDs is explained by the difference in position of the top of the valence band with respect to the redox energy level of the thiol molecule. Capping exchange with 4-mercaptophenol results in quenching of the exciton emission for both CdSe and CdTe QDs and is explained by the high redox energy level of this thiol with respect to other thiols investigated in this work.

References:

[1] A.P. Alivisatos, *J. Chem. Phys.* **1996**, 100, 13226
[2] L.E. Brus, *J. Chem. Phys.* **1986**, 90, 2555
[3] Z.A. Peng, X. Peng, *J. Am. Chem. Soc.* **2002**, 124, 3343
[4] D.V. Talapin, A.L. Rogach, E.V. Shevchenko, A. Kornowski, M. Haase, H. Weller, *J. Am. Chem. Soc.* **2002**, 124, 5782
[5] C. de Mello Donega, S.G. Hickey, S.F. Wuister, D. Vanmaekelbergh, A. Meijerink, *J. Phys. Chem. B* **2003**, 107, 489
[6] M. Bruchez Jr., M. Moronne, P. Gin, S.A. Weiss, A.P. Alivisatos, *Science* **1998**, 281, 2013
[7] B. Dubertret, P. Skourides, D.J. Norris, V. Noireaux, A.H. Brivanlou, A. Libchaber, *Science* **2002**, 298, 1759
[8] V.I. Klimov, A.A. Mikhailovsky, S. Xu, A. Malko, J.A. Hollingsworth, C. A. Leatherdale, H.J. Eisler, M.G. Bawendi, *Science* **2000**, 290, 314
[9] S. Coe, W.K. Woo, M.G. Bawendi, V. Bulovic, *Nature* **2002**, 420*,* 800
[10] H. Mattoussi, J.M. Mauro, E.R. Goldman, G.P. Anderson, V.C. Sundar, F.V. Mikulec, M.G. Bawendi, J. Am. Chem. Soc. 2000, 122, 12142
[11] W. J. Parak, R. Boudreau, M. Le Gros, D. Gerion, D. Zanchet, C. M. Micheel, S. C. Williams, A.P. Alivisatos, C. Larabell, *Adv. Mater.* **2002**, 14, 882
[12] D.V. Talapin, A. L. Rogach, I. Mekis, S. Haubold, A. Kornowski, M. Haase, H. Weller, *Coll. Surf. A* **2002**, 202, 145
[13] S. F. Wuister, I. Swart, F. van Driel, S. G. Hickey, C. de Mello Donegá, *Nano Lett.* **2003**, 3, 503
[14] A.L. Rogach, A. Kornowski, M. Gao, A. Eychmueller, H. Weller, *J Phys. Chem. B* **1999**, 103, 3065
[15] N. Gaponik, D.V. Talapin, A.L. Rogach, K. Hoppe, E.V. Shevchenko, A. Kornowski, A. Eychmueller, H. Weller, *J Phys. Chem. B* **2002**, 106, 7177
[16] M. Gao, S. Kirstein, H. Möhwald, A. L. Rogach, A. Kornowski, A. Eychmüller, H. Weller, *J. Phys. Chem. B* **1998,** 102*,* 8360
[17] D.V. Talapin, S. Haubold, A.L. Rogach, A. Kornowski, M. Haase H. Weller, *J. Phys. Chem. B* **2001**, 105, 2260
[18] S.F. Wuister, A.F. van Driel A. Meijerink, *Phys. Chem. Chem. Phys.* **2003,** 5, 1253
[19] Y. Ebenstein, T. Mokari, U. Banin, *Appl. Phys. Lett.* **2002**, 80, 4033
[20] B. R. Fisher, H. J. Eisler, N. E. Stott, M. G. Bawendi, *J. Phys. Chem. B.* **2004**, 108, 143
[21] S. F. Wuister, C. de Mello Donegá, A. Meijerink, *J. Chem. Phys.* **2004**, 121, 4310
[22] M. Kuno, J. K. Lee, B. O. Dabbousi, F. V. Mikulec, M. G. Bawendi, *J. Chem. Phys.* **1997,** 106, 9869

[23] A. Hagfeldt, M. Graetzel, *Chem. Rev.* **1995**, 95, 49
[24] M. J. Natan, J. W. Thackeray, M. S. Wrighton, *J. Phys. Chem.* **1986,** 90, 4089
[25] C. -H Fischer, A. Henglein, *J. Phys. Chem.* **1989**, 93, 5578
[26] J. Aldanan, Y. A. Wang, X. Peng, *J. Am. Chem. Soc.* **2001**, 123, 8844
[27] M. Tata, S. Banerjee, V. T. John, Y. Waguespack, G. L. McPherson, *Coll. Surf. A* **1997**, 127, 39

Chapter 5.

Local-field effects on the spontaneous emission rate of CdTe and CdSe quantum dots in dielectric media

Abstract

The refractive index dependence of the spontaneous emission rate is determined using organically capped CdSe and CdTe quantum dots as probes. The radiative lifetime of the exciton emission is measured in a variety of apolar solvents with refractive indices n between 1.37 and 1.50. It is demonstrated that quantum dots provide a model system for testing theories on the influence of local field effects on the spontaneous emission rate. The experimentally observed influence of n on the radiative lifetime is smaller than predicted by well-known models for local field corrections but is in good agreement with a recently developed fully microscopic model for the local-field enhancement of the spontaneous emission rate.

5.1 Introduction

The influence of local-field effects on the spontaneous emission rate of a two level system has been the topic of both theoretical and experimental work since long [1-4]. In the absence of local field effects the radiative lifetime of a two level system decreases with increasing refractive index *n* of the surrounding medium as [5]

$$\tau_{rad}(n) = \frac{\tau_{vac}}{n} \tag{5.1}$$

where τ_{rad} (n) is the radiative lifetime of the emission in a medium with refractive index n and τ_{vac} is the radiative lifetime in vacuum. This simple relation between the radiative lifetime and the refractive index follows from solving the macroscopic Maxwell equations assuming a homogeneous dielectric constant over space. In reality, the two level system interacts with all surrounding microscopic dipoles of the medium in which it is embedded. This complicates the analysis. To incorporate the influence of local interactions, local field corrections have to be introduced [6]. Already since the 1940's local-field effects were included in a quantitative description of the absorption and emission of light [1-3]. In the past 15 years theoretical work has resulted in the development of models in which the two-level system is placed in a cavity to account for microscopic interactions with local dipoles. The exact dependence of the radiative lifetime $\tau_{rad}(n)$ on the refractive index n is very sensitive to the choice of the cavity. Two limiting cases have been analyzed in detail: in the empty-cavity model the oscillator is situated in an empty spherical cavity and the dependence of the radiative lifetime on the refractive index follows [7]

$$\tau_{rad}(n) = \left(\frac{3n^2}{2n^2+1}\right)^{-2} \frac{\tau_{vac}}{n} \tag{5.2}$$

In the other limit, the full- or virtual-cavity model, the two-level system is placed in a cavity with the same refractive index as the surrounding medium but the dipoles inside the cavity do not contribute to the local electric field. In this situation the radiative lifetime is described by [8,9]

$$\tau_{rad}(n) = \left(\frac{n^2+2}{3}\right)^{-2} \frac{\tau_{vac}}{n} \tag{5.3}$$

The two models described above still rely on a macroscopic description of the dielectric. More recently, a fully microscopic model for local-field effects was presented using a quantum-electrodynamical, many-body derivation of Langevin-Bloch operator equations for two-level atoms embedded in a dielectric host. In the limit of no interaction between the two-level systems (a single system in a dielectric host) the radiative lifetime shows a dependence on the refractive index of

the (non-absorbing) dielectric host that is much weaker than predicted with the empty-cavity and full-cavity models and is given by [10]

$$\tau_{rad}(n) = (\frac{n^2+2}{3})^{-1}\tau_{vac} \quad (5.4)$$

In order to test the validity of the different models, experimental work has been done in which the luminescence lifetime is measured as a function of the refractive index of the surrounding medium. In contrast to the large number of papers discussing theoretical models for local field effects, the number of experimental studies to verify the theoretical work is very limited. The reason is that these experiments are not as trivial as they may seem [11]. One of the complications is that the surrounding medium may influence both radiative and non-radiative decay rates through mechanisms other than a variation in the refractive index. This complicates a quantitative analysis of the influence of local-field effects on τ_{rad} and only a few experimental studies have been reported in which the theoretical models could be compared with experiment. Most insightful experiments have been done using Eu^{3+}. The intraconfigurational $4f^6$ transitions of the Eu^{3+} ion are characterized by a long luminescence lifetime. Rikken and Kessner studied the luminescence lifetime of the Eu^{3+} emission for complexes (Eu^{3+}-hfa-topo, Eu^{3+}-dpa) dissolved in hydro- and fluorocarbons with different refractive indices [12]. They found that for the electric dipole transition the dependence of τ_{rad} on n is best described by the empty-cavity model [Eq. (2)]. Schuurmans et al. did experiments on a Eu^{3+}-fod complex in supercritical CO_2 [13]. The refractive index of the surrounding medium was varied between 1 and 1.3 by changing the pressure between 1 and 1000 bar. These experiments confirmed the applicability of the empty-cavity model for Eu^{3+} complexes. Luminescence lifetime measurements by Meltzer et al. for Eu^{3+} in Y_2O_3 nanocrystals embedded in media of different refractive index indicated that the full- or virtual-cavity model [Eq.(3)] gives a better agreement with the experimentally observed relation between n and τ_{rad} [14].
In all experiments involving Eu^{3+} a complicating factor is the sensitivity of radiative and non-radiative relaxation rates to small changes in the immediate surroundings of the Eu^{3+} ion (in spite of the shielding of the $4f^6$ shell of Eu^{3+} by the outer $5s^2$ and $5p^6$ shells). Subtle changes in the local symmetry strongly affect the radiative decay rate of the forced electric dipole transitions within the $4f^6$ configuration, as is for example clear from the strong variation of the lifetime of the Eu^{3+} emission within the inhomogeneously broadened emission line for Eu^{3+} in the yttrium oxide nanocrystals [14]. In addition, the local dielectric surroundings will be different for Eu^{3+} located in the middle of the nanoparticles in comparison to Eu^{3+} ions close to the surface. As a result, the local field effects are expected to vary between different ions in the system. This complicates the analysis of their

influence on the radiative lifetime. For the Eu^{3+} complexes corrections need to be made for non-radiative (multi-phonon) relaxation to derive the radiative decay rate from luminescence lifetime measurements. The non-radiative relaxation rates may vary as the solvent is changed [13]. For the Eu^{3+} complexes in supercritical CO_2 the change in pressure could affect the distance between the central Eu^{3+} ion and the coordinating atoms from the ligand molecules or the complex geometry. Even a small change in distance can influence the radiative decay rates. In spite of the complications arising from the sensitivity of the intraconfigurational $4f^6$ transition rates to the local surroundings, the experiments on Eu^{3+} to establish the relation between τ_{rad} and n have up until now been the most insightful ones demonstrating the influence of n on τ_{rad}.
In this chapter nanocrystalline organically capped CdSe and CdTe quantum dots (QDs) are used to probe the influence of the refractive index on the radiative decay rate. Due to quantum confinement effects, discrete levels arise at the band edges and as a result semiconductor QDs are also known as artificial atoms [15-17]. By placing these artificial atoms in media with different refractive indices, an ideal test case is obtained to determine the relation between τ_{rad} and n if the QD luminescence is dominated by radiative decay (i.e. $\tau_{exp}= \tau_{rad}$). An important advantage of QDs over Eu^{3+} is the insensitivity of the radiative decay rate of the exciton emission to changes in the local symmetry since the exciton emission of QDs is a fully allowed electric dipole transition. It is the aim of the present work to measure the influence of refractive index of the medium surrounding QDs on the radiative decay rate of the excitonic emission and to compare the results with theoretical models described above.

5.2 Experimental

Choice of the system

The synthesis of efficiently luminescing quantum dots is crucial for the experiment. Highly efficient II-VI semiconductor nanocrystals like CdSe and CdTe can be grown in a hot solvent of organic molecules that coordinate to ions at the surface of the growing nanocrystal [18]. Typical coordinating molecules are TOPO (tri-octylphosphineoxide), HDA (hexadecylamine), DDA (dodecylamine) and TOP (tri-octylphosphine). After synthesis, the surface of the semiconductor nanocrystals is well-passivated with these molecules and non-radiative recombination at surface sites is suppressed. Various groups have shown that it is possible to grow CdSe and CdTe QDs which are characterized by a high luminescence quantum yield (up to 80%) and a single exponential (radiative) decay [21-24]. It is for these QDs that the influence of the refractive index on the radiative decay rate can be studied. To this effect, the highly luminescent QDs are dissolved in various organic solvents. The refractive index of the surrounding solvent can be changed without influencing the capping of the QD. Caution should be taken to only use ‘inert’ organic solvents i.e.

solvents that cannot bind to surface atoms of the semiconductor core and replace the capping molecules. High refractive index organic solvents like pyridine and carbon disulfide are not useful since capping exchange with these solvent molecules can take place. The solvents used in this experiment are commonly used for the dispersion of QDs and no capping exchange with the solvent molecules is expected.

Synthesis of highly luminescent QDs

Two types of semiconductor QDs have been prepared to investigate refractive index dependence of the spontaneous emission rate. All syntheses were carried out in a glovebox under Argon employing standard oxygen and moisture free conditions (less than 2 ppm O_2 and H_2O).

CdTe QDs are synthesized at 165ºC in a mixture of TOP/DDA by a modified version of the method reported by Talapin *et al.* [19,20]. In a three necked flask 10 g of dry DDA and 7 mL of TOP were heated to 50^{o}C. To this solution 0.22 g (1.54 mmol) $Cd(Me)_2$ in 7 mL of TOP and 0.16 g (1.25 mmol) Te powder were added. The reaction mixture was heated to 165ºC for 3 hours. The final product is a viscous liquid.

To obtain a stable colloidal solution of the CdTe QDs in a variety of organic solvents, the TOP/DDA capping is exchanged by a hexanethiol capping. Capping exchange is achieved by adding 100 µl of hexanethiol to 50 µl of the crude solution of the CdTe QDs in TOP/DDA. After one day 5 ml of an organic solvent (hexane, octane, cyclohexane, toluene or chloroform) is added and a stable and transparent colloidal suspension of QDs is obtained for all solvents. The quantum efficiency of the CdTe suspensions is around 40%.

CdSe QDs are synthesized in a mixture of TOP/TOPO/HDA [19,21]. A total of 20 g of TOPO, 10 g of HDA, and 2 mL of triethylorthoformate were placed into a 250 mL three necked, round-bottom flask and heated slowly to 330 °C. A portion of 0.79 g (10 mmol) of Se was dissolved at room temperature in 10 mL TOP. To this solution 0.28 g (2 mmol) of $Cd(Me)_2$ was added. The temperature of the TOPO/HDA mixture was allowed to fall (the heating mantle was removed) to 300 °C at which point the TOP/Se/$Cd(Me)_2$ solution was quickly injected into the mixture using a syringe. After the injection, the temperature was allowed to drop further to 180°C. The reaction temperature was then stabilized at a growth temperature of 240 °C. CdSe QDs were dispersed in the same five organic solvents as used for CdTe for luminescence and lifetime measurements. The quantum efficiency of the CdSe QDs prepared in this way for the present experiments is around 55%.

Apparatus

Luminescence spectra and luminescence lifetimes were measured using a Pico Quant diode laser (λ_{ex}=406 nm, 2.5 MHz repetition rate, 55 ps pulse width) as an

excitation source. Emission spectra were recorded with a 0.25 m Acton Research monochromator fitted with a Princeton Instruments liquid nitrogen cooled CCD camera. To determine the lifetime of the luminescence a monochromator (0.1 m focal length, 1350 lines mm^{-1} grating, blazed at 500 nm) was used for wavelength selection and a fast Hamamatsu H5738P-01 photomultiplier tube (PMT) was used for light detection. With the monochromator an emission band around the emission maximum was selected for recording the luminescence decay curves. Since the luminescence lifetime is expected to depend on the particle size (and thus emission wavelength) the decay curves were recorded at the same emission wavelength for the QDs in the different solvents. The spectral width of the detection is however not expected to give a large variation in life times as it was recently demonstrated the there is only a weak dependence of the luminescence life time of the QD emission on the particle size [25]. Luminescence decay curves were obtained using time-correlated single-photon counting via time-to-amplitude conversion (TAC) with a Time Harp 100 computer card. The laser power used for excitation was low (less than 1 mW/cm^2) for two reasons: First, the ratio of stop to start pulses needs to be small (below 0.05) to assure good statistics. In addition, by using a low excitation power the formation of bi-excitons (with a different decay rate) is prevented. Measurements were done on very dilute solutions (OD below 0.1 in the visible) to prevent an influence of reabsorption. The time resolution of the measurements is better than 0.5 ns and is mainly limited by the spread in transit times for the PMT. Luminescence quantum efficiencies (QE) were determined using a SPEX Fluorolog spectrofluorometer and Rhodamine B (QE=90%) as a standard. Further experimental details can be found in Refs. 20 and 21.

5.3 Results

5.3.1 CdTe QDs

In Figure 5.1 room temperature emission spectra are shown of CdTe quantum dots after capping exchange with hexanethiol and transfer into hexane (Figure 5.1a) and toluene (Figure 5.1c). The quantum dots show a bright yellow emission with a maximum at 570 nm. The position of the emission maximum is the same in all five solvents.

From the position of the exciton emission band the particle diameter can be estimated to be 3.0 nm [19,20]. On the right hand side of Figure 5.1 luminescence decay curves are depicted for the emission of CdTe dots in two of the solvents (hexane and toluene). The luminescence lifetime is around 18 ns in both cases. This is in agreement with the radiative decay time reported for CdTe exciton emission and indicates that the experimentally observed luminescence lifetime is indeed determined by radiative decay [20,24]. Also the single exponential character of the decay curves provides strong evidence that the luminescence is dominated by radiative decay. Exciton emission is characterized by a weak electron-phonon

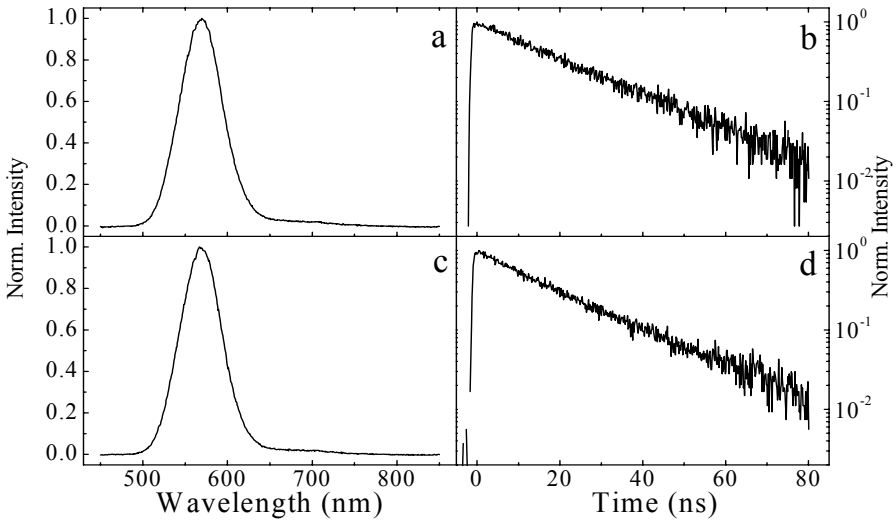

Figure 5.1 Emission spectra of hexanethiol-capped CdTe quantum dots dissolved in hexane (a) and toluene (c) and luminescence decay curves of the exciton emission at 570 nm for the same solutions of QDs in hexane (b) and toluene (d). The measurements are done for 406 nm excitation at 295 K.

coupling (also in QDs [23]). As a result, non-radiative relaxation of the exciton by phonon relaxation processes can be neglected. The lifetime of the QD exciton emission is thus dominated by radiative decay unless energy transfer occurs to quenching centers in or close to the QD. In case of quenching by energy transfer, non-radiative decay rates will vary between QDs (due to differences in quenching rates between QDs) and non-exponential decay curves are expected. Indeed, for CdSe and CdTe QDs prepared via a different synthesis method non-exponential decay curves are observed and the faster initial decay is attributed to quenching centers [21,24-26]. The present observation of a purely exponential luminescence decay in Figure 5.1 shows that the emission from the CdTe QDs is dominated by radiative decay. Further support for the fact that the presently observed decay curves reflect only radiative decay is obtained by measuring the wavelength dependence of the luminescence lifetime. The luminescence lifetime decreases for shorter wavelength according to the well-known λ^3 dependence, which is valid for radiative decay only [29,30].

In spite of the strong evidence showing that the luminescence decay curves are determined by radiative decay only, the luminescence quantum efficiency of the QD solutions is around 40% and not 100%. The lower quantum yield indicates that there is partial quenching of the luminescence. This is ascribed to the presence of

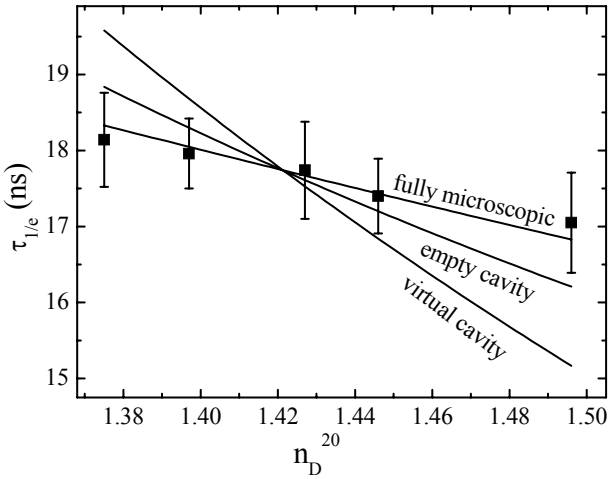

Figure 5.2 Radiative lifetime of the exciton emission at 570 nm for hexanethiol-capped CdTe QDs as a function of the solvent refractive index for QDs is apolar solvents. The filled squares represent the experimental results and drawn lines are fits to the theoretical models described by Eq. (5.2) (empty cavity), Eq. (5.3) (virtual cavity) and Eq. (5.4) (fully microscopic).

two types of CdTe quantum dots: bright dots, showing radiative exciton recombination and 'dark' (i.e. non-luminescent) dots for which the luminescence is almost completely quenched. The luminescence decay curves for the emission from the ensemble of QDs are dominated by the radiative decay time of the bright QDs that have quantum efficiencies close to 100% and reflect the radiative exciton lifetime. Convincing evidence for the co-existence of bright dots with a purely radiative decay and dark dots in the same ensemble is presented in Refs. 26, 28. Luminescence measurements on single QDs show the presence of bright QDs with quantum efficiencies near unity and dark QDs with a very low quantum efficiency [26].

To measure the influence of the refractive index on the radiative lifetime the hexanethiol-capped CdTe QDs were dissolved in five apolar solvents spanning a range of refractive indices as wide as possible, viz. hexane (n=1.375), octane (n=1.397), cyclohexane (n=1.427), chloroform (n=1.446) and toluene (n=1.496) [31]. In all these solvents the QDs dissolve readily and form a stable and clear colloidal suspension. The luminescence decay curves were measured for the CdTe QDs in the five solutions under identical circumstances (same optical density of the QD suspension, O.D ~ 0.1 at 406 nm, and same laser excitation power) and the measurements were repeated ten times in order to reduce the experimental error. For the QDs in all five solvents single exponential luminescence decay curves, similar to those shown in Figure 5.1 are measured. The radiative luminescence

lifetimes ($\tau_{1/e}$) are plotted as a function of the refractive index in Figure 5.2. The radiative lifetime decreases from 18.2 ns for CdTe QDs in hexane to 17.0 ns in toluene. The error bars in Figure 5.2 represent the experimental error as determined from analysis of the ten measurements. It is evident that the variation in refractive index gives only a small variation in the luminescence lifetime which will be discussed below.

5.3.2 CdSe QDs

The exciton luminescence of CdSe QDs has been studied more extensively in the literature than the luminescence of CdTe QDs. The efficient luminescence from TOP/TOPO capped CdSe QDs is well-known and in various studies the luminescence lifetimes of this type of capped CdSe QDs have been reported [15,21,26-28]. The presently studied TOP/TOPO/HDA capped CdSe QDs show a bright yellow emission peaking at 572 nm. From the position of the emission maximum the particle diameter is determined to be 3.4 nm. The capped CdSe QDs readily dissolve in the same five solvents as used for the CdTe QDs. The quantum efficiency is not strongly influenced by dissolving the QDs in the various solvents and is around 55%. Just as for CdTe the exciton emission for the CdSe QDs shows single exponential decay curves in the maximum of the emission band. As an example, the decay curves measured for CdSe QDs in the solvents with the highest (toluene, n=1.496) and the lowest refractive index (hexane, n=1.375) are shown in Figure 5.3. The luminescence decay curves are single exponential which indicates that the decay times reflect the radiative decay rate of the excitonic emission (see also the section above). The luminescence lifetime is around 26 ns, in good agreement with the radiative decay times reported for the exciton emission from

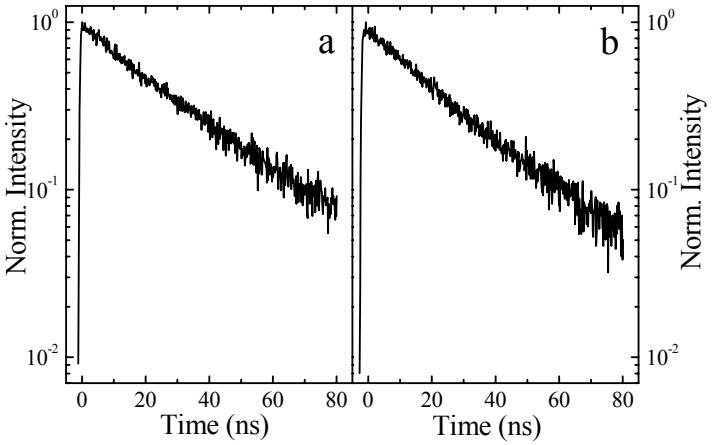

Figure 5.3 Luminescence decay curves of the exciton emission at 570 nm for TOP/TOPO/HDA capped CdSe quantum dots dispersed in hexane (a) and toluene (b). The measuements are done at 295 K under 406 nm excitation.

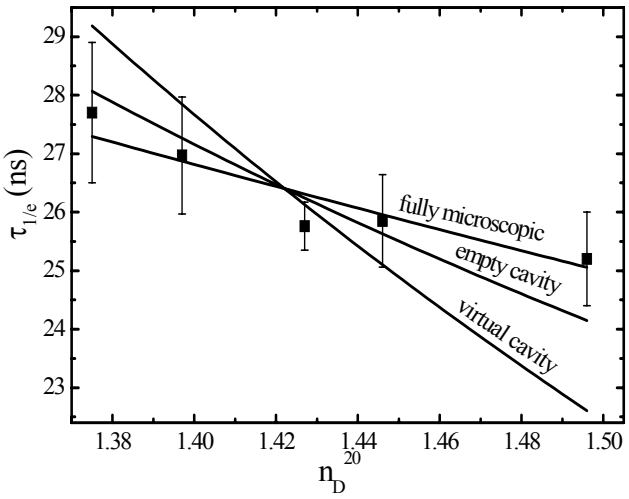

Figure 5.4 Radiative lifetime of the exciton emission from TOP/TOPO/HDA capped CdSe quantum dots as function of the solvent refractive index for quantum dots in apolar solvents. The filled squares represent the experimental results and drawn lines are fits to the theoretical models described by Eq. (5.2) (empty cavity), Eq. (5.3) (virtual cavity) and Eq. (5.4) (fully microscopic).

CdSe QDs [21,26-28,32]. In a recent study on the fluorescence life time of the emission from single quantum dots it was demonstrated that the non-radiative decay rate can vary for a single dot [33]. Analysis of the luminescence decay behavior of a large number of dots during different time intervals showed that the life time measured during the period of maximum brightness are around 27 ns and can be considered as the radiative life time. This observation provides strong support for the observation that the single exponential decay curves measured for the QD emission reflect the radiative decay rate and that the radiative life time for CdSe QDs is of the order of 26 ns.

The luminescence lifetimes for the exciton emission from CdSe QDs in the five solvents are plotted in Figure 5.4. The luminescence lifetime decreases from 27.7 to 25.2 ns as the refractive index of the solvent increases from 1.38 to 1.50. Just as observed for CdTe the influence of the refractive index on the luminescence lifetime is small. This observation is consistent with the reported insensitivity of the absorption cross-section of CdSe QDs on the solvent refractive index reported by Leatherdale *et al.* [34].

5.4 Discussion

The results described above show that both the CdTe and the CdSe QDs are ideal probes for monitoring the influence of the refractive index on the radiative decay

rate. The quantum dots are small (much smaller than the wavelength of light) luminescent species that are shielded from direct contact with the surrounding medium of variable refractive index by a thin (~0.4 to 0.9 nm) capping layer. For this two-level like system the radiative decay rate will be influenced by the solvent only through a variation of the refractive index of the surrounding medium assuming that the surrounding medium does not affect the thickness or interaction with the capping layer. In view of the similar apolar character of the solvents used to dissolve the capped QDs no influence of the solvent on the capping layer is expected. As a result, the measurements of the variation of the lifetime of the quantum dot emission in media of different refractive index will provide insight into which of the theoretical models discussed in the introduction can explain the observed relation between τ_{rad} and n.

In order to determine which of the various models can account for the experimental results, the data in Figs. 5.2 and 5.4 were fitted to the empty-cavity model [Eq. (5.2)], the full-cavity model [Eq. (5.3)] and the fully microscopic model [Eq. (5.4)]. The resulting fits are plotted in Figs. 5.2 and 5.4. For both types of QD the empty cavity and the full-cavity models strongly overestimate the influence of the refractive index on the radiative lifetime and cannot explain our experimental results. The recently published fully microscopic model [Eq. (5.4)], however, can explain the observed (small) decrease in radiative lifetime with increasing refractive index. This shows that neither the empty-cavity nor the full-cavity model can describe the dependence of the spontaneous emission rate on the refractive index for the QDs studied. It is encouraging to see that the fully microscopic model does reproduce the measured influence of the refractive index on the radiative decay rate. More in general, the present results provide reliable experimental data on the relation between radiative decay rates and the refractive index of the medium in which a two-level system is embedded. As such, the results are important in the further development of theories that account for the influence of local field effects on the spontaneous emission rate. It should be noted that typically QDs are not completely spherical but are slightly prolate with an aspect ratio of about 1.1. Orientation of the dipole may influence the coupling with the dielectric medium and complicate the theoretical analysis.

The difference between the present results, which show a relatively small influence of n on τ_{rad}, and the results for Eu^{3+} complexes, for which a much stronger influence has been reported, may also be related to the different nature of the systems. In Figure 5.5 a schematic drawing showing the difference for the Eu^{3+} complexes and the semiconductor QDs is depicted. In the case of the Eu^{3+} complexes the optical transition is localized within the $4f^6$ configuration of the Eu^{3+} ion and the transition dipole moment of the transition involved is small. The Eu^{3+} ion is placed in a relatively large cavity (the organic complex) with a low polarizability. The interaction with the surrounding dielectric occurs through this region of low

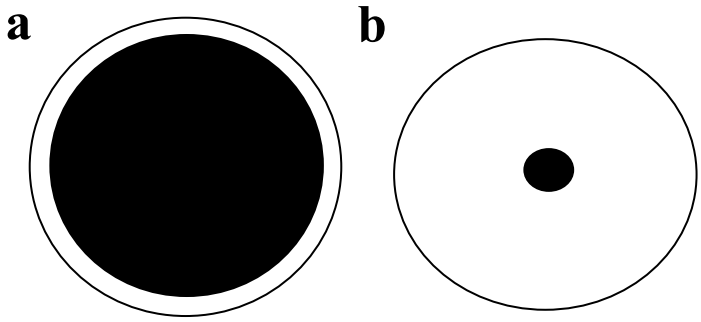

Figure 5.5 Schematic picture of a quantum dot with organic capping (a) and of a $Eu(fod)_3$ complex (a). The black part indicates the luminescing core and the white part the organic capping. The two pictures have not the same scale.

polarizability and the boundary conditions for the empty-cavity model form a good description for the Eu^{3+} complex in a dielectric. The presently studied system is different. The optical transitions in the QDs have large transition dipole moments and the QDs have a high polarizability. The interaction with the surrounding dipoles occurs through a relatively thin capping layer of capping ligands. This situation resembles the boundary conditions for the fully microscopic model presented in Ref. 10 where Eq. (5.4) was obtained by considering the interaction of an embedded atom with the nearby polarizable particles of the host via the electromagnetic field. The origin of the local field renormalization of the spontaneous emission rate is the microscopic near-dipole-dipole interaction in which the influence of the atom on each nearby oscillator is fed back to the atom. In the presently studied system an artificial atom (the CdTe or CdSe QD) is embedded in a dielectric and near-dipole-dipole interaction between the large excitonic electric dipole and dipoles of the surrounding dielectric can occur through the thin capping layer. The good agreement between the experimentally observed dependence of the spontaneous emission rate on the refractive index with Eq. (5.4) provides experimental support for the applicability of the fully microscopic model for the local-field enhancement of the spontaneous emission rate. It will be interesting to extend the experiments in the future to QDs in polar solvents and to widen the range of refractive indices over which the relation between n and τ_{rad} is measured. It may also be interesting to vary the thickness of a capping layer with low polarizability around the QD to investigate how the relation between n and τ_{rad} changes beyond a certain width of the capping layer when the boundary conditions change to those of the empty or full-cavity models.

5.5 Conclusions

The radiative lifetime of the excitonic luminescence of CdTe and CdSe QDs has been measured as a function of the refractive index of the surrounding dielectric by dissolving capped QDs in a variety of solvents with n varying between 1.37 and 1.50. The radiative lifetime of the exciton emission is observed to decrease from 18.2 to 17.0 ns for CdTe and from 27.2 and 25.2 ns for CdSe. This dependence of τ_{rad} on n is weaker than in previously reported experiments for Eu^{3+} complexes and the dependence predicted by theoretical models for an oscillator in an empty or full cavity. The results are well explained by a recently reported fully microscopic model based on near-dipole-dipole interactions of an embedded atom with dipoles in the surrounding medium. The results show that capped semiconductor QDs are ideal probes for studying the influence of the refractive index on the spontaneous emission rate and provide reliable experimental data which can serve as input in the further development of theoretical models describing the influence of local field effects on the radiative decay rate for electric dipole transitions.

References

[1] E. M. Purcell, *Phys. Rev.* **1946**, 69, 681
[2] D. L. Dexter, *Phys. Rev.* **1956,** 101, 48
[3] V. L. Ginzburg, *J. Phys. USSR* **1940**, 2, 441
[4] P. W. Milonni, J. Mod. Optics **42**, 1991 (1995).
[5] G. Nienhuis and C. Th. J. Alkemade, *Physica* (Amsterdam) **1976**, 81 C, 181
[6] A. von Hippel, *Dielectrics and Waves*, (John Wiley and Sons, New York, **1954**)
[7] R. J. Glauber and M. Lewenstein, *Phys. Rev. A* **1991** 43, 7
[8] J. Knoester and S. Mukamel, *Phys. Rev. A* **1989**, 40 7065
[9] S. M. Barnett, B. Huttner and R. Loudon, *Phys. Rev. Lett.* **1992**, 68, 3698 ;
S. M. Barnett, B. Huttner, R. Loudon and R. Matloob, *J. Phys. B* **1996**, 29, 3763
[10] M. E. Crenshaw and C. M. Bowden, *Phys. Rev. Lett.* **2000**, 85, 1851
[11] F. J. P. Schuurmans and A. Lagendijk, *J. Chem. Phys.* **2000**, 113, 3310
[12] G. L. J. A. Rikken and Y. A. R. R. Kessener, *Phys. Rev. Lett.* **1995**, 74, 880
[13] F. J. P. Schuurmans, D. T. N. de Lang, G.H. Wegdam, R. Sprik and A. Lagendijk, *Phys. Rev. Lett.* **1998**, 80, 5077
[14] R.S. Meltzer, S. P. Feofilov, B. Tissue and H. B. Yuan, *Phys. Rev. B* **1999**, 60, 14012
[15] U. Woggon, *Optical properties of semiconductor quantum dots*, Springer, New York, **1997**
[16] A. P. Alivisatos, *J. Phys. Chem.* **1996**, 100, 13226
[17] C. B. Murray, C. R. Kagan and M. G. Bawendi, *Annu. Rev. Mater. Sci.* **2000**, 30, 546
[18] C. B. Murray, D. B. Norris, M. G. Bawendi, *J. Am. Chem. Soc.* **1993**, 115, 8706
[19] D. V. Talapin, A. L. Rogach, A. Kornowski, M. Haase and H. Weller, *Nano Lett.* **2001**, 1, 207
[20] S. F. Wuister, F. van Driel and A. Meijerink, *Phys. Chem. Chem. Phys.* **2003**, 5, 1253
[21] C. de Mello Donega, S.G. Hickey, S.F. Wuister, D. Vanmaekelbergh and A. Meijerink, *J. Phys. Chem. B* **2003**, 107, 489
[22] D.V. Talapin, S. Haubold, A. L. Rogach, A. Kornowski, M. Haase and H. Weller, *J. Phys. Chem. B* **2001**, 105, 2260
[23] S. A. Empedocles, R. Neuhauser, K. Shimizu and M. G. Bawendi, *Adv. Mater.* **1999,** 11, 1243
[24] S. F. Wuister, I. Swart, F. van Driel, S. G. Hickey and C. de Mello Donegá, *Nano Lett.* **2003**, 3, 503

[25] A. M. Kapitonov, A. P. Stupak, S. V. Gaponenko, E. P. Petrov, A. L. Rogach and A. Eychmüller, *J. Phys. Chem. B* **1999**, 103, 10109
[26] Y. Ebenstein, T. Makari and U. Banin, *Appl. Phys. Lett.* **2002**, 80, 4033
[27] S. A. Crooker, J. A. Hollingworth, S. Tretiak and V. I. Klimov, *Phys. Rev. Lett.* **2002**, 89, 186802-1
[28] O. Labeau, P. Tamarat and B. Lounis, *Phys. Rev. Lett.* **2003**, 90, 257404-1
[29] F. van Driel, D. A. M. Vanmaekelbergh and W. Vos, to be published
[30] A. Thränhardt, C. Ell, G. Khitrova and H. M. Gibbs, *Phys. Rev. B* **2003**, 65, 035327-1
[31] D.R. Lide, *Handbook of Chemistry and Physics*, *79th ed.*, (CRC Press, Boca Raton, FL., **1999**
[32] M. Nirmal, D. J. Norris, M. Kuno, M. G. Bawendi, A. L. Efros and M. Rosen, Phys. Rev. Lett. **1995**, 3728
[33] B. R. Fischer, H-J Eisler, N. E. Scott and M. G. Bawendi *J. Phys. Chem. B* **2004**, 108, 143
[34] C. A. Leatherdale, W.-K. Woo, F. V. Mikulec and M. G. Bawendi, *J. Phys. Chem. B* **2002**, 106, 7619

Chapter 6.

Luminescence temperature antiquenching of capped CdSe quantum dots

Abstract

The quantum yield of efficient TOP/TOPO/HDA-capped CdSe QDs was investigated as function of temperature. The quantum yield gradually decreases above 20 K but increases sharply when the QDs are heated above a transition temperature around 250 K. This observation is unique as it is the opposite of the commonly observed temperature quenching of luminescence. To understand the mechanism behind the temperature antiquenching, the TOP/TOPO/HDA capping was exchanged with various alkylamines. The transition temperature shifts systematically to higher temperatures as the length of the alkyl chains increases. This indicates that a phase transition in the capping layer is involved and directly affects reconstruction of the CdSe surface. Surface reconstruction is required to remove surface (quenching) states. In addition, our results show how chemical exchange of the capping provides control over the temperature-dependent optical properties of QDs.

6.1 Introduction

Their efficient luminescence and tunable emission color make semiconductor quantum dots (QDs) very promising for application in opto-electronic devices and as luminescent labels [1-3]. Surface passivation with aliphatic capping molecules like tri-octylphosphine (TOP), tri-octylphosphineoxide (TOPO) and hexadecylamine (HDA) plays a crucial role in obtaining luminescence quantum yields close to unity [4,5]. The influence of quantum confinement on the electronic and optical properties of semiconductor nanocrystals is of great fundamental and practical interest. Especially for direct bandgap II-VI semiconductors like CdSe and CdTe the increasing control over the size, shape and surface chemistry has enabled the production of QDs with a tunable (from blue to red) narrow band luminescence and quantum yields close to unity [4-7]. Research on these QDs continues to contribute to a better understanding of the influence of quantum size

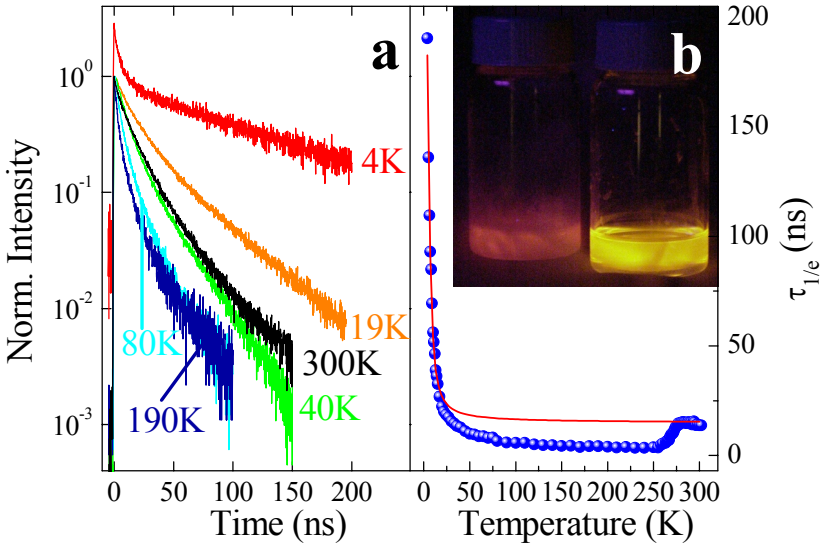

*Figure 6.1 Temperature dependence of the exciton luminescence for TOP/TOPO/HDA capped CdSe QDs. In **a** the luminescence decay curves are shown for TOP/TOPO/HDA capped CdSe QDs at various temperatures between 4 and 300 K. The luminescence lifetime ($\tau_{1/e}$) of the exciton emission as determined from the curves in **a** are shown as a function of temperature in **b**. The drawn line in **b** is a fit to a three level model with a lower energy emitting triplet state and a higher energy singlet state separated by 1.8 meV. The inset shows the quenching of the luminescence at low temperatures. Both vials contain a solution of TOP/TOPO/HDA capped CdSe QDs and are illuminated with a UV-lamp (360 nm). The vial on the left is cooled to 160 K while the brightly luminescing solution in the vial on the right is at 300 K.*

effects in the semiconductor core. The role of the semiconductor surface and the interaction with the passivation layer has not reached the same level of understanding. The capping layer is considered to merely confine the charge carriers by providing a potential barrier and to passivate the dangling bonds of surface atoms. The large surface area makes nanocrystals ideal systems to investigate surface properties that cannot be studied in bulk system. Even though this is recognized to be one of the important new areas of research in solid-state chemistry [8], only few studies address this aspect of semiconductor nanocrystals. The present work provides insight into the role of surface and the interaction with the aliphatic capping layer on the energy level structure of CdSe QDs. The temperature dependence of the quantum efficiency of TOP/TOPO/HDA capped CdSe QDs is investigated. An unexpected sharp increase of the quantum efficiency is observed around 250 K. To gain understanding of the origin of this effect, CdSe QDs are recapped with alkylamines with different carbon chain lengths. The exact transition temperature shifts to higher temperatures with increasing alkyl chain length. This indicates that a phase transition in the capping is involved, which hampers the surface reconstruction which is needed for a high quantum efficiency.

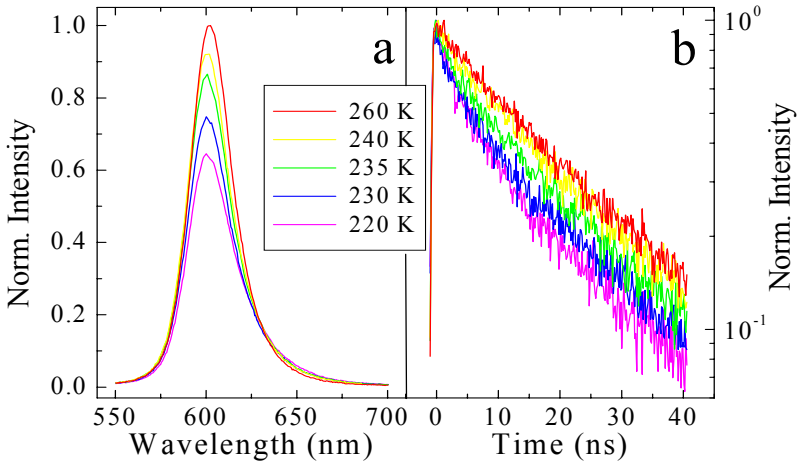

Figure 6.2 Luminescence of CdSe QDs after capping exchange with hexylamine C6). The emission spectra in a show the increase in luminescence intensity with increasing temperature around the antiquenching temperature. Luminescence decay curves of the exciton emission at 604 nm are shown in b for various temperatures around the antiquenching temperature for the same hexylamine capped QDs. Excitation is with a ps diode laser at 406 nm.

6.2 Experimental

Highly luminescent CdSe QDs were prepared by the method reported by de Mello Donegá *et al.* [5]. For the synthesis of CdSe QD's 20 g of TOPO, 10 g of HDA and 2 ml of TEOF (tri-ethylorthoformate) are heated in a three-necked flask to 330 ^{o}C. At this temperature the heating mantle is removed and a solution of 10 ml TOP containing 0.79 g of Se (present as a TOP-Se complex) and 0.28 g $Cd(Me)_2$ is quickly injected as the temperature has dropped to 300 ^{o}C after which the particles were allowed to grow at 240 ^{o}C for 1 h followed by a slow addition of additional precusor solution and annealing for 1 h ar 240 ^{o}C resulting in 4.3 nm CdSe particles emitting around 605 nm. To exchange the surface capping with alkylamines, 0.25 g of the crude product of CdSe QD's was mixed with a twenty fold excess (relative to TOPO/HDA) of hexylamine (C_6), decylamine (C_{10}), dodecylamine (C_{12}), hexadecylamine (C_{16}) or octadecylamine (C_{18}). The mixture was stirred for 12 h at 70 ^{o}C after which 5 ml of toluene was added. Luminescence and luminescence life time measurements are performed on dilute solutions of QD's (with an optical density at 500 nm of 0.04) in toluene with a diode laser set-up described in detail in Ref. 5).

6.3 Results and discussion

The most widely applied synthesis methods for strongly luminescent QDs are based on the growth of nanometer-sized crystallites of the semiconductor material inside a shell of coordinating molecules.[4-7] The role of the ligand molecules is two-fold. Firstly, inside a shell of coordinating ligands the semiconductor crystallites grow to a size that is determined by the kinetics of attaching and detaching of the ligands. The second role of the ligand molecules is to passivate dangling bonds in order to prevent non-radiative recombination at surface sites. The luminescence quantum yield is known to be very sensitive to subtle changes in the synthesis procedure indicating that the surface structure is a key factor for the occurrence of band gap states that quench the exciton luminescence [5,9].

For the present study, high-quality CdSe QDs were synthesized by hot injection into a coordinating solvent mixture (TOP/TOPO/HDA) [5,9]. The suspension of QDs shows a bright orange exciton luminescence with a quantum efficiency of 60% at room temperature. Luminescence decay curves are shown in Figure 6.1a at various temperatures between 4 and 300 K. At 4 K a bi-exponential decay is observed with a fast component due to emission from the singlet exciton state (spin-allowed) and a slow component due to emission from the triplet state (spin-forbidden). As the temperature is raised, the radiative lifetime decreases due to thermalization between the triplet and singlet states similar to what has been reported [10-12]. The temperature dependence of the lifetime is well described by a three-level model with decay rates for the triplet and singlet states of $5x10^6$ s^{-1} and $1.25x10^8$ s^{-1}, respectively, and an energy difference of 1.8 meV between the two states. Above 20 K the decay curves become increasingly non-exponential until a

relatively fast ($\tau_{1/e}$ ~ 4 ns) and strongly non-exponential decay curve is observed at220 K. Luminescence life times ($\tau_{1/e}$) for the non-exponential decay curves are defined as the time in which the intensity drops to 1/e of the initial intensity. As the temperature is raised from 250 to 300 K the decay time becomes longer and the decay curves return to a single-exponential with $\tau_{1/e}$ ~ 20 ns. In Figure 1b the $\tau_{1/e}$ times determined from the decay curves are plotted as a function of temperature. The drawn line represents the temperature dependence of the radiative lifetime, calculated using the three level model. The luminescence lifetimes are in good agreement with the measured $\tau_{1/e}$ values between 4 and 20 K and above 280 K. Between 20 and 280 K the luminescence decay is faster than that calculated suggesting that non-radiative relaxation provides an additional recombination channel in this temperature regime. The non-exponential character of the decay curves shows that the non-radiative decay rates vary for different QDs. The observation that the luminescence intensity decreases between 20 and 250 K confirms the presence of non-radiative relaxation. Temperature quenching of luminescence is commonly observed and ascribed to thermally activated (phonon-induced) processes. Temperature quenching above 20 K has previously been reported for TOP/TOPO capped CdSe QDs but not a recovery of the luminescence at higher temperatures [11].

Luminescence intensity measurements between 250 and 300 K show that the lengthening of $\tau_{1/e}$ in this temperature range is accompanied by a recovery of the luminescence intensity. This is a striking observation; as non-radiative relaxation processes are usually thermally induced it is unexpected to observe a rise in quantum efficiency with increasing temperature. The long (radiative) lifetime (~20 ns), almost single exponential decay and high quantum efficiency (~60%) for the CdSe QDs at room temperature show however that the temperature quenching of the luminescence between 20 and 250 K is reversed to temperature antiquenching above 250 K. We conjecture that the striking recovery of purely radiative decay above the threshold temperature is due to subtle displacements of the semiconductor surface atoms induced by a phase transition in the molecular capping layer. To verify if a phase transition is involved, the capping layer of the CdSe QDs was exchanged for alkylamines with linear chains varying in length between six and eighteen carbon atoms. In Figure 6.2 luminescence decay curves and emission spectra are shown for CdSe QDs after capping exchange with hexylamine. Just as for the TOP/TOPO/HDA capped QDs the exciton luminescence intensity increases (Figure 6.2a) in the same temperature regime where the decay curves evolve towards a single-exponential while $\tau_{1/e}$ increases (Figure 6.2b). The temperature at which this transition takes place (~ 235 K) is however considerably lower than that for the TOP/TOPO/HDA capped QDs. In Figure 6.3 the temperature dependence of the luminescence intensity and $\tau_{1/e}$ are plotted as a function of temperature for CdSe QDs after capping exchange with

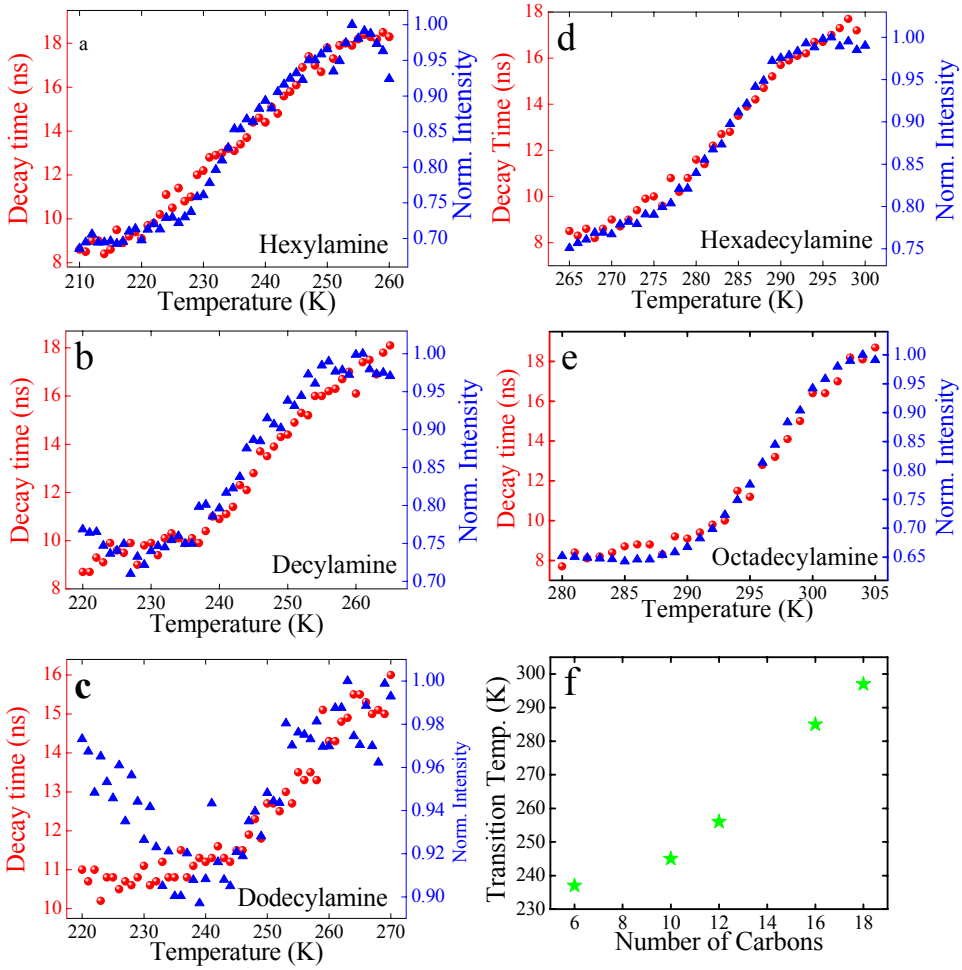

*Figure 6.3 Influence of the capping molecules on the antiquenching temperature for CdSe QDs. The temperature dependence of the luminescence lifetime (●, λ_{em}=604 nm) and the integrated luminescence intensity of CdSe QDs (▲) after capping exchange with hexylamine (**a**), decylamine (**b**), dodecylamine (**c**), hexadecylamine (**d**) and octadecylamine (**e**) are shown for excitation at 406 nm. In **f** the antiquenching temperatures obtained from figures **a-e** are plotted as a function of the number of carbon atoms in the alkyl chains of the passivating alkylamine capping molecules.*

hexylamine, decylamine, dodecylamine, hexadecylamine and octadecylamine. Figures 6.3a-6.3e show that for all types of capping layers there is an excellent correlation between the temperature dependence of the lifetime and the luminescence intensity which proves that the lengthening of the lifetime with

increasing temperature corresponds to a decrease in the non-radiative relaxation rates. The antiquenching temperature shifts to higher temperatures as the length of the alkyl chain increases. In Figure 6.3f the antiquenching temperature, defined as the temperature at which the intensity and luminescence lifetime have increased to 50% of the total recovery, is plotted as a function of the number of carbon atoms in the alkylamine capping molecules, clearly showing the effect.

With the experimental support for the role of a phase transition in the ligand shell on the luminescence of CdSe QDs the next step is to understand the nature of the phase transition and how it affects the luminescence efficiency. Theoretical modelling of TOPO capped CdSe QDs indicates that small displacements of the surface Cd and Se atoms are required to prevent surface (quenching) states with energies in the forbidden gap [13]. If the capping layer of alkyl chains is in a frozen state this surface relaxation may be hampered, which means that the luminescence quenching centers remain active. The phase behavior of alkylamine passivation layers on QDs has been studied and can be described by the same interactions as those in self-assembled monolayers (SAM) [14]. Experimental and theoretical work on the phase behavior of n-alkanes, n-alkylamines and n-alkylthiols (SAM and also bulk) shows a complex behavior with various phase transitions [15,16]. A solid-liquid phase transition for long-chained alkylamines occurs above room temperature and cannot explain the present changes below room temperature. At lower temperatures phase transitions occur in the ordered phase. In the lowest temperature phase the alkyl chains are orientationally ordered. At higher temperatures (typically between 200 and 300 K for C6 to C20 alkanes) a transition occurs to a phase in which rotational motion is possible (the locked rotator phase). At even higher temperatures a second phase transition takes place to the unlocked rotator phase in which the tilt direction of the alkyl chains can fluctuate between nearest-neighbor molecules. For this phase transition molecular dynamics simulations show that for SAMs of hexadecylamine the transition temperature is around 275 K [15]. This temperature is very close to the temperature at which the recovery of the luminescence intensity and lengthening of the decay time is observed for the QDs capped with hexadecylamine. A transition to a phase in which neighboring ligand molecules can have different tilt angles is consistent with an onset of relaxation of atoms bound to the ligands. As the tilt angle for neighboring alkyl chains can change, a vertical displacement of surface atoms bound to the polar head groups becomes possible. This surface reconstruction is not possible when the alkyl chains are ordered and have fixed tilt angles. Further evidence for the role of a phase transition is provided by the shift to 10-15 K higher temperatures each time the alkyl chain length increases with two carbon atoms (Figure 3f) which is very similar to shifts reported in the literature [15,16]. Future experiments can provide more insight. For example, room temperature x-ray scattering experiments have shown the outward displacement of surface Se atoms and the inward displacement of Cd atoms in CdSe QDs at 300 K [17].

Temperature-dependent x-ray scattering experiments are expected to show that this surface reconstruction is hampered as the sample is cooled below the transition temperature of the capping layer.

6.4 Conclusions

The surprising observation of temperature antiquenching of the luminescence from capped CdSe QDs gives insight in the importance of the interaction between the capping layer and the semiconductor core on the energy level structure of QDs. It shows that the organic passivation layer not only passivates dangling bonds but also plays an active role in surface reconstruction. A phase transition in the capping layer affects the relaxation of the surface atoms and strongly influences the luminescence properties. Chemical exchange of the capping can be adapted to gain control over the temperature-dependent optical properties of QDs.

References

[1] J. Ouellette, *Ind. Phys.* **2003**, 9, 14
[2] C. M. Niemeyer, *Angew. Chem. Int. Ed.* **2001,** 40, 4128
[3] S. A. Empedocles, R. Neuhauser, K. Shimizu, M. Bawendi, *Adv. Mater.* **1999,** 11, 1243
[4] C. B. Murray, D.J. Norris, M. G. Bawendi, *J. Am. Chem. Soc.* **1993**, 115, 8706
[5] C. de Mello Donega, S. G. Hickey, S. F. Wuister, D. Vanmaekelbergh, A. Meijerink, *J. Phys. Chem. B,* **2003**, 107, 489
[6] D. V. Talapin, A. L. Rogach, A. Kornowski, M. Haase, H. Weller, *J. Phys. Chem B*, **2001,** 105, 2260
[7] X. Peng, L. Manna, W. Yang, J. Wickham, E. Scher, A. Kadavanich, A. P. Alivisatos, *Nature* **2000**, 404, 59
[8] R. J. Cava, F. J. DiSalvo, L. E. Brus, K. R. Dunbar, C. B. Norman et al., *Progress in Solid State Chemistry,* **2002**, 30, 1
[9] D. V. Talapin, A. L. Rogach, A. Kornowski, M. Haase, H. Weller, *Nano Lett.* **2001**, 1, 207
[10] O. Labeau, P. Tamarat, B. Lounis, *Phys. Rev. Lett.* **2003,** 90, 257404-1
[11] S. A. Crooker, T. Barrick, J. A. Hollingsworth, V. I. Klimov, *Appl. Phys. Lett*. **2003**, 82, 2793
[12] M. Nirmal, D. J. Norris, M. Kuno, M. G. Bawendi, A. L. Efros, M. Rosen, *Phys. Rev. Lett.* **1995**, 75, 3728
[13] K. Leung, K. B. Whaley, *J. Chem. Phys.* **1999**, 110, 11012
[14] R. W. Meulenberg, G. F. Strouse, *J. Phys. Chem. B* **2001,** 105, 7438
[15] J. Hautman, M. L. Klein, *J. Chem. Phys.* **1990,** 93, 7483
[16] G. Ungar, *J. Phys. Chem* **1983**, 87, 689
[17] M. G. Bawendi, A. R. Kortan, M. L. Steigenwald, L. E., *J. Chem. Phys.* **1989**, 91, 7282

Chapter 7.

Luminescence temperature antiquenching of the of water-soluble CdTe quantum dots: role of the solvent

Abstract

Luminescence temperature antiquenching (LTAQ) is observed for water-soluble CdTe quantum dots (QDs) capped with amino-ethanethiol (AET). The efficient exciton emission (quantum efficiency of ~ 40% at 300 K) is quenched almost completely as the QD solutions are cooled to below 230 K and is fully recovered around 270 K upon warming up to room temperature (LTAQ). Temperature dependent life time measurements show that the quenching rate is high resulting in an 'on/off' behavior. No LTAQ is observed for CdTe QDs capped with amino-undecanethiol (AUT). The LTAQ is explained by the influence of solvent freezing on the surface of the QD core. Freezing of the solvation water molecules surrounding the QD will induce strain in the capping shell, due to the interaction between water and the charged heads of the capping molecules. Short carbon chains (AET) will propagate the strain to the QD surface, creating surface quenching states, whereas long and flexible chains (AUT) will dissipate the strain thus avoiding surface distortion. Freezing point depression by the addition of methanol results in a lowering of the transition temperature. Additional support is provided by the size dependence of the LTAQ: smaller particles, with higher local ionic strength due to a higher density of charged NH_3^+ surface groups, experience a lower transition temperature due to stronger local freezing point depression.

7.1 Introduction

Quantum dots (QDs) are an interesting class of materials since their electronic and optical properties mark a transition between bulk material and molecules [1,2]. Especially the variation of the bandgap with the size of the crystal has attracted much attention. Efficiently luminescing semiconductor QDs can be used in applications like biological labels [3,4], quantum dot lasers [5] and LEDs [6]. Monodisperse and highly luminescent II-VI quantum dots of CdSe and CdTe can currently be prepared via different high temperature syntheses [7-10]. The choice of the capping molecules used in the synthesis of the QDs is subtle but crucial for the formation of stable and highly luminescent semiconductor QD suspensions [11].

The role of the capping molecules is threefold. Firstly the capping molecules function as passivating agents for surface states. The surface to volume ratio of nanocrystals is large and many luminescence quenching processes occur at the crystal surface. To prevent non-radiative recombination at surface sites capping molecules cover the QD surface, passivating dangling bonds. Secondly the growth kinetics of the QDs are determined by the affinity of the precursors for the capping molecules and the stability of the capping ligand precursor intermediate complex (e.g. TOP-Se) . If the complex is too stable, no QD formation occurs. If the affinity with the capping molecules is too weak, the control over the crystal growth is poor, resulting in uncontrolled growth and large particles are formed (outside the quantum size regime). Finally the capping molecules prevent the QDs from aggregation via sterical hindrance (e.g. long aliphatic chains) [9-11] or by charge stabilization (e.g. COO^- or NH_3^+ groups at the surface) [12].

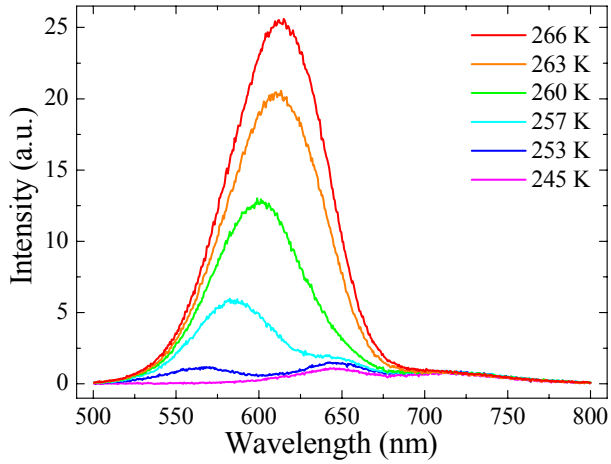

Figure 7.1. Temperature dependent emission spectra (λ_{ex}=400 nm) of AET capped CdTe QDs (d=3.4 nm) in water at temperatures between 245K and 266K.

Although the role of the capping molecules is critical for the creation of a luminescent core, research on QDs has mainly focused on the properties of the semiconductor core. The capping layer of organic molecules is often regarded as an energy barrier to confine the exciton to the semiconductor core. The question if and how the capping molecules play an *active* role in the passivation and surface reconstruction of the QD core has recently been addressed for CdSe QDs capped with aliphatic amines [13]. There evidence was presented for a strong influence of a phase transition in the capping molecules shell on the luminescence behavior of highly luminescent CdSe QDs. A sharp increase in lifetime and quantum efficiency was observed when diluted samples of CdSe QDs were heated from 200 K to 300 K. This unusual luminescence behavior is called luminescence temperature antiquenching (LTAQ) [13]. The transition-temperature for the recovery of the luminescence was found to increase with the chain length of the alkylamine capping molecule (from C6 to C18), consistent with a phase transition in the capping layer [13].
In this chapter LTAQ is reported for highly luminescent water-soluble CdTe QDs capped with amino-ethanethiol (AET). Cooling of the CdTe QDs aqueous solutions below 230 K results in an almost complete quenching of the exciton emission, which fully recovers at 270 K upon heating to room temperature. The transition temperature is dependent on the size of the QD. For CdTe QDs capped with Amino-undecanethiol (AUT) no LTAQ is observed. Experimental evidence is presented which shows that a phase transition in the solvent (water) around the QDs is responsible for the LTAQ of the CdTe QDs.

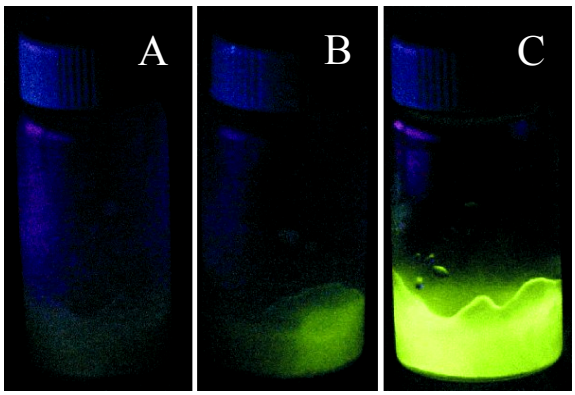

Figure 7.2. Photographs of a vial containing an aqueous solution of green emitting CdTe QDs capped with AET (d=2.7 nm) in ice illuminated with a handheld mercury lamp (365 nm) at ~77 K (A) and just below 273 K (C). Figure 7. 2 B shows a vial warmed up at the right hand side.

7.2 Experimental

Synthesis of DDA capped CdTe QDs.

DDA capped QDs were prepared following the method reported by Wuister *et al.* [14]. In a three necked flask 10 g of dry DDA and 7 mL of TOP were heated to 50ºC. To this solution 0.22 g (1.54 mmol) $Cd(Me)_2$ in 7 mL of TOP and 0.16 g (1.25 mmol) Te powder were added. A Cd/Te ratio of about 1.2 was used in all syntheses performed. The reaction mixture was heated to 145ºC for three hours to yield green emitting QDs (d = 2.7 nm). Orange emitting (d = 3.0 nm) QDs were prepared by heating the reaction mixture to 185ºC for two hours. Red emitting QDs (d = 3.4 nm) were grown in two steps. First QDs were prepared by heating a TOP-DDA mixture containing 0.22 g $Cd(Me)_2$ and 0.16 g Te to 200ºC for four hours. The reaction mixture was then cooled to room temperature and 1.25 mL of a 0.3 M TOP-Te solution (prepared by dissolving Te in TOP overnight at 200ºC) was added. The resulting mixture was subsequently heated slowly to 185ºC for two hours.

Synthesis of aminoethanethiol capped CdTe QDs by capping exchange

To prepare water-soluble CdTe QDs with a positively charged capping [12], 50 μL of the crude solution of CdTe QDs in the TOP/DDA coordinating mixture was dissolved in 5 mL chloroform. Subsequently 50 μL of 0.5 M methanolic solution of AET was added. The stronger affinity of the thiol group (of AET) with the CdTe surface in comparison to the affinity of the amine group of DDA will cause a capping exchange of DDA by AET: the change of a surface with aliphatic chains (of DDA) to a surface with amine groups (of AET) causes flocculation of the QDs in chloroform. Subsequently 5 mL deairated ultrapure water (16 MΩ·cm) was added to the suspension, resulting in a two-phase system (water above chloroform). Upon shaking, the flocculated QDs were dissolved into the water phase forming a clear suspension. The same procedure was followed for the preparation of AUT capped QDs.

Apparatus

Emission spectra were recorded with a SPEX Fluorolog spectrofluorometer, equipped with two monochromators (double-grating, 0.22 m, SPEX 1680, model F2002) and a 450 W Xenon lamp as the excitation source. Emission spectra were also recorded in this setup by collecting the emission with an optical fiber connected to a 0.25 m Acton Research monochromator fitted with a Princeton Instruments liquid nitrogen cooled CCD camera. Luminescence lifetime measurements were performed with a Pico Quant picosecond laser (λ_{ex} = 406 nm, 2.5 MHz) and monochromator (1350 lines mm^{-1} grating, blazed at 500 nm) in combination with a fast Hamamatsu photo-multiplier tube (H5738P-01) for light detection. Luminescence decay curves were obtained by pulse height analysis using a Time Harp 100 computer card. The ratio of stop to start pulses was kept

low (below 0.05) to assure good photon counting statistics. Temperature-dependent PL emission and lifetime measurements were recorded using a liquid helium flow-cryostat. Samples were first cooled to ~ 200 K and slowly warmed to room temperature (typical heating rates are ~ 0.2 K/min.).

7.3 Results and Discussion

7.3.1 LTAQ of water-soluble CdTe QDs

Water-soluble, amino-ethanethiol (AET) capped CdTe QDs show strong exciton emission at room temperature with quantum efficiencies up to 60% [12]. In Figure 7.1 the temperature dependence of the emission spectra is depicted for red emitting AET capped CdTe QDs (d = 3.4 nm) in water from 245 K to 266 K. At 266 K an emission band around 615 nm is observed that is ascribed to the exciton emission of the CdTe QDs. A weak emission band centered around 725 nm also observed in Figure 7.1. This weak emission band (~3% of the total emission intensity) is ascribed to a defect related emission of CdTe [14]. The intensity of this defect related emission is temperature independent in the 245K–266K range. The intensity of the exciton peak however, decreases rapidly with the temperature until almost total quenching at 245 K. The emission intensity does not recover when the sample is cooled further to 4 K. As the sample is allowed to warm up a peak around 555 nm appears (from 250 K on) that strongly increases in intensity with temperature. This emission is ascribed to the recovered exciton emission of CdTe QDs. The emission intensity is completely recovered when the temperature reaches 266 K, just below the melting point of pure water. This surprising LTAQ behavior of the exciton emission of CdTe QDs is reproducible and fully reversible. The behavior of the luminescence intensity for cooling down and heating up are identical (no hysteresis has been observed). The LTAQ can also be visually observed. Fig 7.2 illustrates the LTAQ with three photographs of a frozen aqueous solution of green emitting CdTe QDs (d=2.7 nm) under 365 nm excitation (a real-time movie is also available as supporting information). In Fig 7.2A the sample temperature is close to 77 K (thermal equilibrium with liquid N_2) illustrating the complete quenching of the QD emission. Fig 7.2C shows the same sample just below the melting point of ice. The exciton emission of the green emitting QDs has fully recovered. Fig 7.2B shows the intermediate case where only the right part of the vial was warmed up resulting in a half bright/half dark sample.

Figure 7.1 shows that as the temperature of the CdTe QDs sample is raised, not only the intensity of the exciton emission increases, but also its maximum shifts towards lower energy (longer wavelengths). In Figure 7.3 (green diamonds) the maximum of the exciton emission peak of CdTe QDs is plotted versus the sample temperature. The exciton emission peak is observed to shift to lower energies

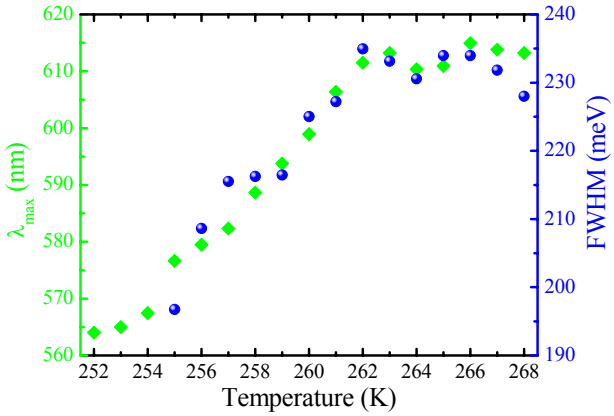

Figure 7.3 Emission maximum (green diamonds) and FWHM (blue dots) of the exciton emission of 3.4 nm AET capped CdTe QDs in water as function of sample temperature.

by 175 meV (564 nm to 614 nm) from 252 K to 263 K. No further shift of the emission maximum occurs when the sample temperature is raised above 263 K.
The change of the emission color from green/yellow to orange/red is also noted by eye during the experiment. Furthermore, the full width at half maximum (FWHM) of the exciton emission peak increases with temperature in the same range where the emission peak shifts to the red (from 255 K to 263 K, Figure3 blue dots). Note that both effects occur over a very narrow temperature range (less than 10K).
Figures 7.1 and 7.3 indicate that the LTAQ of the AET capped CdTe QDs is dependent on the crystal size. First the smallest QDs in the ensemble (largest bandgap) start to emit. This results in a strongly blue shifted emission band (compared to the emission at room temperature). In view of the Gaussian–like size distribution in a QD sample, only a small fraction of very small particles emitting around 570 nm is present in the ensemble. This results in a low emission intensity at the blue side of the room temperature emission spectrum. As the sample temperature increases further also larger QDs start to emit and contribute to the total emission, resulting in a red shift of the exciton emission and a higher luminescence intensity. The increase of the FWHM with temperature is consistent with a size dependent quenching of the exciton luminescence. At temperatures higher than 263 K the FWHM, the position of the emission maximum and the luminescence intensity remain constant, indicating that all the different sizes of QDs contribute to the total emission peak at 268K.
To confirm that the LTAQ of AET capped CdTe QDs is indeed size dependent three different sizes of QDs were prepared, recapped with AET and dissolved in

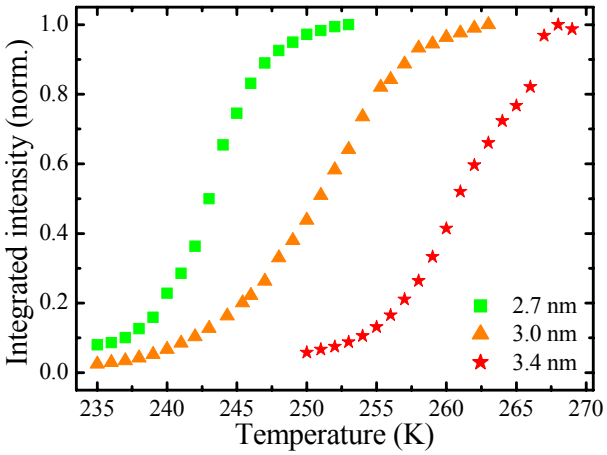

Figure 7.4 Normalized integrated intensity of the emission spectrum (λ_{ex}=400 nm) for three different sizes (2.7 nm, 3.0 nm and 3.4 nm) of AET capped CdTe QDs in water as function of sample temperature.

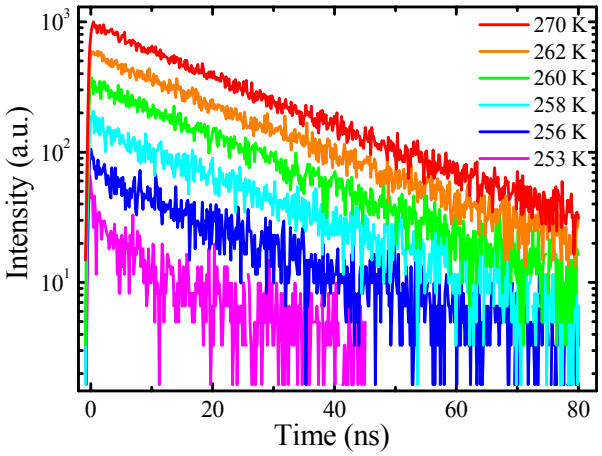

Figure 7.5 Temperature dependent luminescence decay curves (λ_{ex}=400 nm, measured at the emission maximum) of AET capped CdTe QDs (d=3.4 nm) in water.

water. The temperature dependence (from 235 K to 270 K) of the (normalized) integrated emission intensity of these CdTe QD samples is shown in Figure 7.4. A sharp transition (only 10 K from total quenching to total recovery) is observed for all three sizes. The filled stars give the integrated intensity of the emission spectra depicted in Figure 7.1 (for particles with a diameter of 3.4 nm). The total intensity increases sharply slightly above 260 K. The S-shape of the curve reflects the size dispersion of the sample of QDs. Since only few relatively small and large particles are present, the contribution to the change in the total intensity is small in the low and high temperature regime of the curve. The particles with sizes close to the average size of the sample are abundantly present. As the temperature at which these particles start to emit is reached, a rapid change in the total intensity with temperature is observed. The steepness of the transition is dependent on the size distribution: as the size distribution decreases the steepness of the transition increases. For smaller sizes (2.7 nm) and (3.0 nm) the same type of S-shaped curve is obtained. However the transition temperature (the temperature at which the intensity has increased to 50% of the total intensity) decreases with decreasing size. This temperature behavior of the different CdTe samples confirms the size dependence of the LTAQ observed within an ensemble of CdTe QDs: for CdTe QDs with smaller sizes the transition occurs at lower temperatures.

The luminescence decay curves can provide information about the decay kinetics of the CdTe exciton emission [14]. CdTe QDs capped with AET in water have a monoexponential decay with a (radiative) decay time close to 20 ns at room temperature [12]. Figure 7.5 shows the luminescence decay curves of AET capped CdTe QDs (3.7 nm in size) measured at the maximum of the exciton emission as a function of temperature. The area under the luminescence decay curve of the exciton emission increases with temperature in the same way as the integrated intensity determined from Figure 7.1. This is expected as the integral of the luminescence decay curves is proportional to the total light output and therefore to the photoluminescence quantum efficiency.

The decay curves at temperatures above 256 K are monoexponential and have similar decay times (~20 ns), whereas those measured at the lowest temperatures (253 K and 256 K) show a faster initial decay. The monoexponential character of the decay at higher temperatures indicates that purely radiative decay dominates the excitonic emission. The similar slopes also indicate that the nature of the dominant radiative process does not change during temperature increase. No shortening of the decay time is observed here as was detected for the LTAQ of alkylamine capped CdSe QDs. For CdSe QDs a decrease of 30% of the room temperature intensity is observed [13]. Here the quenching is very effective leading to a complete quenching of the exciton emission intensity, leaving only a weak defect related emission to be observed below the transition temperature. This indicates that a high non-radiative decay rate is associated with the

quenching of the exciton emission. This results in an 'on/off' behavior of the exciton luminescence. If the particle is 'on' the luminescence is dominated by radiative decay [12,15,16]. Below the transition temperature (of the individual particle) the luminescence of a given QD is completely quenched (the 'off' state). Since the particle is completely dark, it does not contribute to the luminescence and is therefore not detected in the luminescence decay curve. Consequently luminescence life time determined from the luminescence decay curve does not change, since only the QDs in the 'on' state (with a monoexponential decay) contribute to the luminescence signal.

7.3.2 Mechanism behind LTAQ

The LTAQ of the luminescence from CdTe QDs in water is more pronounced than the LTAQ observed from CdSe QDs reported previously [13]. Before discussing the mechanism behind the presently reported LTAQ it is important to outline the differences between the two systems and to give a brief description of the mechanism proposed for LTAQ in CdSe QDs.

The system studied here (AET capped CdTe QDs in water) differs in several aspects from the previously reported system where LTAQ was observed (alkylamine capped CdSe QDs in toluene). In addition to a different semiconductor core material also the capping and solvent molecules differ. Here, a thiol instead of an amine group is bound to the QD surface and a protonated amine group instead of an hydrophobic alkyl chain will interact with the solvent molecules. This makes the CdTe QD soluble in water instead of organic solvents. For CdSe QDs (in toluene) the solvent is still a liquid while for AET capped CdTe LTAQ is observed in the solid phase (ice).

The mechanism behind LTAQ for CdSe QDs is discussed in detail in Ref 13. In brief, the model for LTAQ considers the influence of a phase transition in the capping layer on surface states of the QD. Total energy minimalization calculations for TOPO capped CdSe QDs have shown that the surface Cd and Se atoms shift slightly from their regular lattice position [17]. This surface relaxation minimizes the energy and it also removes surface states which are present in the bandgap for the unrelaxed surface. Surface states in the bandgap act as quenching centers and to obtain high luminescence quantum yields removal of these surface states by surface relaxation is essential. The LTAQ in CdSe QDs is explained by a phase transition in the layer of capping molecules at the QD surface. The long aliphatic chains of the alkylamine capping molecules have a strong interaction. In a low temperature phase the stacking of the capping molecules induces strain to the relaxed QD surface and the surface atoms are removed from their positions. As a result, surface quenching states are created that lower the luminescence quantum yield. At higher temperatures the increased mobility of the capping molecules in a higher temperature phase lifts the strain

on the surface and allows for surface relaxation, resulting in the recovery of the high luminescence quantum yield.

For AET capped CdTe QDs a similar mechanism is considered to be responsible for the LTAQ of the exciton emission. CdTe QDs are capped with a short chain thiol amine with a positively charged amine group. As a CdTe sample in water is cooled below 273 K the water freezes. The NH_3^+ groups of the AET molecules that have strong interaction with the solvent will be incorporated in the solid. This strongly reduces their mobility and strain is induced to the QD surface. As a result the relaxation of surface atoms of the CdTe QD is hampered and surface states in the bandgap are created due to the unrelaxed surface. Fast non-radiative decay at the surface states becomes possible and quenches the exciton luminescence efficiently (the 'off' state). When the sample is warmed up the ice melts in the direct proximity of the QD. This liberates the NH_3^+ groups from their fixed positions, releases the strain induced to the surface and allows for relaxation of the CdTe surface. The QD will then start to efficiently luminesce again (the 'on' state).

Although the freezing point of (pure) water is 273 K, the transition temperatures observed for LTAQ of the CdTe QDs are lower, as can be seen from Figure 7.4. The reason for the difference between the phase transition temperature of the (pure) solvent and the transition temperature is due to charge located at the QD surface as NH_3^+ groups from the AET capping molecules. The freezing point of water can be lowered by adding e.g. salts or alcohols (freezing point depression). The AET capped CdTe QDs are charge stabilized by protonated amine groups leading to a high positive charge density at the QD surface. The presence of this charge at the QD surface will decrease the freezing point temperature of the water in the direct proximity of the QD surface (local freezing point depression). The freezing point of the solvent remains almost unaffected since the average ion concentration in the solvent is lower than at the positively charged QD surface due to the presence of the AET capping molecules. As pointed out above it is the freezing of the solvent that surrounds the QDs that hampers surface relaxation bringing the QD in the 'off' state. Due to the presence of charge at the QD surface the local freezing point lowers the transition temperature to below 273 K.

This local freezing point depression can also give insight in the question why the LTAQ of AET capped CdTe QDs is dependent on the QD size. For QDs the surface to volume ratio increases as the QD size decreases. Since AET is located at the QD surface, the charge density per volume is dependent on the size of the QD. Smaller QDs will therefore have a larger charge density per volume which gives a stronger freezing point depression in the local environment of the QD. Lower temperatures are needed to freeze the water in the direct surroundings of the AET at the QD surface. The overall effect is a lower quenching temperature of the exciton emission from the smaller QDs.

It is hard to obtain direct evidence for the presented model as it is not possible (in the present experiment) to probe the positions of the surface atoms of the CdTe QDs. To support the explanation presented above and provide evidence that indeed a liquid-solid phase transition in the solvent surrounding the QD is responsible for the LTAQ of CdTe QDs in water, additional experiments were performed.

To confirm that (local) freezing point depression is responsible for the lowering of the transition temperature for LTAQ the freezing point of the solvent can be lowered by addition of methanol. Figure 7.6 shows the temperature dependence of the integrated emission intensity of AET capped CdTe QDs (the mean size is 3.7 nm) without MeOH (spheres), with 12.5% of MeOH (stars) and with 25% of MeOH (diamonds). It was carefully verified that the addition of methanol to the solution of QDs did not result in flocculation. Figure 7.6 shows that the transition temperature decreases if more MeOH is added to the solution of QDs in water.

Since the freezing point of the solution is lowered by the addition of MeOH, the formation of ice at the QD surface is now not only hampered by the charge of the AET molecules but also by the MeOH molecules in the solvent. This experiment provides additional proof that (a phase transition in) the solvent is responsible for the quenching of the exciton luminescence. The previous experiments show the important role of both the solvent and the capping.

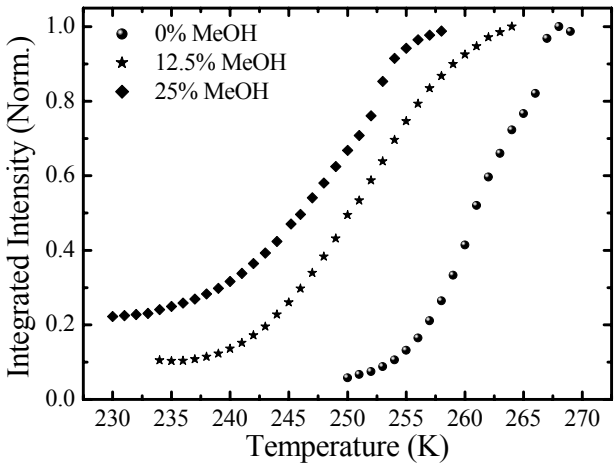

Figure 7.6 Integrated intensity of the emission spectra (λ_{ex}=400 nm) as function of sample temperature of AET capped CdTe QDs (d= 3.4 nm) in water and in water with methanol (12.5 vol% and 25 vol%).

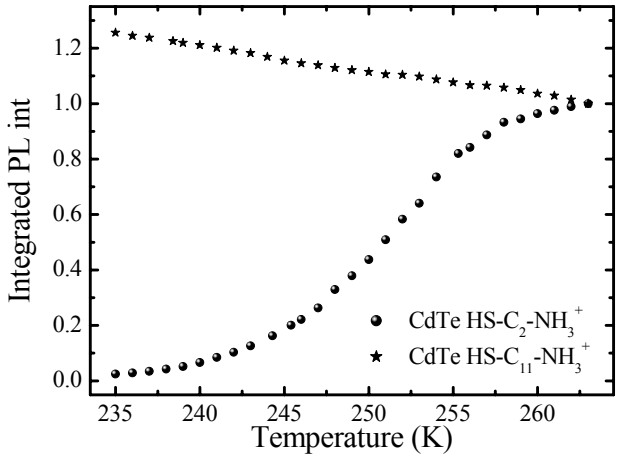

Figure 7.7 Temperature dependence of the integrated emission spectra (λ_{ex}=400 nm, normalized to the intensity at 263 K) of AET (C2, spheres) and AUT (C11, stars) capped CdTe QDs (d= 3.0 nm) in water.

To obtain a deeper understanding of the role of the capping, the influence of the length of the carbon chain of the capping molecules was investigated. Two identical samples of orange luminescing QDs (3.0 nm in diameter) were prepared, with a AET (C_2) and amino-undecanethiol (AUT, C_{11}) capping, respectively. Fig 7.7 shows the temperature dependence of the integrated emission intensity of AET capped (spheres) and AUT capped (stars) CdTe QDs in water.

For AET capped QDs the above reported LTAQ is observed. For AUT capped QDs a gradual temperature quenching of the luminescence instead of a sharp antiquenching is observed. The integrated luminescence intensity of the AUT capped CdTe QDs decreases with temperature in a similar manner as reported for TOPO capped CdSe QDs [18] and CdSe(ZnS) capped QDs [18, 19]. The absence of LTAQ for the AUT capped QDs indicates that surface relaxation is not hampered by the freezing of the solvent surrounding the QD. The reason for the difference in temperature dependence is ascribed to the length of the amino-alkylthiol molecule. Since the chain length has increased considerably for the AUT molecules fixation of the NH_3^+ outer head does not hamper a relaxation of the surface Cd and Te atoms since the movement can be dissipated in the long (C_{11}) chain. This prevents the LTAQ and the CdTe cores respond to the increasing temperature with a gradual decrease of the integrated intensity similar to that observed for CdSe(ZnS) QDs. The results shown in Fig 7.7 demonstrate the important role of both capping molecules and solvent on the luminescence behavior of semiconductor QDs.

7.4 Conclusions

The exciton luminescence of amino-ethanethiol (C_2) capped CdTe QDs in water is completely quenched when cooled below 230 K. The recovery of the luminescence is dependent on size and occurs over a very narrow temperature (<10 K) regime transition. The LTAQ is explained by the influence of a phase transition in the solvent on the surface relaxation of the CdTe QD. Local freezing point depression by the charged amine groups at the QD surface shifts the transition temperature to lower values. Freezing point lowering of the solvent by addition of methanol enhances this effect. No LTAQ is observed when a C_{11} amine thiol is used as capping. This demonstrates the crucial role of the solvent and capping molecules on the exciton luminescence properties of QDs.

References:

[1] A. P. Alivisatos, A. P. *J. Chem. Phys.* **1996**, 100, 13226
[2] C. B. Murray, C. R. Kagan, M. G. Bawendi, *Annu. Rev. Mater. Sci.* **2000**, 30*,* 545
[3] M. Bruchez Jr., M. Moronne, P. Gin, S. Weiss, A. P. Alivisatos, *Science* **1998**, 281*,* 2013
[4] B. Dubertret, P. Skourides, D. J. Norris, V. Noireaux, A. H. Brivanlou, A. Libchaber, *Science* **2002**, 298*,* 1759
[5] V. I. Klimov, A. A. Mikhailovsky, S. Xu, A. Malko, J. A. Hollingsworth, C. A. Leatherdale, H. Eisler, M. G. Bawendi, *Science* **2000**, 290*,* 314
[6] S. Coe, W. -K. Woo, M. G. Bawendi, V. Bulovic, *Nature* **2002**, 420*,* 800
[7] Z. A. Peng, X. Peng, *J. Am. Chem. Soc.* **2002**, 124, 3343
[8] D. V. Talapin, A. L. Rogach, E. V. Shevchenko, A. Kornowski, M. Haase, H. Weller, *J. Am. Chem. Soc.* **2002**, 124, 5782
[9] C. de Mello Donegá, S. G. Hickey, S. F. Wuister, D. Vanmaekelbergh, A. Meijerink, *J. Phys. Chem. B* **2003**, 107*,* 489
[10] D. V. Talapin,S. Haubold, A. L. Rogach, A. Kornowski, M. Haase, H. Weller, *J. Phys. Chem. B* **2001**, 105*,* 2260
[11] D. V. Talapin, A. L. Rogach, A. Kornowski, M. Haase, H. Weller, *Nano Lett.* **2001**, 1, 207
[12] S.F. Wuister, I. Swart, F. Van Driel, S. G. Hickey, C. de Mello Donegá, *Nano Lett.* **2003**, 3 503
[13] S. F. Wuister, A. Van Houselt, C. de Mello Donegá, D. Vanmaekelbergh, A. Meijerink, *Angew. Chem. Int. Ed*. **2004**, 43, 3029
[14] S. F. Wuister, F. Van Driel, A. Meijerink, *Phys. Chem. Chem. Phys.* **2003**, 5, 1253
[15] Y. Ebenstein, T. Mokari, U. Banin, *Appl. Phys. Lett.* **2002**, 80, 4033
[16] B. R. Fisher, H. J. Eisler, N. E. Stott, M. G. Bawendi, *J. Phys. Chem. B.* **2004**, 108, 143
[17] K. Leung, K. B. Whaley, *J. Chem. Phys.* **1999**, 110, 11012
[18] S. A. Crooker, T. Barrick, J. A. Hollingsworth V. I. Klimov, *Appl. Phys. Lett.* **2003**, 82, 2793
[19] G. W. Walker, V. C. Sundar, C. M. Rudzinski, A. W. Wun, M. G. Bawendi, D. G. Nocera, *Appl. Phys. Lett.* **2003**, 83, 3555

Chapter 8.

Temperature dependent energy transfer in CdTe quantum dot solids

Abstract

Efficiently luminescing colloidal CdTe QDs were used for the preparation of monodisperse and mixed size QD solids. Luminescence spectra and decay times of the QD emission were measured as a function of temperature to study energy transfer (ET) between the QDs. In the luminescence decay curves of the emission of the largest QDs (acceptors) a rise time of the luminescence signal is observed due to energy transfer from smaller QDs. Both the rise time (a measure for the energy transfer rate) and the luminescence decay time lengthen upon cooling. This is explained by a decreased dipole strength of the excitonic emission of the QDs in the solid due to the presence of a singlet and a lower lying triplet level. Studies of energy transfer in heteronuclear QD solids reveal that single step ET dominates.

8.1 Introduction

Quantum dots (QDs) are widely studied because of their size dependent electronic and optical properties [1, 2]. Recently, they have been used as building blocks for QD solids, that may find application in e.g. QD solid lasers [3] and QD based LEDs [4]. Energy transfer (ET) between neighboring QDs is an important process in these applications. Assuming ET via dipole-dipole interaction, the ET rate scales with the distance via an R^{-6} dependence [5]. Provided that there is spectral overlap (i.e. that the emission spectrum of the donor overlaps with the absorption spectrum of the acceptor) ET can occur between QDs in a QD solid. Since the exciton emission of the QDs has a large dipole moment at room temperature (reflected by the short radiative decay time) the ET rate can be fast if the distance between the QDs is sufficiently small [6-8]. Kagan *et al.* reported ET between TOPO capped CdSe QDs in an (ordered) QD solid [9, 10]. In a QD solid ET from smaller QDs (larger bandgap) to larger QDs (smaller bandgap) can occur due to the size distribution. Recently CdSe(ZnS) QDs were proposed for the preparation of a QD solid with engineered directional energy flows [5]. In a QD solid with a layered energy-gradient ET rates between QDs of 10^8-10^9 s^{-1} were reported. By fine-tuning the resonance conditions for ET, rates close to 10^{10} s^{-1} can be obtained [6, 7]. Up till now the work on ET in QD solids has involved room temperature measurements. In a few studies low temperature results were reported but temperature dependent studies of ET between QDs are still lacking.

In this chapter we report temperature dependent studies of ET in QD solids, both homonuclear (only orange emitting QDs) and heteronuclear (green and orange emitting QDs). QD solids were prepared from a solution of hexanethiol capped CdTe QDs. For these high quality QDs the luminescence decay curves are dominated by pure radiative decay. Time resolved measurements on QD solids show pronounced rise times in the luminescence decay curves of the larger QDs (acceptors) reflecting the ET rate from donors. Both the radiative decay rate and the ET rate decrease upon cooling, due to the smaller dipole moment of the excitonic emission at lower temperatures.

8.2 Experimental

The preparation of the CdTe QDs and of the CdTe QD solids was performed in a glovebox under a dry argon atmosphere.

Synthesis

Green emitting (λ_{em} ~ 550 nm, quantum efficiency of 10%) and orange emitting (λ_{em} ~ 600 nm, quantum efficiency of 27%) DDA capped QDs were prepared following a previously reported method (see ref. 11 for a detailed description). Capping exchange with hexanethiol (HT) was achieved by adding 200 µL

hexanethiol to 400 µL of the crude solution of CdTe QDs in the TOP/DDA coordinating mixture. These particles were either dissolved in anhydrous chloroform or used for the preparation of QD solids.
Quantum dot solids were prepared by combining green and orange luminescing QDs in their original liquid matrix (TOP/DDA) in the desired ratio of green to orange to a total volume of 400 µL. Capping exchange with hexanethiol was performed by addition of 200µL hexanethiol. After one day to allow for capping exchange this mixture was injected into 8 mL of anhydrous methanol to precipitate the QDs and remove most of the excess TOP, DDA and hexanethiol. The precipitate was removed from the methanol solution, redissolved in a small amount of hexane and slowly dried on a quartz substrate.

Apparatus

Emission spectra, recorded with a monochromator (Acton SP-300i, 0.3 m, 150 lines mm^{-1} grating, blazed at 500 nm) fitted with a Princeton Instruments liquid nitrogen cooled CCD camera, and luminescence decay curves were measured simultaneously using a PicoQuant laser (λ_{ex} = 406 nm, 2.5 MHz repetition rate, 55 ps pulse width) as excitation source. For luminescence lifetime measurements a monochromator (1350 lines mm^{-1} grating, blazed at 500 nm) in combination with a fast Hamamatsu photo-multiplier tube (H5738P-01) was used for light detection. The luminescence decay curves were obtained by time correlated single photon counting (TCSPC) via time-to-amplitude conversion (TAC) with a Time Harp 100 computer card. The ratio of stop to start pulses was kept low (below 0.05) to assure good statistics. Temperature-dependent photo-luminescence and lifetime measurements were carried out using a liquid helium flow-cryostat equipped with a sample heater to stabilize the temperature at different temperatures between 4 K and room temperature. Samples were first cooled to 4 K and slowly heated to room temperature.

8.3 Results and Discussion

8.3.1 QD solids prepared from homonuclear QDs

In this section the room temperature optical properties of the QDs used for the QD solids are discussed. Next the temperature dependence of the emission and luminescence decay curves of orange emitting CdTe QDs in solution and in a QD solid are discussed.
Figure 8.1 shows the absorption and emission spectra of a dilute solution of hexanethiol (HT) capped CdTe QDs in chloroform for two different sizes. The green emitting QDs (G-QDs) are 2.5 nm in diameter and show excitonic emission with a maximum at 555 nm. The orange emitting QDs (O-QDs) are

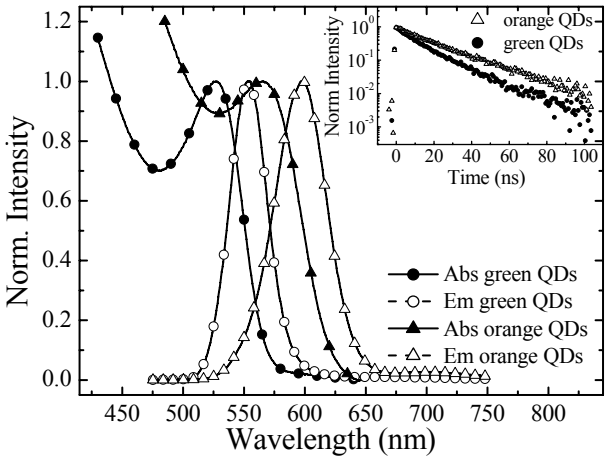

Figure 8.1 Normalized emission (λ_{ex} = 400 nm) and absorption spectra of green and orange luminescing hexanethiol capped CdTe QDs at room temperature. The inset shows luminescent decay curves (measured on the emission peak maximum, λ_{ex} = 406 nm) of both samples.

3.0 nm in size and emit at 600 nm (λ_{max}). The inset shows the luminescence decay curves for both samples measured at the exciton peak maximum. The luminescence decay of the O-QDs shows a monoexponential behavior [12] with a $\tau_{1/e}$ of 19 ns ($\tau_{1/e}$ is defined as the time at which the intensity reaches 1/e of its initial intensity). This luminescence decay time is the radiative decay time for CdTe QDs and shows the high quality of the O-QDs after capping exchange with hexanethiol. The decay of the G-QDs is not monoexponential and has a $\tau_{1/e}$ of 11 ns. This shorter decay is attributed to partial quenching of the exciton luminescence by surface and lattice defects. The fast initial luminescence decay reflects the presence of fast non-radiative processes which lower the quantum efficiency.

Figure 8.2 A shows the temperature dependent emission spectra of O-QDs (normalized to the emission maximum) in solution for two different temperatures (20 K and 200 K). A blue shift of the exciton peak is observed upon lowering the temperature which is explained by the temperature dependence of the band gap of CdTe [13,14]. The temperature dependence of the exciton decay time as function of temperature has been studied in the last years for CdSe QDs [15-17]. The lowest level has a triplet character (also called dark state) while a slightly higher energy level has a singlet character (bright state). The energy difference between these two levels is a few meV [15-17]. At low temperatures the excited state population of the QD will be mainly in the triplet state. The transition from

this state to the ground state is spin-forbidden and characterized by a long decay time (~1 μs) [16]. As the temperature increases the singlet state becomes increasingly thermally populated (Boltzmann distribution). Since the transition from the singlet excited state to the ground state is spin-allowed, the dipole strength of the exciton emission will increase with increasing temperature. As a result the radiative decay time decreases upon raising the temperature. For CdTe QDs a similar temperature dependence of the luminescence life time has been observed [18].

Figure 8.2 B shows the temperature dependence of the (normalized) emission spectra of a QD solid prepared from O-QDs. The excitonic emission is red shifted for all temperatures with respect to the exciton peak of the O-QDs in solution. This is evidence for the occurrence of ET in the QD solid. The QD ensemble used to prepare the QD solid is not monodisperse in size (~15% size dispersion). ET occurs from donors to nearby accepting QDs with a slightly smaller band gap (larger size) and this results in a red shift of the ensemble exciton emission peak. The significant enhancement of the defect related emission compared to the O-QDs in solution is also explained by ET. QDs with a defect act as a trap for the migrating energy. This leads to energy relaxation and the observation of defect related emission.

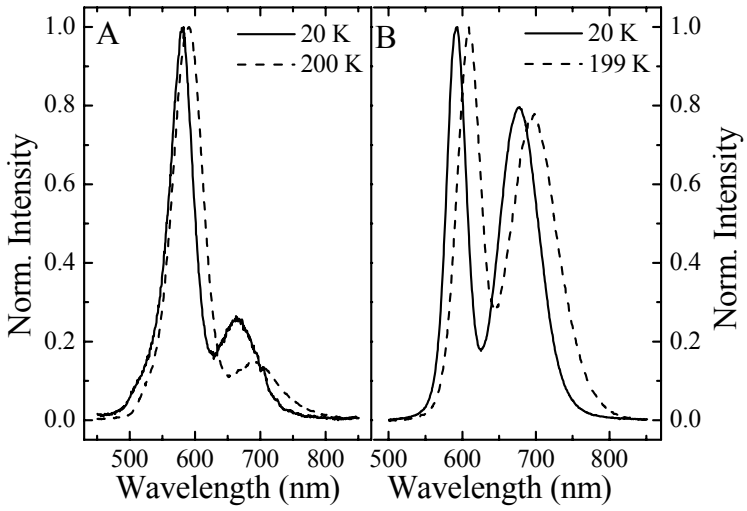

Figure 8.2 Normalized emission spectra (λ_{ex} = 406 nm) of orange luminescing HT capped CdTe QDs dissolved in chloroform (A) and as QD solid on quartz (B) recorded at 20 K (solid line) and 200 K (dashed line).

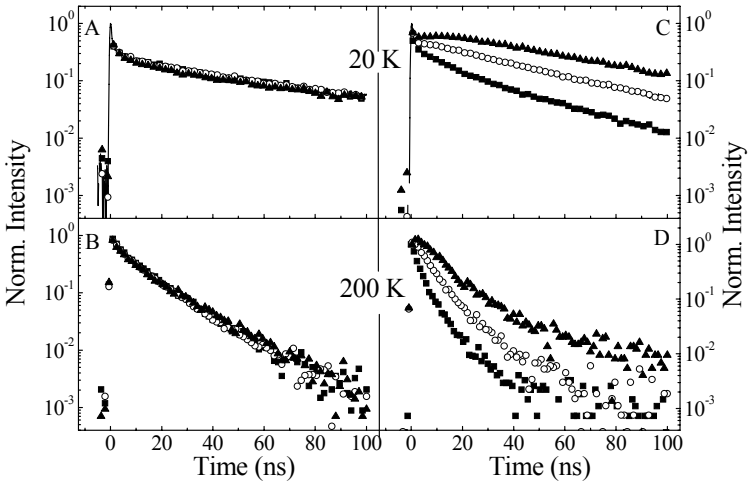

Figure 8.3 Normalized luminescence decay curves (λ_{ex} = 406 nm) of orange emiting hexanethiol capped CdTe QDs dissolved in chloroform (left) and as QD solid on quartz (right), recorded at 20 K and 200 K. The decay curves are measured at the exciton peak maximum (○),20 nm red shifted of the peak maximum (▲) and 20 nm blue shifted of the peak maximum (■).

Figure 8.3 shows the luminescence decay curves at 20 K (A) and 200 K (B) of O-QDs dispersed in chloroform. Each graph in Figure 8.3 shows three decay curves recorded at the emission maximum (○), 20 nm blue shifted from the emission maximum (■) and 20 nm red shifted from the emission maximum (▲). The dependence of the luminescence decay behavior on the emission wavelength isweak, indicating that ET is absent in these diluted QD solutions due to the large distance between the QDs. A longer luminescence decay time is observed at 20 K which becomes increasingly shorter at higher temperatures (200 K). At 20 K a fast initial decrease in the luminescence decay curve is also observed. This is ascribed to fast decay from the singlet level, similar to observations for CdSe QDs reported in ref. 16.

Figure 8.3 shows the luminescence decay curves of a QD solid of O-QDs at 20 K (C) and 200 K (D). At 20 K a fast initial drop in intensity is observed for all emission wavelengths and is due to singlet emission before thermal equilibrium is reached between the singlet and the triplet state. Contrary to the situation for the QDs in solutions, the luminescence decay curves are strongly dependent on the emission wavelength at both temperatures: the decay curves recorded at the shorter emission wavelength (in purple, corresponding to the smaller QDs) show

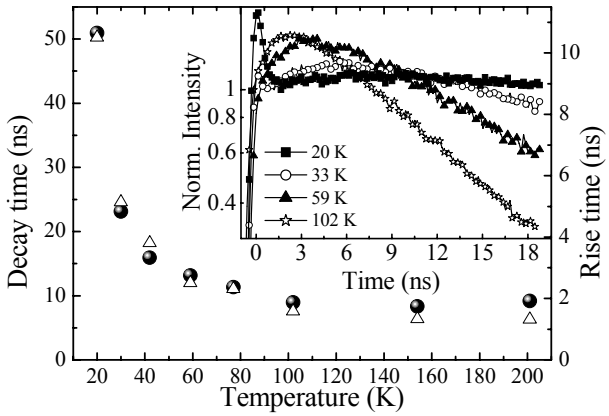

Figure 8.4 Luminescence decay (●) and rise time (△) of a QD solid on quartz, prepared from orange luminescing hexanethiol capped CdTe QDs recorded as function of temperature, measured 20 nm red shifted of the excitonic peak maximum. The inset shows an enlargement of the normalized luminescence decay curves at different temperatures in the first 18 nanoseconds.

a faster decrease in emission intensity than the decay curves recorded at longer wavelengths. In contrast to the fast decay for the smaller QDs, a rise in the luminescence intensity is observed in the curves for the emission at longer wavelength (filled triangles, corresponding to the larger QDs). This is due to feeding by ET from smaller QDs to the larger QDs.

The strong wavelength dependence of the luminescence decay curves provides clear evidence that efficient ET occurs from the smaller O-QDs to the larger O-QDs in the CdTe QD solids. Qualitatively, the results are similar to time-resolved studies reported for CdSe QD solids [5,6]. The smallest QDs, emitting at the shortest wavelength, have a large number of neighboring acceptors to which ET can occur. As a result these QDs have the shortest luminescence decay time. The largest O-QDs act as acceptors only and show, after a rise time due to feeding by ET from the smaller QDs, an exponential decay reflecting the radiative decay rate (Figure 8.3 C and D, filled triangles). A quantitative analysis of the ET rates is complicated by several factors. The luminescence decay curves for the small QDs (the donors) are strongly non-exponential due an inhomogeneous distribution of acceptors around the donors. In addition, both non-radiative decay and ET to non-luminescent QDs may contribute to the observed decay curves of the luminescence for QD donors. The luminescence decay curves of the acceptors shows an initial rise of the luminescence intensity with a rise time that is related to the transfer rate from the donating to the accepting QDs. Analysis of the rise time gives information on the transfer rate from the donor QDs. To

obtain information on the temperature dependence of the ET rate, the decay curves of the acceptor emission (recorded 20 nm red shifted of the emission maximum) were fitted to a bi-exponential function:

$$y(t) = y_0 + A_1 e^{+\tau 1/t} + A_2 e^{-\tau 2/t} \tag{8.1}$$

where y_0 is the off-set (noise level), $\tau 1$ is the rise time of the luminescence intensity and $\tau 2$ is the luminescence decay time. Figure 8.4 presents the decay times (dots, left-hand axis) and rise times (stars, right-hand axis) as a function of temperature. The inset of figure 8.4 shows the first 18 ns of the luminescence decay curves of the acceptors, showing the rise time in more detail than in Figure 8.3. Figure 8.4 shows that the rise and decay time have the same temperature dependence. Over the full temperature range the rise time is proportional to the decay time of the QD emission. This is an interesting observation. For ET via dipole-dipole interaction the ET rate is expected to be proportional to both the donor and acceptor oscillator strengths (see also below). In the present situation the oscillator strength of the transition on the acceptor can be assumed to be constant as a function of temperature (the donor emission overlaps with the same excitation transitions on the acceptor). But the oscillator strength of the donor emission is strongly temperature dependent and decreases at lower temperatures due to an increase of population in the triplet excited state upon cooling. The fact that the experimentally observed ET rate scales with the (radiative) decay rate over the full temperature range gives evidence that the ET proceeds via dipole-dipole interaction. ET via an exchange interaction mechanism can be excluded since for this mechanism the transfer rate is not influenced by the dipole strengths of the donor and acceptor transitions [19], but only by the overlap between the donor and acceptor wavefunctions.

From the values of the rise time an estimate can be made of the ET rate. The rise time at 20 K is about 10 ns and it drops to about 1 ns at 200 K. The rise time is much shorter than the radiative decay time, showing that ET has a higher probability than radiative decay. The corresponding ET rates are 10^8 s^{-1} at 20 K and increase to 10^9 s^{-1} at 200 K. As indicated above, these numbers give the order of magnitude of the average ET rates from the donor QDs to multiple acceptors and cannot be taken as an accurate ET rate between one nearest neighbor donor-acceptor pair. Nevertheless, it is interesting to compare the experimentally observed transfer rate with the theoretically calculated transfer rate. Using the Förster theory the ET rate via dipole- dipole interaction can be derived to be [20]:

$$k_{\text{Förster}} = \frac{Q_D}{\tau_D}\left(\frac{8.785 \cdot 10^{-25} I}{n^4 R^6}\right) \tag{8.2}$$

where Q_D quantum efficiency of the donor (1), τ_D is the radiative decay time of the donor (19 ns), *n* is the refractive index of the surrounding media (2.2) and *R* is the distance between the dipoles. The overlap integral I is given by:

$$I = \int_0^\infty \alpha_A(\lambda) f_D(\lambda) \lambda^4 d\lambda \tag{8.3}$$

where α_A is the extinction coefficient of the acceptor (1.5 10^5 M^{-1} cm) , f_D is the oscillator strength of the donor (1.4 10^{-12}) and λ is the absorption or emission wavelength (550 nm). Using these numbers an ET rate at room temperature of 1.5 10^9 s^{-1} is calculated for ET between nearest neighbors at 3.5 nm, the expected average distance between the O-QDs. The calculated ET rate is of the order of magnitude of the experimentally observed ET rate.

8.3.2 Heteronuclear QD solids

In addition to using the polydispersity of a sample of QDs to observe ET, also QD solids prepared from two sizes of QDs were used to study the ET between the QDs. Two QD solids have been prepared with a molar ratio of G-QDs:O-QDs of 9:1 and 165:1. Temperature dependent emission spectra are shown at two temperatures (20 K and 200 K) in figure 8.5 for a QD solid with a G-QDs:O-QDs ratio of 9:1 (A) and 165:1 (B). In Figure 8.5 A three emission peaks are observed

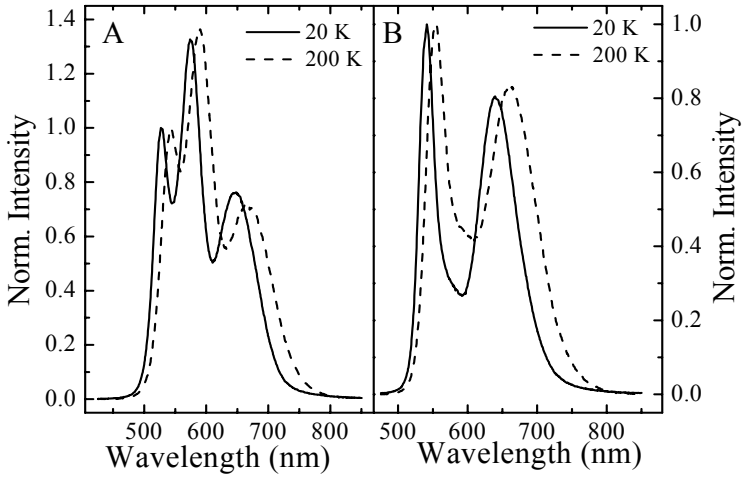

Figure 8.5 Normalized emission spectra (λ_{ex} = 406 nm) of mixed hexanethiol capped CdTe QD solids on quartz. The ratio of green luminescing QDs to orange luminescing QDs is 9:1 (A) and 165:1 (B).

over the full temperature regime: a peak around 550 nm (the excitonic emission from the G-QDs), a peak around 590 nm (the excitonic emission from the O-QDs) and a broad band around 675 nm which is ascribed to the defect related emission of both G-QDs and O-QDs. The relative intensities of the green and orange emission remain constant in the temperature range from 20 K- 200 K. This can be understood since both the radiative decay and the ET rate are dependent on the dipole strength of the exciton emission (as discussed above, see figure 8.4). For the QD solid with the 165:1 ratio (figure 8.5 B) an emission peak around 550 nm is clearly visible corresponding to the excitonic emission of the G-QDs. The broad peak around 650 nm is ascribed to the defect related emission of the G-QDs. The exciton emission of the O-QDs is present as a weak shoulder between these two peaks. With temperature this peak increases in intensity with respect to the exciton emission of the G-QDs, but the emission from the O-QDs is weak over the temperature range studied. For both samples the intensity ratio of the excitonic and defect related emission is almost independent of the sample temperature between 20 K to 200 K. The emission spectra of the mixed QD solids show that in the presently studied QD solids the ET is dominated by single step energy transfer from donors to acceptors. In the 9: 1 mixed QD solid the acceptor concentration is high and 60-70% of the G-QD donors have one or more O-QDs as nearest neighbors and efficient donor-acceptor ET is observed. The probability of finding one or more O-QDs as nearest neighbors is dependent on the coordination number in the QD solid. Since the here studied QD solids are not expected to be ordered the coordination number was varied between 8 (BCC packing) and 12 (FFC/HCP packing) to get an estimate for the probabilities.

In the 165: 1 sample the ET from the G-QD donors to the O-QD acceptors is not probable by direct ET due to the low acceptor concentration: only 5-7% of the G-QDs have a O-QD as nearest neighbor. The absence of a significant fraction of orange emission shows that ET via (multi-step) energy migration over the G-QDs is not efficient. This is also reflected in the ratio of the intensities of the exciton peak of the G-QDs and the O-QDs in the 9:1 sample. Based on only radiative emission from the QDs, the intensity ratio of the G-QDs:O-QDs, after correction for the QEs, should be 10:3. However, the emission of the O-QDs is much stronger than expected: an intensity ratio of approximately 10:17 is observed. From the difference in these two ratios it was calculated that 50% of the G-QDs transfers its excitation energy to O-QDs. The probability of finding a G-QD that has one or more neighboring O-QDs is 60% to 70% in a QD solid with a G-QDs:O-QDs ratio of 9:1. This shows that nearly all G-QDs that have a O-QD as neighbor, transfer their energy, indicating that ET between nearest neighbors is a very efficient process compared to radiative decay, as expected from the rates estimated above (at room temperature the ET rate is $2\ 10^{9}\ s^{-1}$ and the radiative decay rate is $5\ 10^{7}\ s^{-1}$).

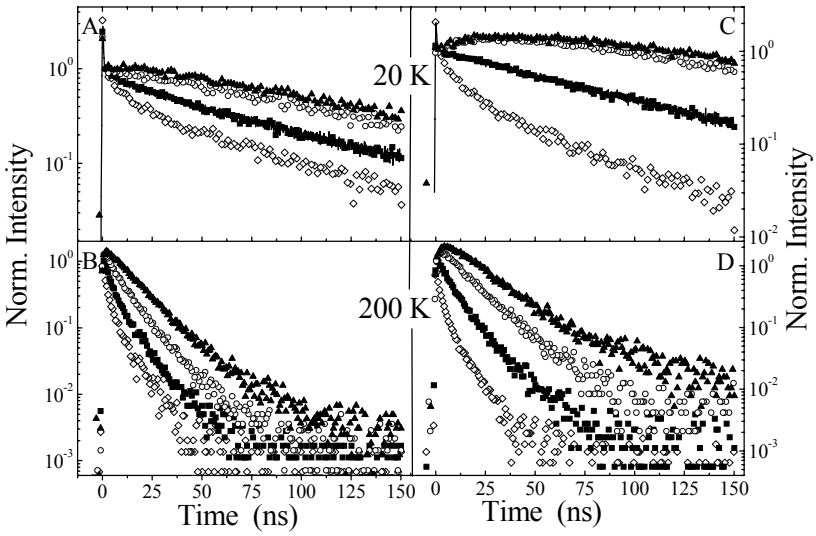

Figure 8.6 Normalized luminescence decay curves (λ_{ex} = 406 nm) of mixed hexanethiol capped CdTe QDs as QD solid on quartz, recorded at 20 K and 200 K. The ratio of G-QDs to O-QDs is 9:1 (A and B) and 165:1 (C and D). The decay curves are measured at the exciton peak maximum of the G-QDs (■),20 nm red-shifted of this peak maximum(○), 20 nm blue-shifted of this peak maximum(◇) and at the exciton peak maximum of the O-QDs(▲).

Figure 8.6 shows the luminescence decay curves of the QD solid with a G-QD:O-QD ratio of 9:1 at two selected temperatures: 20K (A), and 200K (B) and of the QD solid with a G-QD:O-QD ratio of 165:1 at 20K (C), and 200K (D) In each graph four curves are depicted, all recorded at different emission wavelengths: at the excitonic peak maximum of the G-QDs (■), 20 nm blue shifted (◇) or red shifted (○) of this peak maximum and at the excitonic peak maximum of the O-QDs (▲). A similar wavelength dependence of the decay curves is observed as in figure 8.3: the luminescence decay is faster at shorter wavelengths and becomes faster as the emission wavelength (i.e. the particle size) increases. This shows that ET occurs in both heteronuclear QD solids. Comparing the luminescence decay curves of the two heteronuclear QD solids, interesting differences are observed. At 200 K the decay curves recorded 20 nm blue shifted from the G-QDs exciton peak maximum are identical, showing that the ET rate of the smallest particles in both solids is comparable. For the O-QDs (red curves) the rise time is more pronounced in the sample with a G-QDs:O-QDs ratio of 165:1. The rise time in the decay curves of these QDs reflects their role as acceptors. The main difference between the two heteronuclear QD solids is the concentration of O-QD. For the QD solids with a G-QDs:O-QDs ratio of 9:1 the

higher O-QD concentration gives rise to a probability of finding a larger O-QD as nearest neighbor for an O-QD of 30-35%, while for the QD solid with a G-QDs:O-QDs ratio of 165:1 this probability is 2-4%. ET between two O-QDs will diminish the rise time of the (smaller) O-QDs. Since the probability of finding one or more O-QDs as nearest neighbors is much larger in the QD solid with a G-QDs:O-QDs ratio of 9:1, the rise time of the O-QDs is less pronounced due to ET between O-QDs. In the QD solid with a G-QDs:O-QDs ratio of 165:1 the ET between O-QDs is negligible. For this QD solid the rise in intensity observed in the decay curve of the O-QDs reflects the feeding by G-QDs.

8.4 Conclusions

QD solids are prepared from efficiently luminescing colloidal CdTe QDs. Energy transfer (ET) is observed in both homonuclear and heteronuclear QD solids from smaller to larger QDs. Both the radiative decay rate and the ET rate are dependent on temperature and decrease upon cooling. The rise times in the luminescence decay curves of the larger (energy accepting) QDs reflect the ET rate. Over the temperature range studied here the ET rates are observed to be proportional to the radiative decay rate which is consistent with a dipole-dipole mechanism for ET. Studies of ET in heteronuclear QD solids show that ET is dominated by a single step ET process.

References:

[1] A. P. Alivisatos, *J. Chem. Phys.* **1996**, 100, 13226
[2] L. E. Brus, *J. Chem. Phys.* **1986**, 90, 2555
[3] V. I. Klimov, A. A. Mikhailovsky, S. Xu, A. Malko, J. A. Hollingsworth, C. A. Leatherdale, H. Eisler, M. G. Bawendi, *Science* **2000**, 290*,* 314
[4] S. Coe, W.-K. Woo, M. G. Bawendi, V. Bulovic, *Nature* **2002**, 420*,* 800
[5] S. A. Crooker, J. A. Hollingsworth, S. Tretiak, V. I. Klimov *Phys. Rev. Lett.* **2002**, 89, 186802-1
[6] M. Achermann, M. A. Petruska, S. A. Crooker, V. I. Klimov *J. Phys. Chem. B* **2003**, 107, 13782
[7] T. Franzl, D. S. Koktysh, T. A. Klar, A. L. Rogach, J. Feldmann, N. Gaponik, *Appl. Phys. Lett.* **2004**, 84, 2904
[8] T. Förster, *Naturwissenschaften*, **1946**, 33, 166
[9] C. R. Kagan, C. B. Murray M. Nirmal, M. G. Bawendi, *Phys. Rev. Lett.* **1996**, 76, 1517
[10] C. R. Kagan, C. B. Murray, M. G. Bawendi, *Phys. Rev. B* **1996**, 54, 8633
[11] S.F. Wuister, F. Van Driel, A. Meijerink, *Phys. Chem. Chem. Phys.* **2003**, 5, 1253
[12] S. F. Wuister, I. Swart, F. Van Driel, S. G. Hickey, C. de Mello Donegá, Nano Lett. **2003**, 3, 503
[13] J.F. Suyver, T. van der Beek, S. F. Wuister, J. J. Kelly, A. Meijerink. *Appl. Phys. Lett.* **2001**, 79, 4222
[14] Y. P. Varshni, *Physica,* **1967**, 34, 149
[15] M. Nirmal, D. J.Norris, M. Kuno, M.; M. G. Bawendi,. Al. L. Efros,; M. Rosen, *Phys. Rev. Lett.* **1995**, 75, 3728
[16] O. Labeau, P. Tamarat, B. Lounis, *Phys. Rev. Lett.* **2003**, 90, 257404-1
[17] Al. L. Efros, M. Rosen, M. Kuno, M. Nirmal, D.J. Norris, M. G. Bawendi, *Phys. Rev. B* **1996**, 54, 4843
[18] C. de Mello Donegá, C. Kleijer, A. Meijerink, unpublished
[19] G. Blasse and B. C. Grabmaier, *Luminescent materials*, Springer-Verlag
[20] G. D. Scholes, *Annu. Rev. Phys. Chem.* **2003**, 54, 57

Chapter 9

Efficient energy transfer between nanocrystalline YAG:Ce and TRITC

Luminescent nanocrystalline (NC) Ce^{3+}-doped yttrium aluminum garnet ($Y_3Al_5O_{12}$:Ce - YAG:Ce) is prepared by a combustion synthesis technique that yields a highly porous three-dimensional network of interconnected 18 nm nanocrystals. Tetramethyl rhodamine isothiocyanate (TRITC) was conjugated to NC YAG:Ce by using glycine as a bridging molecule. Efficient energy transfer is observed from the Ce^{3+} ions to the TRITC molecules upon photoexcitation of the NC YAG:Ce – TRITC conjugates.

9.1. Introduction

Resonant energy transfer (ET) between a donor in the excited state and a neighboring acceptor is commonly observed between dyes [1], quantum dots and dyes [2,3], quantum dots [4,5], and metal ions [6]. The ET process can occur via several mechanisms, but the electric dipole-electric dipole interaction is the most effective one over relatively long distances (up to several tens of angstroms, with a r^{-6} distance dependence) [6]. This mechanism is particularly efficient when both donor and acceptor have allowed electric dipole resonant transitions.

ET between suitable probes can be used to obtain structural information or monitor dynamic processes in biological systems but its usefulness is severely limited by fast photobleaching when dyes are used for tagging the target molecules. Semiconductor quantum dots are more stable then dyes [7] but still suffer from photoinduced degradation processes. Luminescent ions in inorganic phosphors offer the prospect of a greatly superior photo-stability associated with high quantum yields. Intermittence in emission (blinking), which is a problem in certain applications of single quantum dots, is not expected for inorganic phosphor nanocrystals as they contain a large number of luminescing ions (typically between 10 and 10000 depending on the size of the nanocrystal and the concentration of luminescing ions). In the past few years there has been a growing interest in the properties of nanocrystalline lanthanide-doped insulating phosphors, and several well-known materials, such as $Y_2O_3:Eu^{3+}$ [8-9], $Lu_2O_3:Eu^{3+}$ [10], $YVO_4:Eu^{3+}$ [11], $LaPO_4:Ln^{3+}$ (Ln= Eu or Ce/Tb [12]), $YbPO_4:Er^{3+}$ [13], and $Y_3Al_5O_{12}:Ln^{3+}$ Ln= Nd, Eu, Tb, Tm or Ce [14-18]), have been prepared in nanocrystalline form. The application of lanthanide-doped nanocrystalline phosphors as biological labels would however strongly limit the photon turnover rates due to the long (μs to ms) decay time of their intraconfigurational $4f^n$ luminescence. One of the few exceptions for visible-emitting phosphors is $Y_3Al_5O_{12}:Ce$ (YAG:Ce). In YAG:Ce the 5d state of Ce^{3+} is situated at a low energy resulting in a fast intraconfigurational 5d→4f luminescence in the visible. The luminescence life time of this emission is 65 ns [19]. This luminescence decay time is ideally suited for time-gated detection of biological species, since it is slower than the autofluorescence background decay common to many biological species (typically a few ns), but is still fast enough to ensure a high turnover rate. Additional attractive features are the excitation in the blue (which further decreases the autofluorescence background obtained under UV excitation) and the large stokes shift of the luminescence. The strong electric dipole of the Ce^{3+} f-d emission also makes NC YAG:Ce a promising candidate as donor for efficient ET processes to dyes.

In order to evaluate the potentiality of NC YAG:Ce as a probe in biological systems the ET from NC YAG:Ce to tetramethyl rhodamine isothiocyanate (TRITC) was investigated. TRITC is chemically conjugated to highly

luminescent NC YAG:Ce by using glycine as a linker molecule. Steady state (excitation and emission spectra), time-domain (fluorescence decay times) measurements and photobleaching experiments clearly demonstrate the occurrence of ET from Ce^{3+} to TRITC molecules in the NC YAG:Ce - TRITC conjugates.

9.2 Experimental

Nanocrystalline YAG:Ce (0.5 mol%) was prepared by using a combustion synthesis technique similar to that reported in [9], but optimized to yield nanoparticles smaller than 20 nm with a small degree of sintering. Glycine was used as a fuel and the metal nitrates as oxidizers. Typically, 3 mmol of $Ln(NO_3)_3.4H_2O$ (Ln= Y and Ce), 5 mmol of $Al(NO_3)_3.9H_2O$ and 14 mmol of glycine were dissolved in 4 mL of demi-water and the resultant solution was dried overnight at 80^{o}C. The resulting transparent gel was placed into a preheated furnace at 650^{o}C for 30 minutes in air. The as-synthesized product was a foamy porous gray body, which was shown by X-ray powder diffraction to be amorphous. This product was subsequently treated at 1150^{o}C for 90 s under air, yielding a highly porous yellow body.

Steady-state emission and excitation spectra were recorded with a SPEX Fluorolog spectrofluorometer, model F2002, equipped with two monochromators (double-grating, 0.22 m, SPEX 1680) and a 450 W xenon lamp as the excitation source. Luminescence decay curves were measured using a Pico Quant PDL 800-B laser (λ_{ex}=440 nm, 2.5 MHz repetition rate, 55 ps pulse width) as an excitation source. The luminescence was dispersed by a monochromator (0.1 m focal length, 1350 lines/mm grating, blazed at 500 nm) and detected by a fast Hamamatsu H5738P-01 photomultiplier tube. The decay curves were obtained by time correlated single photon counting (TCPCS) via time-to-amplitude conversion (TAC) with a Time Harp 100 computer card. The ratio of stop to start pulses was kept low (below 0.05) to assure good statistics.

9.3 Results and discussion

Figure 9.1 shows the X-ray powder diffraction patterns of the final product and of a microcrystalline powder sample of YAG:Ce (commercial phosphor purchased from Nichia Co.). It can be concluded that the product consists of single phase crystalline YAG. The peak broadening and the small shift of the peak maxima to lower angles can be ascribed to a finite size effect, indicating that the sample consists of nanocrystalline domains. The mean size of these domains, determined from the full width at half maximum of the peak with the Debye-Scherrer formula [20] is 18 nm. Thermal treatments at temperatures higher than 1150^{o}C and/or for longer times yield larger average nanocrystal sizes and more pronounced sintering. Temperatures below 1000^{o}C yield amorphous

white samples (non-luminescent). The use of other fuels such as urea or citric acid leads to slightly larger YAG:Ce nanocrystals (23 nm), lower quantum yields and a larger degree of sintering.

The NC YAG:Ce samples are highly friable and can be easily ground to a powder and broken apart into NC clusters (100-1000 nm) by sonic waves (sonic bath). The transmission electron microscopy (TEM) image of one such NC YAG:Ce cluster is depicted in figure 9.2A, which clearly shows that the NC YAG:Ce samples consist of a highly porous and interconnected three-dimensional network of nanoparticles. The high degree of crystallinity of these YAG:Ce nanoparticles is confirmed by both high-resolution TEM (figure 9.2B) and selected area electron diffraction (inset of figure 9.2A. The size of the YAG:Ce nanocrystals obtained from TEM and HR-TEM is consistent with the average size determined from XRD (~20 nm).

To conjugate TRITC to NC YAG:Ce a portion of 35 mg NC YAG:Ce (a slightly yellow powder) in 10 mL ultra-pure water was mixed thoroughly with 35 mg glycine (aminoacetic acid) and left overnight. Excess of glycine was removed by centrifuging and several times rinsing with ultra pure water. Glycine was chosen as the linker molecule because it can bind to both TRITC and NC YAG:Ce. The carboxylic group of glycine is expected to strongly bind to the surface of the YAG:Ce nanocrystals via the Y^{3+} and Al^{3+} ions, whereas its primary amine group reacts with the isothiocyanate group of TRITC. The use of TRITC as functionalised dye allows for selective excitation of the YAG:Ce at 440 nm since the absorption of TRITC at this wavelength is very low. A disadvantage of TRITC as a dye is the spectral overlap between the emission of YAG:Ce and TRITC which complicates a quantitative analysis of the energy transfer

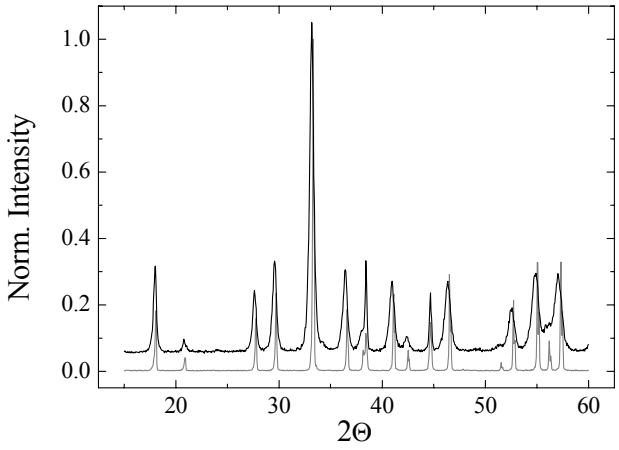

Figure 9.1. X-ray powder diffraction patterns (Cu Kα) of NC YAG:Ce (black) and microcrystalline YAG:Ce (dark gray).

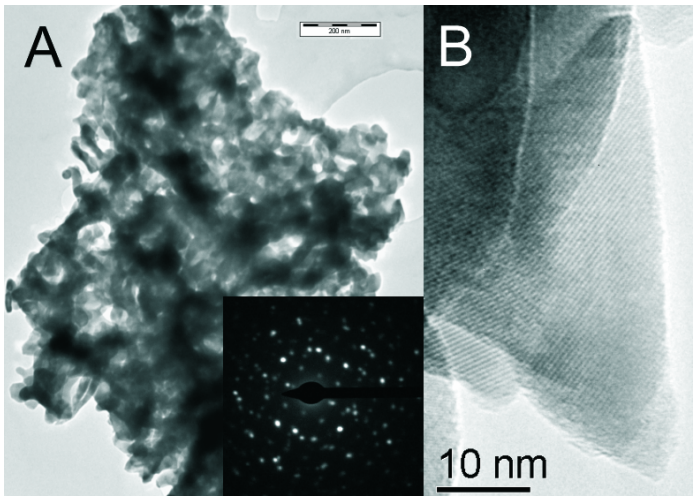

Figure 9.2. (A) Transmission electron micrograph of NC YAG:Ce. A selected area electron diffraction pattern is presented in the inset. Figure 9.2 (B) shows a HR-TEM image of a selected region in the same sample of NC YAG:Ce.

efficiency from the emission spectra. To the glycine capped NC YAG:Ce 35 μg of TRITC in 10 mL methanol was added and the sample was left overnight. The excess of TRITC was removed by centrifuging and rinsing twince with methanol. The sample (hereafter named TRITC-NC YAG:Ce conjugate) is a light pink powder and was dried in air prior to characterization. It should be mentioned that treatment of YAG:Ce with glycine and Rhodamine B (a dye molecule similar to TRITC, but without the isothiocyanate group) did not lead to a dye-NC YAG:Ce conjugate, showing that the presence of an isothiocyanate group is crucial for the formation of the conjugate.

Figure 9.3 shows the excitation spectra (A, λ_{em} = 580 nm) and emission spectra (B, λ_{ex} = 440 nm) of tetramethyl rhodamine isothiocyanate (TRITC) in water (dark gray curves), NC YAG: Ce (light gray curves) and TRITC-NC YAG:Ce conjugate (black curves). The emission spectrum of NC YAG:Ce (0.5 mol%) consists of a broad band with maximum around 550 nm that is ascribed to a 5d→4f transition. The 4f→ 5d excitation transitions yield broad bands at around 260 nm (not shown), 340 nm and 450 nm. The band at 260 nm is very weak because the upper 5d states of Ce^{3+} in YAG have energies within the conduction band of the host and therefore excitation in these levels results mainly in quenching [19]. The Ce^{3+} 5d level populated by the transition occurring at 340 nm is just below the YAG conduction band and will also be quenched to some

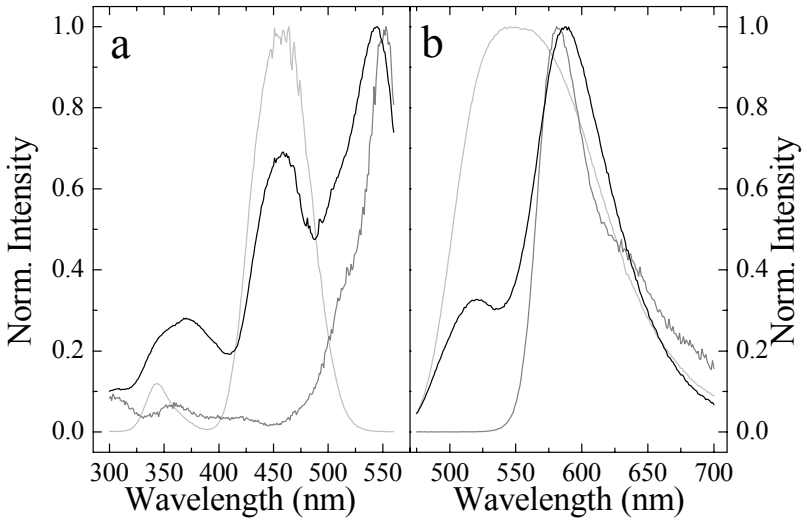

Figure 9.3 (a) Normalized excitation spectra (λ_{em} = 580 nm) and (b) emission spectra (λ_{ex} = 440 nm) of NC YAG:Ce (light gray), TRITC (dark gray), and YAG:Ce-TRITC conjugate (black).

extent at room temperature [19]. There are no significant differences between the emission and excitation spectra of NC YAG:Ce and bulk YAG:Ce, as expected considering that the band-gap of YAG is very large (7 eV) and that the electronic transitions involved in the luminescence are localized on the Ce^{3+} ion. Quantum size effects, as observed for the luminescence of nanocrystalline semiconductors, are not expected for the luminescence of Ce^{3+} in NC YAG. The quantum efficiency of the NC YAG:Ce sample is lower than that of a bulk sample (~50% at λ_{ex} = 430 nm, instead of the 70% observed for commercial Nichia phosphor).
The lower quantum efficiency of the nanocrystalline samples can be ascribed to a decrease in the excitation efficiency due to light scattering and to quenching and competitive absorption by surface defects (e.g. oxygen vacancies and/or disorder at grain boundaries [19]). The quantum efficiencies can be improved by longer thermal treatments or higher temperatures, which however lead to undesired nanocrystal growth and sintering. The luminescence quantum efficiency is given by the number of emitted photons divided by the number of absorbed photons, and was determined by comparison with standard phosphors, following the method of de Mello Donega et. al. [21]. This method is accurate within 10%.
It is clear from the excitation spectra in Figure 9.3a that selective excitation of NC YAG:Ce is possible at 440 nm (TRITC hardly absorbs at this wavelength). The black curve in Figure 9.3b shows the emission spectrum of TRITC- NC

YAG:Ce conjugate under 440 nm excitation. The weak band around 520 nm can be ascribed to Ce^{3+} emission, while the peak around 580 nm is due to TRITC emission. This provides a clear indication that ET from Ce^{3+} ions to TRITC takes place, since the TRITC emission dominates the emission spectrum despite its negligible absorption at 440 nm, whereas the strong absorption of YAG:Ce at 440 nm yields only a weak Ce^{3+} luminescence. We would like to point out that the spectral overlap between the emission of the donor and the absorption of the acceptor, needed for ET via dipole-dipole interaction, is good since the maximum of the donor (Ce^{3+}) emission and the acceptor (TRITC) absorption band are both situated around 550 nm. In the excitation spectrum of TRITC- NC YAG:Ce conjugate (Figure 9.3a, black curve) the peak at ~550 nm is due to direct excitation of the TRITC. The peak around 450 nm is ascribed to direct excitation of Ce^{3+} ions. It is noteworthy that the relative intensity of the peak around 375 nm for the TRITC- NC YAG:Ce conjugate is larger than expected by a simple convolution of the excitation bands of NC YAG:Ce and TRITC, suggesting an increased excitation efficiency due to resonance between the Ce^{3+} 5d level at 3.64 eV (340 nm) and TRITC excited states. This resonance would lead to efficient ET between the two levels, competing with the depopulation of the Ce^{3+} 5d level via the YAG conduction band.

The observation of Ce^{3+} excitation bands in the excitation spectrum of the TRITC emission at 580 nm in the conjugate sample provides further evidence for the occurrence of $Ce^{3+} \rightarrow$ TRITC ET, but it is not unambiguous since the broad emission band of Ce^{3+} overlaps with the emission of TRITC. The luminescence decay curve of the Ce^{3+} emission provides a more direct way to probe whether $Ce^{3+} \rightarrow$ TRITC ET is indeed taking place. Figure 9.4 shows the luminescence decay curves of NC YAG:Ce (in light gray) and of TRITC- NC YAG:Ce conjugate (in black). The decay curves are recorded monitoring luminescence at 520 nm to avoid detection of the TRITC emission. The decay curve of the Ce^{3+} ions in YAG is nearly monoexponential and has a decay time of 60 ns. This is very close to the reported decay time of Ce^{3+} ions in bulk YAG sample (65 ns [19]). This is surprising since the effective refractive index is lower in NC YAG:Ce than in the bulk material due to the presence of a lower refractive index material (liquid helium or air) around the nanocrystals and within a distance of the order of the wavelength of light. It is expected that, through local field effects, the lower effective refractive index would reduce the radiative decay rate of the Ce^{3+} emission in NC YAG:Ce in comparison with the bulk. This effect has already been observed for NC $Y_2O_3:Eu^{3+}$ [22]. In the case of NC YAG:Ce, however, the filling fraction is not known, what makes the comparison with the previous studies on NC $Y_2O_3:Eu^{3+}$ difficult. Further, non-radiative processes are more important for the nanocrystal than for the bulk materials due to the larger surface to volume ratio, which is reflected in an initial deviation from single-exponential decay and a lower quantum efficiency. The slightly faster initial

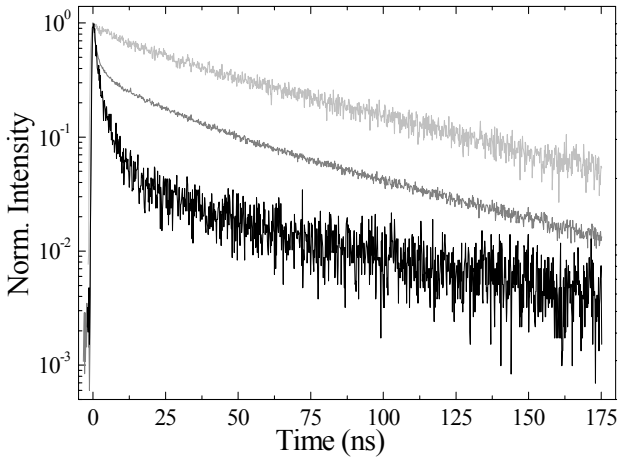

Figure 9.4 Luminescence decay curves (λ_{ex} = 440 nm, λ_{em} = 520 nm) of NC YAG:Ce (light gray) and YAG:Ce-TRITC conjugate (black). The decay curve of YAG:Ce-TRITC conjugate after photobleaching is shown in dark gray.

decay, observed for NC YAG:Ce can explain why the luminescence decay time measured, defined as the time at which the emission intensity has dropped to 1/e of its initial value, is shorter for the NC YAG:Ce despite the lower effective refractive index. For the TRITC- NC YAG:Ce conjugate (black curve) a fast initial decay in the luminescence intensity of the Ce^{3+} ion is observed, indicating the presence of an additional decay channel for the Ce^{3+} ions in the conjugate, which can be ascribed to resonant ET from the 5d excited states of Ce^{3+} in YAG to acceptor excited states of TRITC molecules at the nanocrystal surface. Radiative transfer from the Ce^{3+} ions to the TRITC molecules may also occur, but would not lead to shorter life times for the donor states. The fact that coupling to TRITC results in significantly faster luminescence decay curve shows that non-radiative energy transfer via dipole-dipole interaction is dominant. The *average* ET rate can be estimated from the decay curves and is ~ 10^8 - 10^9 s^{-1}. Since both the Ce^{3+} and the TRITC emissions are allowed electric-dipole transitions, the dipole-dipole interaction will be strong allowing efficient ET to occur if the Ce^{3+}-TRITC distances are sufficiently small. Using the Förster-Dexter theory for energy transfer via dipole-dipole interaction an estimate of the energy transfer rate can be made. The critical distance for energy transfer (where the radiative rate equals the energy transfer rate) is given by [23]

$$R_c^6 = 310^{12} f_A E^{-4} S.O. \qquad (9.1)$$

Here f_A is the oscillator strength of the acceptor transition, E is the energy at the maximum of spectral overlap (in eV) and S.O. is the spectral overlap integral. The oscillator strength as determined from the TRITC absorption spectrum is about 0.5. The spectral overlap determined from the YAG:Ce emission and TRITC absorption spectrum is 2 eV^{-1}. This gives a critical distance for energy transfer from Ce^{3+} to TRITC of about 7 nm. As a result, energy transfer rates of 10^8 s^{-1} and faster are expected for Ce^{3+} ions in an outer shell of 5 nm thick in the NC. This is quite consistent with the observations. The luminescence decay curves show that a majority of the Ce^{3+} show a fast decay due to efficient energy transfer to TRITC. For the average size of 18 nm YAG:Ce nanocrystals more than 90% of the Ce^{3+} ions will be within a 5 nm distance from the surface and will transfer the excitation energy with transfer rates of 10^8 s^{-1} and higher to TRITC molecules at the surface. It should be noted that a 18 nm diameter YAG:Ce (0.5 mol%) nanocrystal contains about 1700 Ce^{3+} ions statistically distributed over all available Y^{3+} sites. This will cause a distribution in the TRITC to Ce^{3+} distances. Since ET by electric dipole-electric dipole interaction scales with r^{-6}, Ce^{3+} ions closer to the surface will transfer their energy much more efficiently then ions in the core of the nanocrystal. This distribution of donor-acceptor distances will result in a distribution of ET rates between Ce^{3+} ions and TRITC molecules. The size polydispersity inherent to the NC YAG:Ce samples further broadens the distribution of ET rates. Therefore only an average ET rate can be determined from the experimental data. ET is not only possible between the Ce^{3+} ions and the TRITC molecules but also between Ce^{3+} ions. Therefore Ce^{3+} ions deep inside the nanocrystals may also transfer their energy to Ce^{3+} ions closer to the surface which subsequently transfer their excitation energy to the TRITC molecules, thus increasing the ET rate. A more quantitative analysis of the energy transfer process is not possible in view of the various uncertainties discussed above.

Photobleaching can be used as a control experiment [24] to show that the decay time shortening of the Ce^{3+} luminescence observed in the TRITC-YAG:Ce conjugate is indeed due to energy transfer. TRITC will degrade after being exposed to UV light for a long period, while YAG:Ce is photostable. Figure 9.5 shows the excitation (a) and emission (b) spectra of the TRITC-YAG:Ce conjugate prior to (dark gray) and after (black) 65 hours of irradiation with 300 nm light from a 450 W xenon lamp. The color of the sample after irradiation changed from pink to slight yellow, indicating that the photo decomposition of the TRITC molecules has occurred. In the excitation spectrum of the photobleached sample (Figure 9.5a) the peak around 550 nm (due to direct excitation of TRITC) is strongly reduced, which implies that the amount of TRITC in the sample has decreased. However, not all the TRITC molecules were bleached, despite the long period of UV radiation, possibly because the strong

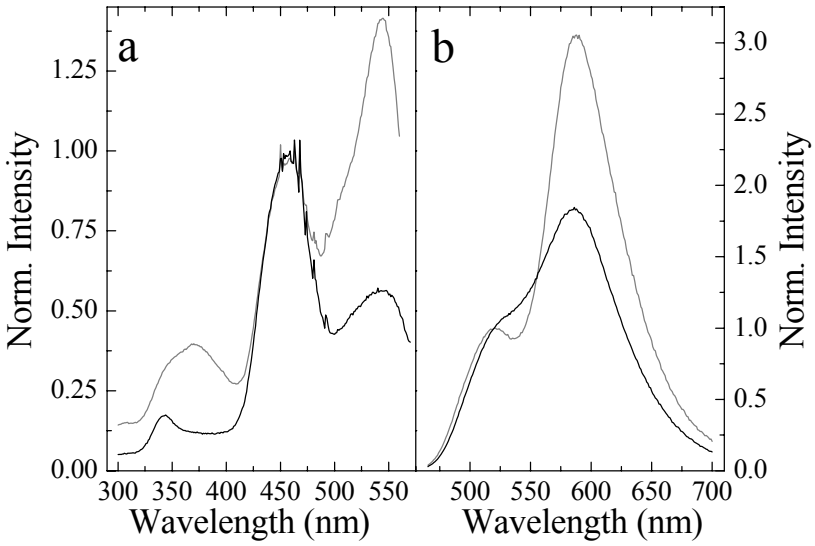

Figure 9.5 (a) Excitation spectra (λ_{em} = 580 nm) and (b) emission spectra (λ_{ex} = 440 nm) of YAG:Ce-TRITC conjugate before (dark gray) and after (black) 65 hours excitation with 300 nm from a 450 W Xenon lamp. Both emission and excitation spectra were normalized to the Ce^{3+} peak.

scattering characteristic of nanoporous materials limits the penetration depth of the light.

In the emission spectra (Figure9.5b) a strong decrease in the emission intensity of the peak around 580 nm (the TRITC emission) is observed after bleaching. Since less TRITC is present at the surface, the average distance between Ce^{3+} ions and TRITC molecules increases. Therefore the likelihood of Ce^{3+} to TRITC energy transfer is diminished and the fraction of radiative recombination of the Ce^{3+} ions increases. Both contributions will be reflected in the decay curves of the photobleached TRITC -YAG:Ce conjugate sample (Figure 9.4, dark gray curve). The fast initial decay is still present, but has a much smaller contribution than prior to the photobleaching, indicating that a smaller population of Ce^{3+} ions have a TRITC molecule at distances short enough to allow efficient ET to take place. This is also reflected in the larger contribution of the exponential decay tail due to the radiative decay of the Ce^{3+} ions without neighboring TRITC molecules.

9.4 Conclusions

In conclusion, we have demonstrated that efficient energy transfer (ET rates of ~10^8-10^9 s^{-1}) from Ce^{3+} ions to TRITC molecules occurs in the TRITC-NC YAG:Ce conjugate. Also, we have shown that nanocrystalline YAG:Ce can be successfully conjugated to organic molecules, therefore establishing its potentiality as a biolabel..

References

[1] T. Förster, *Ann. Phys.* **1948**, VI 2, 55
[2] C. E. Finlayson, D. S. Ginger, N. C. Greenham, *Chem. Phys. Lett.* **2001**, 338 83
[3] O. Schmelz, A. Mews, T. Basche, A. Herrmann, K. Muellen, *Langmuir* 2001,17, 2861
[4] C. R. Kagan, C. B. Murray, M. Nirmal, M. G. Bawendi, *Phys. Rev. Lett.* **1996**, 76, 1517
[5] S. A. Crooker, J. A. Hollingsworth, S. Tretiak, V. I. Klimov, *Phys. Rev. Let.* **2002**, 89, 186802/1
[6] B. Henderson, G.F. Imbusch, *Optical spectroscopy of Inorganic Solids*, Oxford Science Publications, **1989**, Chapter 10
[7] M. Bruchez Jr., M. Moronne, P. Gin, S. A. Weiss, A. P. Alivisatos, S*cience* **1998**, 281, 2013
[8] B.M. Tissue, *Chem. Mater.* **1998**, 10, 2837
[9] R. S. Meltzer, S. P. Feofilov, B. M. Tissue, H. B. Yuan, *Phys. Rev. B* **1999**, 60, R14012
[10] E. Zych, A. Meijerink, A.; C. de Mello Donegá, *J. Phys.:Condens. Matter* **2003**, 15, 5145
[11] K. Riwotzki M. Haase, *J. Phys. Chem. B* **2001**, 105, 12709
[12] K. Riwotzki, H. Meyssamy, H. Schnablegger, A. Kornowski, M. Haase, *Angew. Chem. Int. Ed.* **2001**, 40, 573
[13] O. Lehmann, H. Meyssamy, K. Kömpe, H. Schnablegger, M. Haase, *J. Phys. Chem. B* **2003**, 107, 7449
[14] M. Veith, S. Mathur, A. Kareiva, M. Jilavi, M. Zimmer, V. Huch, J. *Mat. Chem.* **1999**, 9, 3069
[15] H. Yukiya, T. Haganuma, K. Sue, T. Adschiri, K. Arai, *Mat. Res. Bull.* **2003**, 38, 1257
[16] O. A. Lopez, J. McKittrick, L. E. Shea, *J. Lumin.* **1997**, 71, 1
[17] D. Hreniak, W. Strek, *J. Alloys Compounds* **2002**, 341, 183
[18] Chung-Hsin Lu, R. Jagannathan, *Appl. Phys. Lett.* **2002**, 80, 3609
[19] E. Zych, C. Brecher, J. Glodo, *J. Phys: Condens. Matter.* **2000**, 12, 1947
[20] B. D. Cullity, *Elements of X-ray Diffraction*; Addison-Wesley: Massachusetts, **1978**
[21] C. De Mello Donega, S. J. L. Ribeiro, R. R. Gonçalves, G. Blasse, *J. Phys. Chem. Solids* **1996**, 57, 1727
[22] R. S. Meltzer, S. P. Feofilov, B. Tissue and H. B. Yuan, *Phys. Rev. B* **1999**, 60, 14012
[23] G. Blasse, B.C. Grabmaier, *Luminescent materials*, Springer-Verlag, Berlin,**1994** p 93
[24] U. Kubitscheck, M. Kircheis, R. Schweitzer-Stenner, W. Dreybrodt, T. Jovin, I. Pecht, *Biophys. J.* **1991**, 60, 307

Samenvatting

‘Noe giet mie de lamp oet’ had mijn (van origine Twentse) opa vast gezegd als hij dit proefschrift nog had kunnen lezen. En zo vergaat het velen. Deze samenvatting is bedoeld om het werk in dit proefschrift in iets eenvoudiger termen te beschrijven. Voelt u zich niet bezwaard als u, zelfs na deze samenvatting gelezen te hebben, het gevoel hebt nog steeds niet alle finesses te begrijpen.

Het onderzoek beschreven in dit proefschrift gaat over nanokristallijne halfgeleiders ook wel “quantum dots” genoemd. Halfgeleiders zijn materialen met een elektronische structuur, zoals die weergegeven is in figuur 1.2 op pagina 13. Een band bij lage energie is gevuld met elektronen (in zwart) en een band bij hoge energie is leeg (zonder elektronen). De twee banden zijn gescheiden door een “band gap”, een verboden zone. Kristallijn wil zeggen dat de atomen van het materiaal zeer regelmatig geordend zijn, net zoals in suiker- en zoutkristallen. Nano (van het Griekse ‘nanos’: dwerg) is net als milli en micro een term die iets zegt over de afmetingen van deze kristallen. In dit geval gaat het om kristallen met een afmeting van een paar miljoenste millimeter! Een kristal van deze afmetingen bevat slechts tussen de 100 en 10.000 atomen.

Halfgeleiders kunnen licht uitzenden. De kleur van dat licht hangt in eerste instantie af van de grootte van de verboden zone, de band gap. Elk materiaal heeft zijn eigen bandgap en daarbij hoort een specifieke kleur licht die uitgezonden kan worden. Als de band gap groter wordt, verandert de kleur van het licht dat uitgezonden wordt als volgt: rood → oranje → geel → groen → blauw → violet. Deze volgorde komt overeen met de kleuren van de regenboog. Wanneer we het kristal nu heel klein maken, een paar nanometer groot, gebeurt er iets opmerkelijks. De band gap, die per materiaal vast leek te liggen, verandert voor hetzelfde materiaal als de (halfgeleider)deeltjes kleiner worden. De band gap wordt groter naarmate het kristal kleiner wordt en verschuift een band gap die correspondeert met het uitzenden van rood richting het blauw. De precieze grootte van het kristal bepaalt de kleur van het licht dat uitgezonden wordt.

Tot nu toe hebben we aangenomen dat het licht ‘zomaar’ uitgezonden wordt. Aangezien alleen de zon voor niets opgaat, kost het wel wat om een halfgeleider licht te laten uitzenden. In dit proefschrift is dit gedaan met behulp van ultraviolet (UV) licht. Je oog is niet gevoelig voor dit licht (je ziet dus niet dat een UV-lamp aan is), maar de hier bestudeerde halfgeleiders kunnen de UV-straling wel absorberen. Door de absorptie van UV straling wordt een elektron uit de zwarte band in figuur 1.2 geëxciteerd naar de hoger energetische lege (witte) band. De toestand die nu ontstaan is heet ‘aangeslagen toestand’ en is niet stabiel. Het elektron zal eerst snel naar de bodem van de lege band zakken (‘niet-stralende verval’ genoemd) en vandaar naar zijn oude plaats terug gaan onder uitzending

van (zichtbaar) licht. De energie van de fotonen ('lichtdeeltjes') die worden uitgezonden is gelijk aan de band gap. Voorwaarde voor het uitzenden van licht is dat de energie van het licht dat gebruikt wordt bij de bestraling groter moet is dan de band gap van de halfgeleider.
Het bovenstaande geldt voor halfgeleiders in het algemeen. Gaan we nu kijken naar halfgeleiders van enkele nanometers groot dan zijn dezelfde principes van toepassing maar er zijn twee belangrijke verschillen. Ten eerste zal, aangezien de band gap van een halfgeleider nanokristal groter wordt naarmate het kristal kleiner wordt, de energie van het licht dat gebruikt wordt om het kristal in de aangeslagen toestand te brengen, toenemen. In dit proefschrift is steeds violet licht gebruikt met een energie waarmee alle in dit proefschrift bestudeerde nanokristallen aangeslagen kunnen worden. Voor het uitgezonden licht geldt dat als de band gap groter wordt, de energie van de uitgezonden fotonen verandert en daarmee ook de kleur van het uitgezonden licht. Een tweede belangrijk verschil is dat het specifieke oppervlak van een nanokristallijn materiaal heel veel groter is. Als je een groot kristal van 1x1x1 meter opsplitst in nanokristallen van 1x1x1 nanometer, blijft het volume gelijk, maar neemt het totale oppervlak toe met een factor miljard!
Nanokristallen hebben dus een relatief groot oppervlak. Aan het oppervlak kan de aangeslagen toestand, die ontstaat na bestraling met violet licht, niet-stralend (dus zonder uitzending van licht) terug vallen. Dit betekent dat in het ongunstigste geval de nanokristallen geen licht uitzenden na in de aangeslagen toestand te zijn gebracht. Voor het doen van onderzoek aan lichtgevende materialen zijn efficiënt lichtgevende materialen nodig. Een maat voor de efficiëntie is de kwantumefficiëntie. Deze is gedefinieerd als het aantal uitgezonden fotonen gedeeld door het aantal geabsorbeerde fotonen. Een kwantumefficiëntie van enkele tientallen procenten is ruim voldoende voor het onderzoek dat in dit proefschrift wordt beschreven.
Om de nanokristallen licht te laten geven en het niet-stralende verval aan het oppervlak te voorkomen, worden kleine molekulen op het oppervlak geplaatst, zogenaamde "capping molekulen". Deze molekulen zorgen er niet alleen voor dat de nanokristallen efficiënt licht gaan geven, ze zorgen er ook voor dat de nanokristallen die in een oplosmiddel zweven niet gaan klonteren. Zo kunnen de eigenschappen van een heleboel afzonderlijke nanokristallen tegelijk worden bestudeerd.
De eigenlijke inhoud van dit proefschrift bestaat, naast een introductiehoofdstuk, uit 8 hoofdstukken, die bijna allemaal gebaseerd zijn op reeds verschenen publicaties in internationaal gelezen tijdschriften.
Hoofdstuk 2 beschrijft de synthese van cadmiumtelluride (CdTe) nanokristallen uit twee stoffen: een in de aanwezigheid van zuurstof spontaan ontvlambare cadmiumverbinding (dimethylcadmium) en tellurium, een zwart poeder. Vanwege de grote reactiviteit van de uitgangsstoffen met water en zuurstof moet

de synthese worden uitgevoerd in een luchtdicht afgesloten kast waarin de synthese uitgevoerd kan worden via twee handschoenen. De handschoenenkast is gevuld met argon, een edelgas dat niet reactief is. Als er een beetje lucht in de kast lekt, worden water en zuurstof er actief uitgehaald zodat de zuurstof- en waterconcentratie altijd beneden een miljoenste deel blijven.
De synthese van de CdTe nanokristallen is uitgevoerd bij verschillende temperaturen (145°C tot 180°C). De nanokristallen groeien van klein naar groot. De uiteindelijke grootte wordt bepaald door de temperatuur en de aard en concentratie van de capping molekulen. De synthese werd uitgevoerd in een soort twee componenten zeep. De zeepmolekulen gaan als capping molekulen op het oppervlak zitten van de CdTe nanokristallen. De groei van de nanokristallen kan worden gevolgd door tijdens de synthese monsters te nemen. Van die monsters worden absorptie- (welk licht wordt opgenomen?) en emissiespectra (welk licht wordt uitgezonden?) opgenomen. Hiermee wordt informatie over de grootte van de nanokristallen verkregen. De uiteindelijke grootte van de nanokristallen neemt toe naarmate de temperatuur voor de synthese hoger wordt en de binding van de capping molekulen aan het oppervlak zwakker is. Dit maakt het mogelijk nanokristallen van elke gewenste grootte tussen ca. 2 en 6 nm te maken door de syntheseomstandigheden te variëren. Van het uitgezonden licht werd ook bepaald hoe snel de emissie-intensiteit afneemt na een korte puls van het violette excitatielicht.
Hoofdstuk 3 beschrijft hoe de in hoofdstuk 2 gemaakte CdTe nanokristallen vanuit een oliefase in een waterfase overgebracht kunnen worden. Dit werd gedaan met molekulen die thiolen worden genoemd. De hier gebruikte thiolen hebben een hydrofiele (letterlijk: waterminnende) groep aan een kant en een thiolgroep (een zwavel-waterstofgroep), die sterk bindt aan het cadmium van het CdTe nanokristal, aan de andere kant. Door deze thiolen toe te voegen, worden de molekulen, die op het oppervlak van het nanokristallen zitten, vervangen door de thiolmolekulen. Door vervolgens water toe te voegen, ontstaat er onder de olieachtige laag een waterlaag (een tweefasen systeem). De nanokristallen die aan het oppervlak de hydrofiele groepen hebben worden naar de waterfase getrokken. De luminescentie-efficiëntie van de nanokristallen is hoger voor de nanokristallen in water. Voor een groot deel van de nanokristallen is het niet-stralende verval aan het oppervlak zelfs volledig afwezig. Voor de luminescentie van deze nanokristallen wordt, na een korte excitatiepuls, een mono-exponentiele afname van de emissie-intensiteit in de tijd waargenomen met een vervaltijd die bepaald wordt door de kans op stralende terugval van het elektron.
Hoofdstuk 4 laat zien dat deze mooie luminescentie-eigenschappen ook worden waargenomen als andere soorten thiolen op het oppervlak van de nanodeeltjes worden aangebracht. Zo kunnen de efficiënt luminescerende nanodeeltjes oplosbaar worden gemaakt in water, alcohol en olieachtige oplosmiddelen. De luminescentie-eigenschappen van de CdTe worden vergeleken met die van

nanodeeltjes van een materiaal dat heel erg lijkt op CdTe, namelijk cadmiumselenide (CdSe). Als dezelfde thiolmolekulen op de CdSe nanokristallen worden aangebracht, dooft de luminescentie. Dit wordt verklaard door het gemak waarmee het thiol aan het oppervlak een elektron kan afgeven aan het CdSe nanokristal. Hierdoor kan het elektron, dat in de hoogenergetische 'lege' band zit, niet naar zijn oude plek terugvallen en kan er ook geen licht worden uitgezonden. Bij CdTe daarentegen is het, door een energiebarrière, niet mogelijk voor de meeste thiolen om een elektron af te geven aan het kristal.
Hoofdstuk 5 bespreekt de invloed van de brekingsindex van het oplosmiddel op de snelheid waarmee de luminescentie-intensiteit afneemt na een korte excitatiepuls. De metingen worden gedaan voor efficiënt luminescerende CdTe en CdSe nanokristallen waarvoor de levensduur van de emissie bepaald wordt door de kans op stralende terugval. Voor de invloed van de brekingsindex van de omgeving op de stralende levensduur zijn in het verleden veel verschillende modellen afgeleid en in dit hoofdstuk worden theoretische modellen experimenteel geverifieerd door precies dezelfde CdTe en CdSe nanokristallen op te lossen in verschillende olieachtige oplosmiddelen, elk met een andere brekingsindex, en vervolgens de levensduur van de emissie te meten. Er wordt een zwakke afhankelijkheid tussen de levensduur en de brekingsindex van het oplosmiddel gevonden. De invloed van de brekingsindex is veel kleiner dan voorspeld wordt door in het verleden ontwikkelde en algemeen toegepaste modellen maar de resultaten worden wel goed verklaard door een recent gepubliceerde theorie.
In hoofdstuk 6 worden de kwantumefficiëntie en de levensduur van de emissie voor CdSe nanokristallen bestudeerd voor temperaturen tussen -70°C en 30°C. Gewoonlijk gaat een nanokristal minder licht geven als de temperatuur hoger wordt. Dit verschijnsel is algemeen geldig voor lichtgevende materialen en wordt "temperature quenching" (temperatuurdoving) genoemd. Voor de hier bestudeerde nanodeeltjes neemt de kwantumefficiëntie (en ook de levensduur van de emissie) echter toe bij het opwarmen van een oplossing met nanokristallen. Dit is een nieuw en opmerkelijk verschijnsel en de foto in figuur 6.1 geeft een visuele indruk. We hebben het verschijnsel "temperature anti-quenching" genoemd. De precieze temperatuur waarbij de lichtintensiteit begint toe te nemen hangt af van de lengte van de capping molekulen op het oppervlakte van de CdSe nanokristallen. Voor capping molekulen met een langere keten is de temperatuur waarbij de overgang plaatsvindt hoger. Dit duidt er op dat een faseovergang (bijv. van vast naar vloeibaar) in de laag van capping molekulen de oorzaak is van de temperature anti-quenching, aangezien een faseovergang voor korte molekulen bij een lagere temperatuur plaasvindt. De oorzaak voor de doving van de luminescentie bij lage temperatuur is waarschijnlijk spanning in de oppervlaktelaag van het nanokristal door de sterke ordening van de capping molekulen.

Hoofdstuk 7 beschrijft temperature anti-quenching van de luminescentie voor de wateroplosbare CdTe nanodeeltjes die in hoofdstuk 3 gemaakt zijn. Het effect is hier nog veel sterker dan voor CdSe. Het licht van de nanokristallen dooft volledig uit als de deeltjes afgekoeld worden. Dit is mooi te zien in figuur 7.2. Nu is niet een faseovergang in de laag van capping molekulen, maar een faseovergang van het water (naar ijs) verantwoordelijk voor het uitgaan van het licht (noe giet mie de lamp oet?). Deze verklaring wordt bevestigd door methanol als antivries toe te voegen aan een waterige oplossing van nanodeeltjes. Na toevoeging van methanol zakt de temperatuur voor de faseovergang water/ijs en daalt ook de temperatuur waarbij het licht, dat de nanokristallen uitzenden, dooft.
In hoofdstuk 8 worden geen oplossingen van CdTe nanodeeltjes gebruikt maar ‘gedroogde nanodeeltjes’. Bij het indrogen neemt de afstand tussen de nanodeeltjes sterk af en kunnen de nanodeeltjes een interactie met elkaar aangaan. Het blijkt dat kleinere (bijv. groen lichtgevende) nanokristallen energie kunnen overdragen aan de grotere (bijv. rood lichtgevende) nanokristallen. In plaats van groen licht uit te zenden kan een kleiner nanokristal het grotere nanokristal in de aangeslagen toestand brengen en wordt uiteindelijk rood licht uitgezonden. Als je nu 90% groen en 10% rode nanodeeltjes mengt en laat drogen tot een poeder wordt er voornamelijk rood licht uitgezonden door energieoverdracht van de kleinere naar de grotere nanokristallen. Dit hoofdstuk richt zich op de invloed die de temperatuur heeft op energieoverdracht.
Hoofdstuk 9 beschrijft ook energieoverdracht, maar dan tussen nanodeeltjes van YAG (een oxide van aluminium en ytterium) dat ionen (atomen met een lading) van cerium bevat die (geel) licht kunnen uitzenden. Als er een kleurstof op het oppervlak van deze nanodeeltjes wordt gezet, kan de energie van de aangeslagen cerium ionen worden overgedragen aan de (lichtgevende) kleurstof op het oppervlak, zodat deze licht gaat uitzenden.

List of publications

This thesis is based on the following publications:

- Luminescence and growth of CdTe quantum dots and clusters. Sander F. Wuister, Floris van Driel and Andries Meijerink, *Phys. Chem. Chem. Phys.* **2003**, 5, 1253 (chapter 2)

- Highly luminescent water-soluble CdTe quantum dots. Sander F. Wuister, Ingmar Swart, Floris van Driel, Stephen G. Hickey and Celso de Mello Donegá, *Nano Lett.* **2003**, 3, 503 (chapter 3)

- Influence of thiol capping on luminescence and decay kinetics for CdTe and CdSe quantum dots. Sander F. Wuister, Celso de Mello Donegá and Andries Meijerink, *J. Phys. Chem. B* **2004**, 108, (chapter 4)

- Local-field effects on the spontaneous emission rate of II-VI semiconductor quantum dots in dielectric media. Sander F. Wuister, Celso de Mello Donegá and Andries Meijerink, *J. Chem. Phys.*, **2004**, 121, 4311 (chapter 5)

- Temperature antiquenching of the luminescence from capped CdSe quantum dots. Sander F. Wuister, Arie van Houselt, Celso de Mello Donegá, Daniel Vanmaekelbergh and Andries Meijerink, *Angew. Chem. Int. Ed.* **2004**, 43, 3029 (chapter 6)

- Luminescence temperature antiquenching of water-soluble CdTe quantum dots: role of the solvent. Sander F. Wuister, Celso de Mello Donegá and Andries Meijerink *J. Am. Chem. Soc.*, **2004**, 126, 10397 (chapter 7)

- Temperature dependent energy transfer in CdTe quantum dot solids. Sander F. Wuister, Rolf Koole, Celso de Mello Donegá and Andries Meijerink, submitted to *J. Phys. Chem. B* (chapter 8)

- Efficient energy transfer between nanocrystalline YAG:Ce^{3+} and TRITC. Sander F. Wuister, Celso de Mello Donegá, Andries Meijerink, *Phys. Chem. Chem. Phys.* **2004**, 6, 1633 (chapter 9)

Other publications:

- Preparation of conjugated quantum dots via capping exchange. Sander F. Wuister, Ingmar Swart, Celso de Mello Donegá and Andries Meijerink (manuscript in preparation)

- Synthesis and luminescence of CdS quantum dots capped with a silica precursor. Sander F. Wuister, Andries Meijerink, *J. Lum.* **2003**, 105, 35

- Single-step synthesis to control the photoluminescence quantum yield and size dispersion of CdSe nanocrystals. C. de Mello Donegá, S. G. Hickey, S. F. Wuister, D. Vanmaekelbergh,; A. Meijerink, *J. Phys. Chem. B* **2003**, 107, 489

- Luminescence of nanocrystalline ZnSe:Cu. J.F. Suyver, T. van der Beek, S. F. Wuister, J. J. Kelly, A. Meijerink, *Appl. Phys. Lett.* **2001**, 79, 4222

- Synthesis and photoluminescence of nanocrystalline ZnS:Mn^{2+}. J.F. Suyver, S. F. Wuister, J. J. Kelly, A. Meijerink, *Nano Lett.* **2001**, 1, 429

- Luminescence of nanocrystalline ZnSe:Mn^{2+}. J.F. Suyver, S. F. Wuister, J. J. Kelly, A. Meijerink, *Phys. Chem. Chem. Phys.* **2000**, 2, 5445

Dankwoord

De mensen zijn in mijn ogen veel belangrijker dan hun werken. In de wetenschap vergeet men dat vaak! Daar is de inhoud van de artikelen het belangrijkst en een auteur is een pseudoniem voor een reputatie. Gelukkig is er tussen wetenschappers onderling naast veel elektronisch contact ook nog persoonlijke interactie. Dat brengt voor mij dingen terug tot de juiste proporties: wetenschappers zijn mensen. Daarom is het ook volledig terecht dit dankwoord als eerste te lezen. Hieronder noem ik een aantal mensen (niet allemaal wetenschappers!) die ik wil bedanken.

Andries, je bent een erg enthousiaste promotor, vol humor en betrokken bij mijn onderzoek. Je gaf mij ook genoeg ruimte om mijn eigen gang te gaan en was altijd uit je stoel te krijgen met de woorden: “Hé Andries, ik wil je wat leuks laten zien in het lab”. Mede dankzij jouw retoriek zijn er een heleboel mooie artikelen verschenen! Celso, ik heb goede herinneringen aan de brainstormsessies met jou en Steve. Altijd kwam er wel weer een nieuw idee of inzicht. Je deur stond altijd open om even binnen te lopen om wat verse resultaten te bespreken, waarbij je synthese expertise, je enthousiasme en je nauwkeurigheid goed van pas kwamen. Daniël was de afgelopen jaren ook erg betrokken bij mijn onderzoek. Je ambitie en je enthousiasme waardeer ik zeer.

Cees, je interactieve colleges waren erg leerzaam en interessant. Ook in de laatste fase van mijn promotie heb je veel voor mij gedaan :-). Ik heb bewondering voor je ogenschijnlijk simpele vragen (why does the exciton decay?) die precies de vinger op de ‘zere plek’ leggen. Ook de colleges ‘natuurkunde voor chemici’ van Harold de Wijn waren een welkome aanvulling voor een fysisch chemicus als ik. John, bij jou kon ik terecht met vragen over bulk halfgeleider eigenschappen en je bent ook al zo’n retorische reus. Dank voor je vriendelijkheid.

Peter Liljeroth helped me a lot with chapter 4 of this thesis and reminded me when interesting articles appeared (some had titles that were very familiar to me …). Thanks for reading the manuscript of this thesis and for all the constructive comments. Stephen Hickey thanks for all the discussions we had and for your suggestions (especially on the MPS stuff) and of course for all the work you did to fix that green monster. You left too soon.

Met Dave van den Heuvel en Hans Gerritsen heb ik ook leuke discussies en gesprekken gehad. Bedankt voor jullie interesse, expertise en voor het lenen van de PQ 440. Jammer dat we samen geen ‘single dot’ werk hebben kunnen doen. Addy van Dijken van Philips Research heeft geholpen door metingen met hun streak camera aan ‘quantum dot solids’ te doen, bedankt voor je tijd en enthousiasme.

Hans Ligthart is onmisbaar geweest de afgelopen jaren: geen goed onderzoek zonder goede technici! Je stond altijd klaar om de meetapparatuur en de glovebox draaiende te houden en om chemicaliën te bestellen. En natuurlijk zette jij elke ochtend een lekker bakkie koffie! Stefan Zevenhuizen is die andere technicus waar ik meermaals in wanhoop een beroep op heb gedaan als mijn computer het weer eens niet deed. Rustig keek jij waar het probleem zat en fikste het in no-time. Hans Meeldijk wil ik bedanken voor al de tijd die je achter de TEM hebt gezeten op zoek naar onze nanodingetjes. Als er één ondersteunende dienst is die een dikke pluim verdient dan zijn het wel de 'mannen van het gas', Johan, Nico en Jan. Jullie service is perfect, nooit was het jullie te veel om een vaatje te vullen, een fles argon te brengen, een gaslek te zoeken, advies te geven of gewoon een praatje te maken. Ik wil ook de audiovisuele dienst bedanken voor het opmaken van mijn posters en de goede service.
Natuurlijk even een apart bedankje voor Paul: meer dan vier jaar bij elkaar op vier verschillende kamers. Bedankt dat je zo'n gezellige en attente kamergenoot bent geweest. Helaas heeft zelfs Ruben je niet kunnen overtuigen van de juiste kleur van natriumlicht. I would like to thank Xinghua for being my roommate and for selling me his vacuum cleaner and washing machine, they still do their job. Gijs, jij kon losgaan maar wat was je vaak kapot. Dennis en Rolf, hebben inmiddels de leiding op de TOP-kamer overgenomen. Jammer dat ik door 'Michelle' er niet zo vaak was, met z'n drieën was het heel gezellig.
Ik heb geboft met 5 goede studenten die mij wilde helpen bij mijn onderzoek. Susanne Bisschop, Arie van Houselt, Ingmar Swart, Rolf Koole (wie had ooit gedacht dat jij nog eens mijn kamergenoot zou worden!) en Susan Kersjes bedankt voor jullie inzet en creatieve ideeën. Het was een plezier om jullie te begeleiden, het heeft veel opgeleverd en het is goed om te zien dat velen van jullie zijn gaan promoveren. Ook Bart, Jan, Marijn en Veronique hebben mij geholpen met mijn onderzoek en hebben laten zien dat eerstejaars studenten waardevolle en soms zelfs publiceerbare (!) dingen kunnen meten.
Een speciaal bedankje voor Freek Suyver die mij enthousiast heeft gemaakt voor nano en mij tijdens mijn hoofdvak geholpen heeft mijn eerste stapjes in dit fascinerende wetenschapsgebied te zetten. Ik heb nooit spijt gehad van mijn 'terugkeer'. De sectie *Condensed Matter and Interfaces* is niet alleen een professionele maar ook een heel leuke werkomgeving. Het zijn opnieuw een heleboel mensen die de sfeer zo prettig hebben gemaakt. Al die mensen (Aarnoud, Ageeth, Alexander, Arjan, Bert, Fiona, Floris, François, Harold, Jeroen, Jessica, Jan, Karen, Laura, Liesbeth, Marcel, Monica, Peter, Rianne, Stephen, Thijs, Vladimir, Willem, Zeger en .....{mocht ik je naam vergeten zijn, vul hem dan zelf hier in}) wil ik daarvoor bedanken.
Didi en Carmen, bedankt voor de vele potjes squash. Al snel had ik door dat het met vrouwen veel gevaarlijker squashen is dan met mannen. Jullie hebben me

meerdere keren van de baan geslagen (letterlijk), maar toch mocht dat de pret niet drukken.
Arnoud en Linda, bedankt dat jullie mijn paranimfen willen zijn, het zal een speciale dag worden voor de familie Wuister. Reinier en Maaike, bedankt voor jullie vriendschap! We zullen jullie missen als jullie straks een hele tijd bijna tegenvoeters worden. Reinier, misschien kunnen we net in als Nederland (Gouda!) gewoon een keer ergens halverwege afspreken... Mijn familie en schoonfamilie wil ik bedanken voor hun interesse in mijn werk. Het is niet altijd makkelijk uit te leggen wat je nou precies doet. Maar gelukkig zijn er een heleboel andere (belangrijkere) onderwerpen waar we het over kunnen hebben. Het is een voorrecht twee zulke families te hebben!
Tineke en Ruben, jullie zijn het einde! Wetenschap is spannend, maar een leven met jullie is nog veel leuker en spannender. Bedankt voor alles wat we samen hebben doorgemaakt. Ik hou van jullie!

Curriculum Vitae

Sander Frederik Wuister werd geboren op 3 juli 1976 te Leidschendam. Hij behaalde in 1995 zijn VWO diploma aan de GSR (Gereformeerde Scholengemeenschap Randstad) te Rotterdam. In datzelfde jaar begon hij met de opleiding Scheikunde aan de Universiteit Utrecht. In 1996 werd het propedeutisch examen afgelegd en het doctoraal diploma werd in 2000 verkregen (met genoegen). Tijdens zijn studie volgde hij bijvakken bij de secties *Chemie en Samenleving* (wetenschapsfilosofie) en *Fysische en Colloïdchemie*. Het hoofdvak werd gedaan in de sectie *Gecondenseerde Materie*. Tevens was hij in 1998/1999 studentlid van de universiteitsraad die onder andere de voorstellen voor de breedtestrategie goedkeurde.

Op 1 januari 2001 startte hij zijn promotie-onderzoek bij de sectie *Gecondenseerde Materie* (tegenwoordig: *Condensed Matter and Interfaces*) aan de Universiteit Utrecht gefinancierd vanuit de breedtestrategie in het programma 'Physics of Colloidal Matter'. De onderzoeksresultaten die in de afgelopen drie jaar behaald zijn, werden gepubliceerd in een aantal wetenschappelijke publicaties en staan beschreven in dit proefschrift. Een deel van het hier beschreven werk werd ook gepresenteerd op de *International Conference on Luminescence and Optical Spectroscopy of Condensed Matter* in Budapest (in 2002) en op de *Materials Research Society Spring Meeting* in San Francisco (in 2004). Tijdens de laatstgenoemde conferentie werd het onderzoek bekroond met een 'Outstanding Poster Prize' en een 'Graduate Student Silver Award'.

Sander begeleidde studenten bij het scheikundepracticum 'Maken en Meten 1' alsmede bij de eindproef voor eerstejaars scheikundestudenten in de sectie *Condensed Matter and Interfaces*.

Per 1 maart zal hij in dienst treden als Senior Scientist bij Philips Research (Natuurkundig Laboratorium) in Eindhoven.